

Physics 4AL: Mechanics Lab Manual¹

UCLA Department of Physics & Astronomy

August 31, 2017

¹This manual is an adaptation of the work of William Slater by W. C. Campbell, Priscilla Yitong Zhao, Julio S. Rodriguez, Jr., Chandler Schlupf, and Anthony Ransford

Abstract

Physics 4AL is designed to give students an introduction to laboratory experiments on mechanics. This course is intended to be taken after completion of Physics 1A or 1AH and concurrently to the student taking Physics 1B or 1BH. We will be experimentally investigating some of the most foundational concepts in physics, including gravity, energy, momentum, harmonic oscillation and resonance. These concepts are the basis for the classical motion of everything from electrons to galaxies. There are a lot of “science skeptics” in the world; I invite you to come to class with a critical eye and to experimentally test whether we, your instructors, have been lying to you all these years!

i. Introduction to the Data Acquisition (DAQ) system

A crucial part of modern experimental physics is the use of computers to aide in data acquisition and experimental control. Computers can allow us to take data faster, more accurately, and with far less tedium than was possible before their integration into the laboratory. It is therefore crucial that an introductory physics laboratory course include the use of computer-aided data acquisition (DAQ), and we will be using the DAQ throughout the course to allow us to focus on the physics. This chapter will introduce the system we will use and can be regarded as a user manual and general reference for later experiments.

i.1 PASCO DAQ System: Capstone and the 850 Universal Interface



Figure i.1: The PASCO 850 Universal Interface

The data acquisition (DAQ) system we will use in this course is produced by PASCO Scientific for instructional lab courses. The software is called Capstone, and provides the

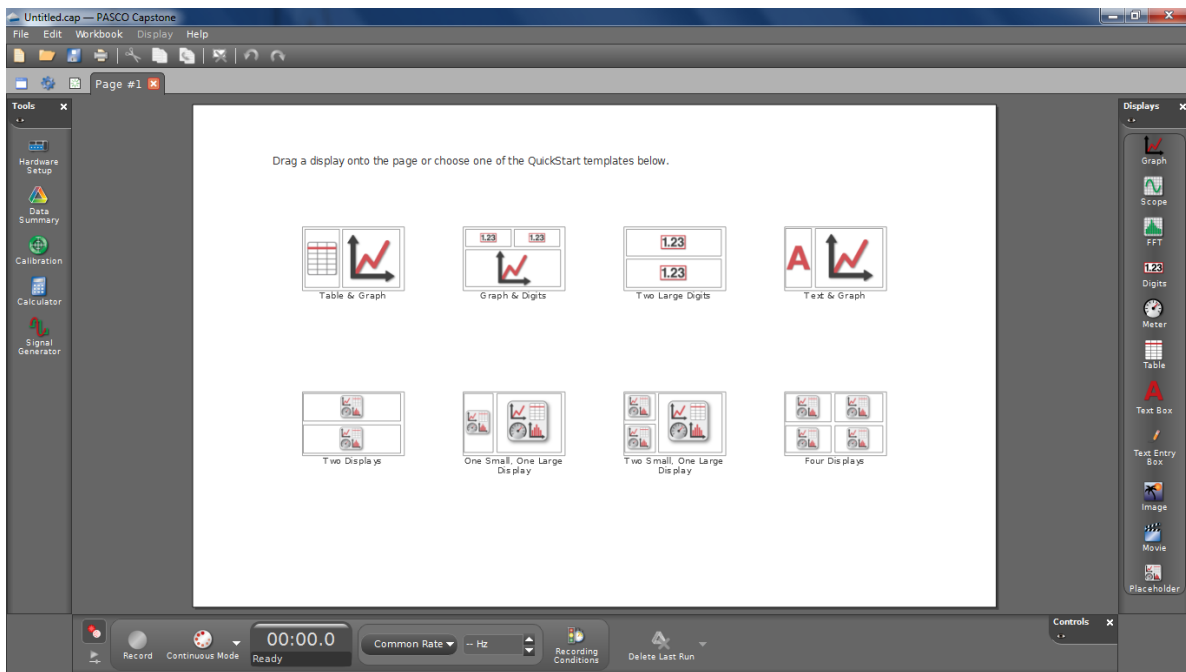
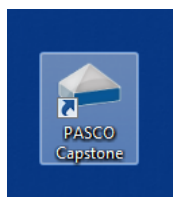


Figure i.2: The default startup screen for PASCO Capstone version 1.0.1. You may be using a slightly newer version that looks a little different, but the basics should be the same.

communication with the hardware interface. This guide is based on PASCO Capstone 1.0.1 and the PASCO 850 Universal Interface, which is the piece of hardware that connects the computer to your instruments, shown in Figure i.1.

i.2 Startup



To begin, ensure that the 850 is connected to the computer (via USB) and power it on by pressing the power button on the front if the 850 is not already on. If the unit is powered up and connected to the computer, the power button will be backlit in blue and the connection indicator light just below the power button will be illuminated in green. If you encounter problems with either of these, check that cables have not come loose or ask for help from your TA.

Next, start the **Capstone** program, which has a logo that looks like, well, a *capstone*. Once running, the program should look something like Figure i.2.

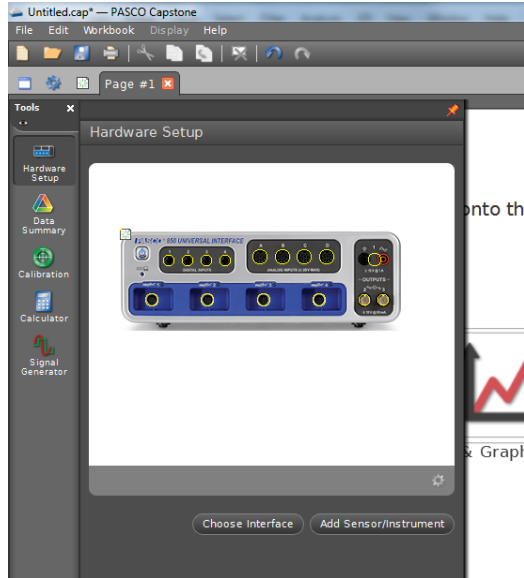
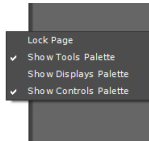


Figure i.3: Clickable **Hardware Setup** screen shot

If the **Tools** palette on the left is missing, click the gear icon in the upper left (“Change properties of current page and Tools Palette”) and check **Show Tools Palette** under **Page Options**. You can also right-click on the gray Capstone desktop and check **Show Tools Palette**. The same thing goes for the **Controls** and **Displays** palettes.



If your palettes are not shown on the screen, right-click the gray desktop and select the appropriate palette.

i.3 Configuring Hardware



To set up the hardware for a specific experiment, click on the **Hardware Setup** icon in the **Tools** palette. If the 850 interface is turned on and is communicating with the computer, this will bring up a clickable picture of the front panel of the 850 interface, as shown in Fig. i.3.

The yellow circles are clickable and will enable you to tell the computer what hardware is attached to each connector on the 850 interface. Clicking on the yellow circle will bring up a drop-down menu showing the possible types of hardware connected to each port. Once you select the appropriate type of hardware from the list, icons will appear indicating how the software thinks the hardware is connected. For example, to configure Capstone for the vibrating string lab, you could choose **Light Sensor** from the drop down menu of the analog input channel used for the photodiode and **Output Voltage Current Sensor** for output channel 1.

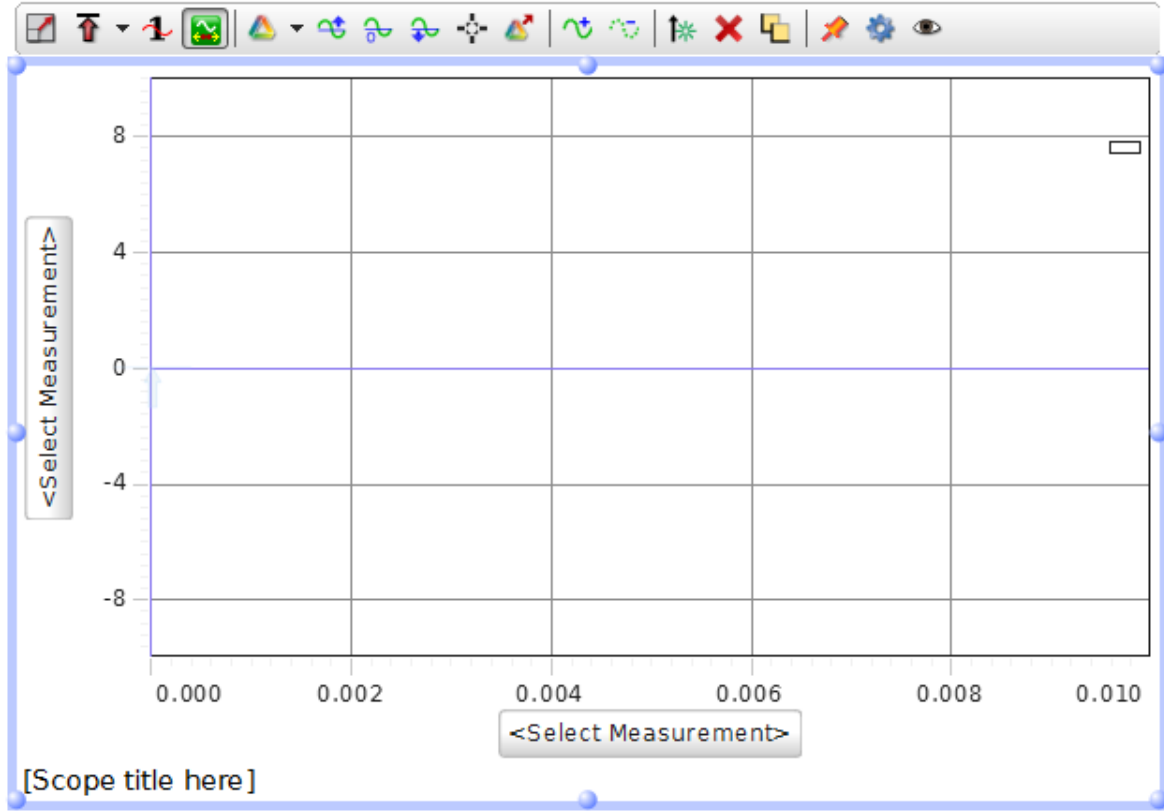
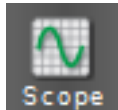


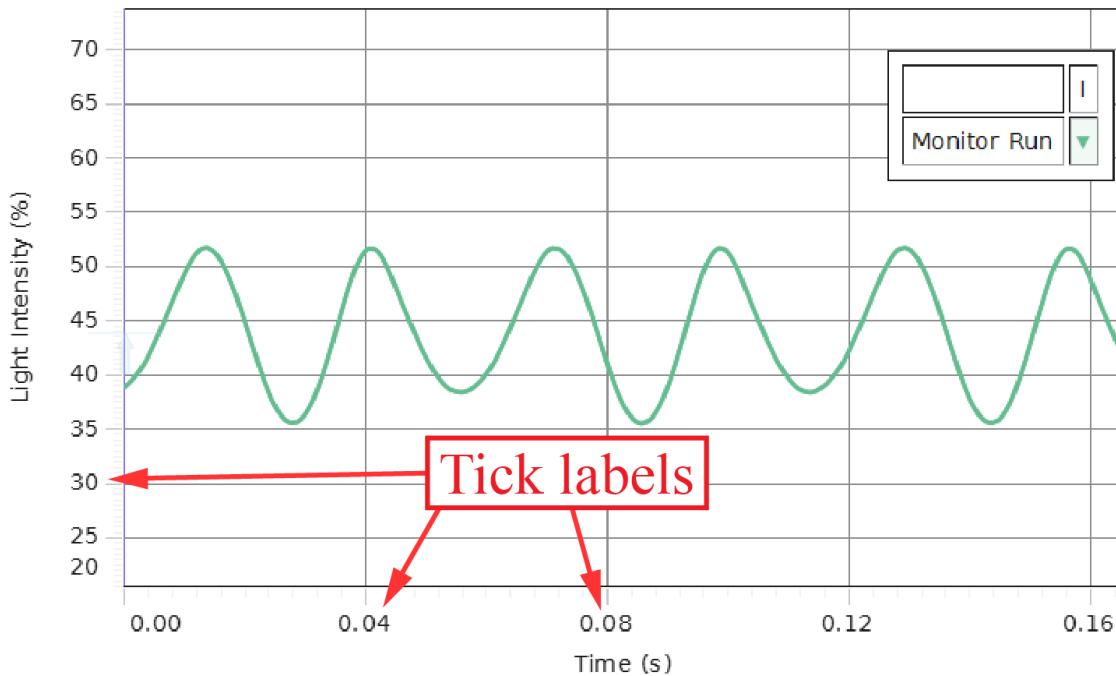
Figure i.4: Clickable **Scope** screen shot

i.4 Scope Display



The **Scope** feature is useful for running diagnostics of your apparatus and setting things up with real-time readout of the results. When all else fails, you can try using the scope to see if your DAQ is receiving input from its transducers. To start a full-screen **Scope** session, double click the **Scope** icon from the **Displays** palette (typically upper right, as shown in Fig. i.2). This will produce a large set of axes on the screen to display the measurement, such as shown in Fig. i.4. If you have the **Hardware Setup** or **Signal Generator** screens open and the left side of the plot is not visible, either close those screens or click the push pin at the upper right side of those windows to force the scope plot to shrink to fit the available space.

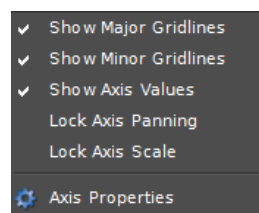
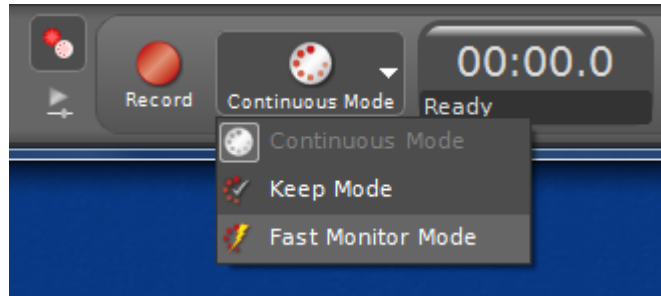
To configure what is being plotted on each axis, click the axis label, which is the button that says to bring up the drop down menu. This menu will have the names of devices that can be used for plotting, but the only selectable items are the actual measurements listed below each device name. Selecting the proper measurement for each axis will display the name of that measurement as the axis label. There is a menu bar for the scope trace that will appear when it is clicked or moused over in the display.



Photodiode Intensity vs. Time

Figure i.5: The scope tool in action, with tick labels pointed out in red.

The x -axis will almost always be time for our purposes, so to begin plotting whatever is on the y -axis vs. time in real-time, you may need to change from **Keep Mode** or **Continuous Mode** to **Fast Monitor Mode**, which can be selected in the **Controls** palette, usually found at the bottom of the screen. This will allow you to start seeing real-time traces on the scope by clicking the **Monitor** button:



Changing the scale and offset of the axes is a little tricky. To change the offset (*i.e.* to move the location of the origin), you can grab the plot region itself and drag it around. If this doesn't work, make sure that axis panning is not locked by right-clicking on a tick label and making sure that **Lock Axis Panning** is not checked. To change the scale of an axis, either mouse over the tick labels and use the scroll wheel, or grab an axis tick label and drag it toward or away from the origin to change the scale.

If nothing appears on the scope trace, make sure the expected signal would be shown in the range that is being plotted. If there is still no trace shown, mouse over the plot area to

bring up the pop-up menu at the top and check to make sure that the trigger button  is *not* depressed. If it is, click it to unselect “normal trigger” mode.¹

To plot multiple traces on the same set of axes, click the **Add new y-axis to scope display** button  on the pop-up menu for the scope trace. (If you don’t see the pop-up menu at the top of the scope trace such as is shown in Fig. i.4, mouse over the plot region.) The new y -axis will appear on the right side. To change the color of the plot, click on the sensor data summary, right click the run, and the option “color picker” will come up.

¹If you understand how to use a trigger on an oscilloscope, feel free to use it; it can be quite handy. The trigger level is indicated by a very faint vertical arrow on the y -axis (at $x = 0$, shown in Fig. i.5 at $t = 0.00$ s, $y = 44\%$) that can be dragged around to change the trigger level. The arrow starts at $(0,0)$ on the plot, so if you click the trigger button and can’t find the arrow, make sure you have $x = 0$ and $y = 0$ visible in your plot region.

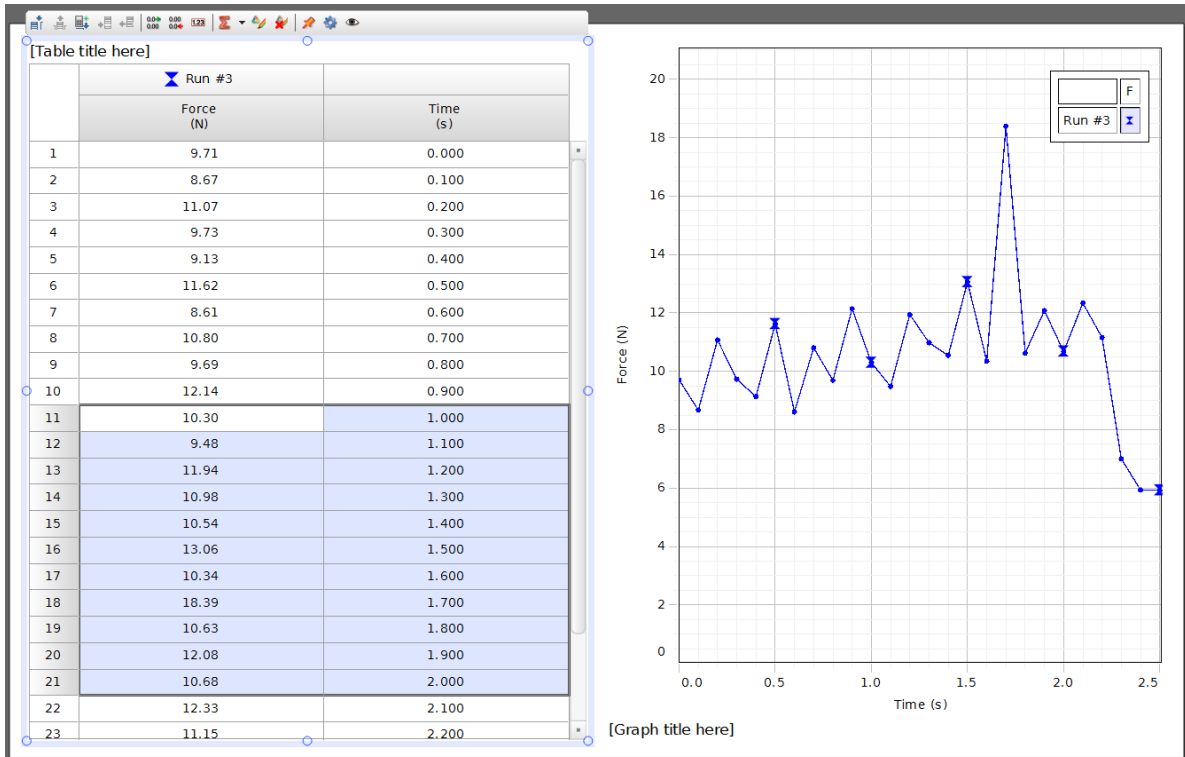


Figure i.6: A **Table** and **Graph** showing the same data. If you only want to save the data between, say, $t = 1$ s and $t = 2$ s, you can highlight just the relevant portion in the **Table** on the left and copy-and-paste it into Excel.

i.5 Exporting your Data

PASCO has not yet provided a way to save your data in a format that is useful. Ideally, you should be able to import your data into an analysis program, such as Matlab, Excel, Mathematica, Open Office Calc, IGOR Pro, Google Spreadsheets, or whatever else is your preferred program. The way we will get around this software limitation is by displaying the data in a table, from which you can later copy and paste the data directly into Excel on the lab computer. Then you can save your Excel file in whatever format you prefer (.xls, .csv, etc.) and, for instance, email it to yourself for analysis at home.



To display the acquired data in a table, first start a new table by clicking the **Table** icon in the **Displays** palette. This will open a new, blank, two-column table on the workspace. The heading of each column will be a clickable drop-down menu just like the **Scope** axes, and you can choose the data you want to save for each column.

For example, Figure i.6 shows the results of a short measurement of force vs. time. Both the **Table** column headings and the **Graph** axis labels have been configured to display force (in Newtons) and time (in seconds). The data were then recorded using, for instance, **Continuous**



	A	B	C	D	E
1	Run #3	Auto			
2	Force (N)	Time (s)			
3	10.3	1			
4	9.48	1.1			
5	11.94	1.2			
6	10.98	1.3			
7	10.54	1.4			
8	13.06	1.5			
9	10.34	1.6			
10	18.39	1.7			
11	10.63	1.8			
12	12.08	1.9			
13	10.68	2			
14					
15					
16					
17					
18					
19					
20					

Figure i.7: The same data highlighted in Fig. i.6 right after being pasted into a new workbook in Excel. Note that the column headers from the table in PASCO were automatically pasted with the data. This spreadsheet can now be used for plotting, analysis, and saving for further analysis and inclusion in a lab report.

Mode from the **Controls** palette, though it may also be acquired using **Fast Monitor Mode** and **Keep Mode** if those are better suited to the particular experiment.

If we only want to save the section of data with the large peak in it for analysis and plotting in a lab report, we can do this by highlighting the relevant portion of the **Table** and copying it to Excel using copy (**ctrl-c**) and paste (**ctrl-v**). Figure i.7 shows the data that was highlighted in Fig. i.6 as it appears in Excel directly after pasting it into a new workbook. The data are now available for saving, plotting, curve fitting, and inclusion in a lab report.

ii. Determining and Reporting Measurement Uncertainties

Throughout this course, we will be making and reporting quantitative measurements of experimental parameters. In order to interpret the results of a measurement or experiment, it is crucial to specify the uncertainty (often called the “error” or “error bars”) with which the measurement claims to be a report of the “true value” of the quantity being measured. This chapter is designed to be a quick reference for the assignment and propagation of errors for your lab reports. For a more detailed treatment, I recommend the excellent books by Taylor [9] or Bevington and Robinson [1].

ii.1 Statement of measured values in this course

Every measurement is subject to constraints that limit the precision and accuracy with which the measured “best value” corresponds to the “true value” of the quantity being measured. It is fairly standard in physics to use the following notation to specify both the measured best value and the uncertainty with which this value is known:

$$q = q_{\text{best}} \pm \delta q. \quad (\text{ii.1})$$

Here, q is the quantity for which we are reporting a measurement, q_{best} is the measured best value (often an average, but not infrequently generated in other ways) and δq is the uncertainty in the best value, which is defined to be positive and always has the same units as q_{best} . For our purposes in this course, the uncertainty will always be symmetric about the measured best value, so the notation of Eq. ii.1 will be used throughout.

For example, the most accurately measured quantity in the world is currently the ratio of the energy splittings between pairs of special states in two atomic ions [7], which is given by

$$\frac{\nu_{\text{Al}^+}}{\nu_{\text{Hg}^+}} = 1.052\,871\,833\,148\,990\,44 \pm 0.000\,000\,000\,000\,000\,06. \quad (\text{ii.2})$$

Here, the measured best value is $1.052\,871\,833\,148\,990\,44$ and the uncertainty is 6×10^{-17} . This level of precision and accuracy is far beyond anything we will be measuring in this

course, but the notation is nonetheless understandable because it is given in the form of Eq. ii.1.

In this course, you will almost exclusively be measuring quantities with units. *Measured values for quantities that have units must be stated with their units.* Failing to do so results in complete nonsense, the loss of \$300 million space probes [6], dogs and cats living together, mass hysteria [5], not to mention the loss of points on your lab report grade. It is fine for the units to appear as abbreviations, words, in column headers, after the numerical values, or in some combination of these just so long as it is clear what the units are. A good example of how to report a measured value is given by the 2010 CODATA recommended value for the proton mass:

$$m_p = (1.672\,621\,78 \pm 0.000\,000\,07) \times 10^{-27} \text{ kg.} \quad (\text{ii.3})$$

Note that the parentheses are used around the measured best value and the uncertainty because they have the same units (which is always true) and are written with the same exponential factor (which can help to make it easy to read).

There are two last points to make here about reporting measured values. First, in these two examples, the uncertainties are written with the same precision (in scientific notation, the number of digits where we include any leading zeros) as the measured best value. This should always be the case, and *when you report a measured value with an uncertainty, you must make sure the uncertainty is reported with the same precision as the measured best value.*

Second, if we disregard all of the leading zeros, the uncertainty is presented with one nonzero digit. There are times when it is appropriate to use up to two digits for this (particularly when the first digit of the uncertainty is small, say, a 1 or 2), but uncertainties should never have three significant digits. This is because the size of the uncertainty itself sets the scale of where the measurement can no longer claim to be providing useful information.

ii.1.1 Other notation you will encounter

A quick glance at Eq. ii.2 and ii.3 reveals that it is difficult to read off the absolute value of the uncertainty, since one has to count a lot of zeros. For this course, you will be expected to report your measurements in the form of Eq. ii.1, but you should be aware of other methods that are used so that you can interpret their meaning.

Concise notation is useful when the fractional uncertainty becomes very small (as in the examples above). In concise notation, only the significant digit or digits of the uncertainty are written, and they are written in parentheses directly after the best value, which is written to the same precision. For example, the following shows two ways to express the same measured value for the frequency of a laser

$$\nu = (3.842\,30 \pm 0.000\,02) \times 10^{14} \text{ Hz} \quad (\text{ii.4})$$

$$\nu = 3.842\,30(2) \times 10^{14} \text{ Hz.} \quad (\text{ii.5})$$

The second line uses concise notation, where since the number in parentheses has one digit, we are being told that this is the uncertainty in the last digit of the best value. This gets

more complicated when uncertainties are quoted with two digits, which seems to be getting more common in the literature. As a concrete example, the mass of the electron reported by CODATA is actually reported in the following form:

$$m_e = 9.109\,382\,91(40) \times 10^{-31} \text{ kg} \quad (\text{ii.6})$$

Here, we are being told that the last *two* digits have an uncertainty given by the two digits in parentheses. This notation can seem somewhat confusing for a number of reasons, but if we always think of writing the digits in parentheses below the best value so that they end at the same place, it is easier to keep from getting confused, as in

$$\begin{aligned} m_e &= 9.109\,382\,91 \times 10^{-31} \text{ kg} \\ &\pm 0.000\,000\,40 \times 10^{-31} \text{ kg} \end{aligned} \quad (\text{ii.7})$$

Asymmetric uncertainties are also sometimes encountered in the scientific literature, where the upper uncertainty may have a different size than the lower one. In this case, the following three examples show how one may see this written, using an example of a measured radiative decay lifetime:

$$\tau = (37.0 +2.0/-0.8) \text{ ms} \quad (\text{ii.8})$$

$$\tau = (37.0 ^{+2.0}_{-0.8}) \text{ ms} \quad (\text{ii.9})$$

$$\tau = 3.70(^{+20}_{-08}) \times 10^{-2} \text{ s} \quad (\text{ii.10})$$

ii.1.2 “Sig Figs”

There is a system for implicitly including the order of magnitude of the uncertainty of a measured quantity by simply stating the value with a certain number of digits, which is often called the “sig figs” method for reporting uncertainty. Since our uncertainties will be determined with higher precision than their order of magnitude, we will not be using this shorthand method in this course, and you will be expected to explicitly write the uncertainty of your measured quantities, either in the form of Eq. ii.1 or as a separate column entry in a table. However, you should be aware of this shorthand since it does get used, though typically outside of formal scientific literature.

Aside from its lack of specificity, an additional drawback of the sig figs method for reporting uncertainties is that all too often it leads to laziness and people reporting numbers with implicit uncertainties far better than are actually merited. Your author starts to become suspicious that this might be happening when measurements of continuous quantities are reported to 4 or more digits, particularly by non-scientists. At or after the 4th digit, one has to think seriously about things such as the calibration and resolution of measurement equipment, thermal expansion of tape measures and rulers, finite response time and jitter of timing systems, the linearity and stability of spring constants, surface roughness and cleanliness, not to mention whether it makes sense at all to define the quantity you’re measuring to that scale.

Example ii.1 Your author just looked at espn.com and noticed that they report the speeds of NASCAR racers to 6 digits. They claim that, for instance, Kyle Busch just completed a lap with an average speed of 126.648 mph. Can you think of reasons to suspect that some (perhaps half) of these digits should not be believed? Hint: was the length of the track even known to 6 digits at that particular time on that particular day [10]?

ii.1.3 Accuracy and Precision

In physics and other sciences, the words *accuracy* and *precision* mean different things, and it is important to distinguish between them. The *accuracy* of a measurement is how close the measured value is to the true value of the quantity being measured. If the true value is within the uncertainty that is reported, we find that the measurement was accurate.

Estimating the accuracy of a measurement is notoriously difficult without knowing the true value. The standards that must be met to produce quantitative accuracy estimates vary from field to field, but they generally consist of trying to estimate the size of the impact of every possible source of error.

One cheap way to make a measurement that won't be inaccurate is to construct the measurement poorly on purpose so that the uncertainty is gigantic and is thereby highly likely to overlap with the true value. However, this illustrates the point that accuracy is not very useful without another key ingredient of a good measurement: precision.

The *precision* of a measurement is how small the range is that a statistical spread of repeated measurements will fall into. The precision tells us nothing about the accuracy of a measurement, and is determined entirely without knowing the true value of the quantity being measured. Measurement precision is often determined by the statistical spread of repeated measurements, and it will be fairly standard in this course to use the standard deviation of a collection of repeated measurements to set the precision of the reported measured value (see § ii.1.6 for a more sophisticated treatment). However, the resolution of the measurement tool itself could be larger than this spread, in which case the quoted precision will be dominated by the instrument resolution.

Exercise ii.1 A researcher needs to determine the diameter of a 10 cm long quartz rod to make sure it will fit the mirror mounts for an optical cavity. The calipers used have a digital display whose most-precise digit is in the 0.01 mm place. 10 measurements along the length of the rod all yield the same reading on the display, 5.98 mm. It is clear that the measured best value is $d_{\text{best}} = 5.98 \text{ mm}$, but how can the uncertainty δd of the measurement be determined?

ii.1.4 Computer use and too many digits

A common mistake that students make in reporting measured values is to have too many (*way* too many) digits on their numbers. After all, the computer will report a measured value often to 16-bit precision, which gives a relative precision of 10^{-5} . However, just because a

computer gives you a number with 5 digits of precision does not mean that the measurement is accurate at that level. If you have a computer multiply a raw measured value of something by π , for instance, the computer will happily tell you the answer to 50 digits. This may look impressive at first, but if the original number is only measured to 2 digits, all of that extra stuff is nonsense.

For example, if you see that repeated measurements of the same quantity fluctuate at about the 3rd decimal place, there is not going to be much useful information in the 8th decimal place and it should probably not find its way into your report in any form. In this case, it would make sense to hang on to maybe 4 or 5 digits during the calculations and for making tables of your raw data. However, the uncertainty is likely to be in the 3rd digit in the end, in which case you will be throwing out everything after the 3rd digit in your final reported number and there is no reason to keep hauling those 8th digits around, cluttering up your spreadsheets and implying an unrealistic uncertainty in your numbers. If you keep things simple, you will find that the physics is easier to see!

ii.1.5 Sources of uncertainty

There are many factors that can contribute to uncertainty in measured quantities. These sources are often separated into two types, *systematic uncertainty* and *statistical uncertainty*. This is a slight oversimplification, but for our purposes in this course, sources of statistical uncertainty tend to produce a random distribution of data points about the mean upon repeated measurements of the same quantity. As such, *statistical uncertainty* affects the *precision* of measured values, but not the *accuracy*.

Systematic uncertainty, on the other hand, affects all of the measured data points in the same way and therefore does not contribute to the statistical spread. *Systematic uncertainty* limits the *accuracy* of a measurement, but not the *precision* of the measured value. If you need to compare your measured value to a known true value (for instance, perhaps in a measurement of g), you will need to consider systematic effects, particularly if you find that your measurement was inaccurate (the true value does not fall within your uncertainty of your measured best value).

However, we will primarily be concerned with quantitative assessments of statistical uncertainty in this course. To reiterate an earlier point, you are likely to encounter two main types of statistical uncertainty in this course, those due to *finite instrument resolution* and those due to “noise” sources that cause repeated measurements of the same quantity to fluctuate. The quantitative method for combining multiple sources of uncorrelated uncertainties is covered in section ii.2.

ii.1.6 Estimation of Statistical Uncertainty in a Mean

One way to estimate the statistical uncertainty in a measurement is to repeat the measurement many times and to look at the spread in measured points. This method is only applicable in cases where the precision is limited by statistics (instead of, for instance, instrument resolution), but will be commonly encountered and so we provide a summary of

the procedure here.

Let us assume we have a set of N data points x_i that all measure some quantity x . If we do not have a good estimate for the uncertainty in each x_i , we can still combine them to come up with a best value and uncertainty in x by looking at their statistics.

For our purposes in this course, we may assume $x_{\text{best}} = \bar{x}$, which is to say that the best value for our measurement of x is the mean of our measured points

$$\bar{x} = \frac{1}{N} \sum_{i=1}^N x_i. \quad (\text{ii.11})$$

One commonly used method for estimating the uncertainty in our knowledge of x is to use the *standard deviation* (σ_x) of the collection of points x_i . The standard deviation is a measure of the spread of points around a mean value. In our case, we should use the so-called *sample* standard deviation¹, given by

$$\sigma_x \equiv \sqrt{\frac{1}{N-1} \sum_{i=1}^N (x_i - \bar{x})^2}. \quad (\text{ii.12})$$

The reason we divide by $N - 1$ instead of N is that \bar{x} was determined from the data points themselves and not independently. In Microsoft Excel, the functions `STDEV()` and `STDEV.S()` both calculate the sample standard deviation using the formula above and you may use either one if you don't want to enter that formula manually.

While it is probably okay in most cases in this course to use the sample standard deviation as an estimate of the statistical uncertainty in the mean, there is something about this that is missing. Specifically, the problem with using $\delta x = \sigma_x$ is that it does not really get smaller as you collect more data. However, if we take 100 times as many data points as we had and they have the same spread as our original data set, we should be able to use this to come up with a significantly better measurement of x since we get to average over 100 times as many individual data points. Specifically, we should get a statistical uncertainty that is 10 times smaller if we take 100 times as many data points, which fact is evident when we use the following formula to calculate our statistical uncertainty:

$$\delta x = \frac{\sigma_x}{\sqrt{N}} = \frac{1}{\sqrt{N}} \sqrt{\frac{1}{N-1} \sum_{i=1}^N (x_i - \bar{x})^2}. \quad (\text{ii.13})$$

You may apply Eq. ii.13 anytime you are trying to estimate the statistical uncertainty in the mean of a collection of data points based only on the distribution of those points.

ii.1.7 Summary

When writing your lab report, you may at times choose to include *raw data* in your report. This will likely take the form of a table or plot of some kind. Raw data does not need to have

¹There is also something called a *population* standard deviation, which differs from Eq. ii.12 in that the factor of $1/(N-1)$ is replaced by $1/N$. The population standard deviation is appropriate in cases where the mean of the parent distribution is determined independently from the data.

explicit uncertainties for each entry unless you are specifically asked to provide it. However, even your raw data must have units labeled. This can be done in column headers or plot axis labels, but there should not be any room for ambiguity on this point.

- Every single number in your report that describes a quantity that has units must have its units clearly labeled in your report.

When reporting the results of measurements in your report (as opposed to just showing examples of raw data), you will be expected to report the measured best value and the uncertainty. When you quote the final measured value of a quantity in your report, be sure that

- You report the measured best value and the uncertainty: $q = q_{\text{best}} \pm \delta q$
- You include proper units
- The measured best value and the uncertainty are written with the same absolute precision
- The uncertainty has no more than two significant digits

ii.2 Propagation of uncertainties

Fairly often in the laboratory we will be measuring many different quantities and combining those measurements together in some mathematical way to come up with a measured value for a composite quantity. For instance, let's say we wanted to measure the average velocity of a glider on an air track (Fig. 1.1) by using a stopwatch to measure the time t it takes the glider to travel some distance x . Using the guidelines above, we will have assigned an uncertainty to each of these quantities, so we want to know how to turn our measured values for the parameters $x_{\text{best}} \pm \delta x$ and $t_{\text{best}} \pm \delta t$ into a measured value for the composite quantity, the average velocity $v = v_{\text{best}} \pm \delta v$.

The way we do this is by using the functional form of how the composite quantity depends upon the input parameters to mathematically determine the resulting uncertainty in the composite quantity. It is important to use the following methods only in the cases where the uncertainties are uncorrelated, so be sure that the uncertainties are generated by physically independent mechanisms (statistical uncertainties typically fall firmly into this category).

We will write the expression relating the uncertainty δf of some composite quantity f to the uncertainties $(\delta x, \dots, \delta z)$ of the parameters used to compute $f = f(x, \dots, z)$ without proof or derivation (see, e.g., [1]):

$$\delta f = \sqrt{\left(\frac{\partial f}{\partial x} \delta x\right)^2 + \dots + \left(\frac{\partial f}{\partial z} \delta z\right)^2} \Big|_{x_{\text{best}}, \dots, z_{\text{best}}} \quad (\text{ii.14})$$

where the vertical line on the right side instructs us to evaluate the resulting expression at $x = x_{\text{best}}, \dots, z = z_{\text{best}}$.²

If you are not familiar with the notation of those derivatives ($\partial f / \partial x$), they are called *partial* derivatives and simply instruct you to treat everything except the variable of differentiation as a constant when taking the derivative. If we come back to our example of the measurement of the average velocity of a glider, we first identify $f = v = x/t$. We need to determine δv in terms of x_{best} , δx , t_{best} , and δt . We can begin by taking the partial derivatives:

$$\frac{\partial v}{\partial x} = \frac{\partial}{\partial x} \left(\frac{x}{t} \right) = \frac{1}{t} \quad (\text{ii.15})$$

and

$$\frac{\partial v}{\partial t} = \frac{\partial}{\partial t} \left(\frac{x}{t} \right) = -\frac{x}{t^2}. \quad (\text{ii.16})$$

This gives us

$$\begin{aligned} \delta v &= \sqrt{\left(\frac{1}{t} \delta x \right)^2 + \left(-\frac{x}{t^2} \delta t \right)^2} \Big|_{x_{\text{best}}, t_{\text{best}}} \\ &= \frac{1}{\sqrt{t^2}} \sqrt{(\delta x)^2 + \frac{x^2}{t^2} (\delta t)^2} \Big|_{x_{\text{best}}, t_{\text{best}}} \\ &= \sqrt{\frac{x^2}{t^2}} \sqrt{\left(\frac{\delta x}{x} \right)^2 + \left(\frac{\delta t}{t} \right)^2} \Big|_{x_{\text{best}}, t_{\text{best}}}. \end{aligned} \quad (\text{ii.17})$$

Normally, we would say that $\sqrt{x^2/t^2} = \pm x/t$ to reflect the two solutions of that equation. However, we have defined all uncertainties (δq in Eq. ii.1) to be positive, so here we take the absolute value:

$$\sqrt{\frac{x^2}{t^2}} = \left| \frac{x}{t} \right|. \quad (\text{ii.18})$$

We can now evaluate our expression at $x = x_{\text{best}}$ and $t = t_{\text{best}}$ to give us

$$\delta v = \left| \frac{x_{\text{best}}}{t_{\text{best}}} \right| \sqrt{\left(\frac{\delta x}{x_{\text{best}}} \right)^2 + \left(\frac{\delta t}{t_{\text{best}}} \right)^2}. \quad (\text{ii.19})$$

We have identified $v_{\text{best}} = x_{\text{best}}/t_{\text{best}}$, so dividing both sides by the absolute value of this quantity and noting that we can add an absolute value sign to both terms under the radical since they are squared anyway gives us the following symmetric-looking form:

$$\frac{\delta v}{|v_{\text{best}}|} = \sqrt{\left(\frac{\delta x}{|x_{\text{best}}|} \right)^2 + \left(\frac{\delta t}{|t_{\text{best}}|} \right)^2}. \quad (\text{ii.20})$$

²The assumption we are going to invoke here is that $f_{\text{best}} = f(x_{\text{best}}, \dots, z_{\text{best}})$. This is sometimes not strictly correct, but will serve for the purposes of this course.

The quantity $\delta q/|q_{\text{best}}|$ is called the *fractional uncertainty* or *relative uncertainty* of some measurement of q , so we can restate Eq. ii.20 in words by saying that the fractional uncertainty in a ratio of two quantities is given by the quadrature sum of the fractional uncertainties of the two quantities.

ii.2.1 Specific formulas

While the form given in Eq. ii.14 is sufficiently general to allow it to be applied directly for every case encountered in this course, we can summarize some of the most common results that can be derived from it as follows.

- Measured quantity times an exact number: $f = Ax$

$$\delta f = |A| \delta x \quad (\text{ii.21})$$

- Sums and differences (they follow the same rule): $f = x + y - z + \dots$

$$\delta f = \sqrt{(\delta x)^2 + (\delta y)^2 + (\delta z)^2 + \dots} \quad (\text{ii.22})$$

- Products and ratios (they follow the same rule): $f = \frac{x \times \dots \times z}{u \times \dots \times w}$

$$\frac{\delta f}{|f_{\text{best}}|} = \sqrt{\left(\frac{\delta x}{|x_{\text{best}}|}\right)^2 + \dots + \left(\frac{\delta z}{|z_{\text{best}}|}\right)^2 + \left(\frac{\delta u}{|u_{\text{best}}|}\right)^2 + \dots + \left(\frac{\delta w}{|w_{\text{best}}|}\right)^2} \quad (\text{ii.23})$$

- Measured quantity raised to an exact number power: $f = Ax^n$

$$\frac{\delta f}{|f_{\text{best}}|} = |n| \frac{\delta x}{|x|} \quad (\text{ii.24})$$

- Exponential with measured quantity in the exponent $f = Ae^{ax}$

$$\frac{\delta f}{|f_{\text{best}}|} = |a| \delta x \quad (\text{ii.25})$$

You may recognize that Eq. ii.20 is a special case of Eq. ii.23, as is Eq. ii.21. And, of course, all of these are special cases of Eq. ii.14. These cases are not the only possibilities for functional forms of the relationships between measured values, but they are the most common for us in this course. You should be sure to keep in mind that these formulas are valid only for uncertainties that are uncorrelated.

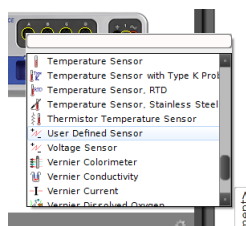
Experiment 0: Sensor Calibration and Linear Regression

Your first experiment is intended to familiarize you with some of the basics of the DAQ system. There will not be a formal report due next week. Instead, there is a short set of homework problems (“Homework 0”) at the end of this chapter that you will complete and turn in online. Be sure to read through the homework problems to make sure you have saved all of the data you will need to complete Homework 0.

For many experiments in this course, you will be using a force sensor similar to the one shown in Fig. 0.1. This device is designed to output a voltage that is proportional to the force applied between the hook and the body of the sensor. The DIN cable allows your computer to read this voltage via the 850 interface. If **Force Sensor** is selected as the type of input, the 850 will assume it knows how to convert voltage to force and will simply read in units of force (N). However, to illustrate how the interface really works, we will not trust this conversion implicitly and will instead be looking at the raw voltage from the sensor.

The process of determining how voltage corresponds to force is an example of a process called *calibration*, and Experiment 0 walks you through a manual calibration procedure for this force sensor. This procedure is not the same as the **Calibration** feature in Capstone, and the manual calibration described here will be far more accurate than that supplied by the manufacturer. Plastic deformations of the sensor components, changes in ambient conditions, and electrical offset sources may all change between experiments, so to increase the *accuracy* of your force measurements, you may consider checking the sensor calibration each week that it is used. Your TA may or may not ask you to do this explicitly.

0.1 Hardware setup



To set up the force sensor to read its raw voltage, start your DAQ system using the instructions in §i.2 and connect the DIN cable to one of the Analog Inputs of the 850. Set up the 850 to read voltage from the appropriate analog input (see §i.3) by choosing **User Defined Sensor** from the drop-down menu of the appropriate input (**Do not choose Force Sensor**), at which point your **Hardware Setup** pane will show a little electricity-looking icon  with a line to the channel you chose.

To test that you have set up the connection correctly and that there are no software or hardware errors happening to keep you from reading the sensor correctly, use the **Scope**

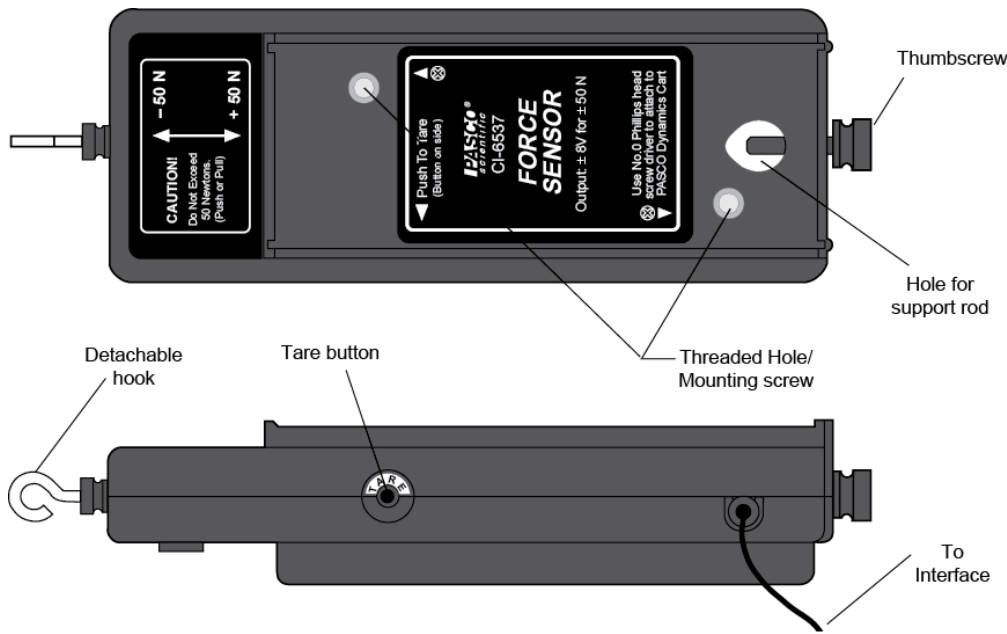


Figure 0.1: PASCO CI-6537 force sensor. This transducer can sense both tension and compression applied between the hook and the body of the unit, up to 50 N in either mode.

feature in **Fast Monitor Mode** to see that the voltage changes when you push or pull a little on the hook. An overview of how to use the **Scope** feature can be found in section i.4. If you cannot see any signal from your sensor on the screen, go back through these steps carefully to see if you missed something; if not, ask your TA for help.

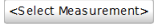
0.2 Manual calibration procedure

Once your DAQ is able to read voltage from the force sensor you are ready to begin the calibration. The procedure will be to attempt to zero, or *tare* the sensor, and then to hang known weights from the hook while monitoring the voltage. You will record several readings, then use Excel or whatever other program you like to fit a line to the data. The slope and offset of this line is the calibration curve for your sensor. The offset will almost certainly not be zero, which will tell you something about how well the tare procedure worked.

0.2.1 Measurement Apparatus

First, attach the force sensor to a horizontal post so that the hook hangs vertically downward, appropriate for hanging weights from it. The best software tool for measuring the voltage is probably the **Digits** feature in the **Displays** palette. If the **Displays** palette is missing, see section i.2 for instructions on how to get it back onto the screen. You can configure your **Digits** display to show the voltage produced



by the sensor by choosing **User Defined (V)** from the drop-down menu of the  button.



Your calibration of the force sensor will be capable of accounting for an offset in the reading caused by a nonzero voltage reading with no applied force. However, it is useful to know how to *tare* the sensor in hardware for calibration and making differential measurements. Using **Fast Monitor Mode** with your **Digits** display, you should be able to read the offset voltage in real-time by clicking **Monitor** in the controls palette.

The voltage you see displayed will fluctuate around some value that is not necessarily zero. You can define this offset to be 0 V by pressing the tare button on the side of the sensor, shown in Fig. 0.1. The voltage reading will now be centered near zero. Your calibration will tell you how well this procedure worked when we produce a fit line.

0.2.2 Changing the Display Precision

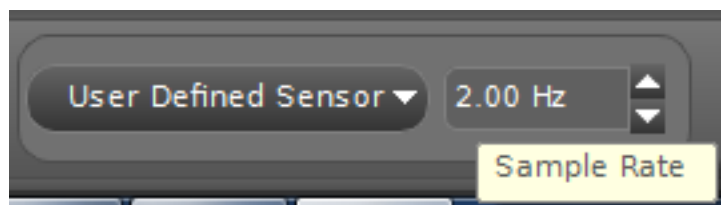
You may notice that your sensor reading fluctuates around as a function of time, even after taring the sensor. This gives you some idea of the *precision of the sensor*, which determines the minimum size of the steps between distinct values. You will need to observe and record the magnitude of fluctuations like this in various sensor readings throughout the course, because they are an important part of your uncertainty determination for measured quantities.

Aside from the precision of the sensor, it is possible that Capstone is only displaying a subset of the digits it actually gets from the sensor. This is called the *display precision* of your DAQ. It will be crucial in later labs to be able to change the display precision to avoid becoming limited by this (which is known as *quantization error*).

To change the display precision, mouse-over the **Digits** display to pop up the menu bar at the top. On the far left side of the menu bar, there will be two buttons to control the display precision, one to increase it and one to reduce it. Click each one a few times while watching your sensor reading to get a feel for how the system works. Determine the maximum number of digits that Capstone is willing to display by increasing the precision until the button no longer changes the display. Typically, the ideal display precision is just at the point where the reading fluctuations show up in the last digit.



Next, we will record the voltage reading for a series of known weights hung from the hook. To get a steady reading, it will be helpful to turn down the sample rate to something on the order of a couple of times per second. This can be done in the **Controls** palette at the bottom of the screen.



	A	B	C	D
1				
2	Mass (g)		Sensor Voltage (V)	
3	0		0.0004	
4	9		-0.005	
5	12		-0.007	
6	15		-0.009	
7	18		-0.011	
8	21		-0.013	
9	24		-0.015	
10	27		-0.017	
11	30		-0.019	
12				
13				

Figure 0.2: Some fake data entered into Excel in two columns with an empty column next to the mass column. Note the unit labels on the column header.

0.2.3 Entering and Plotting Data in Excel

Next, we will be collecting our data in a table, so start a new workbook in Excel and record the voltage reading and mass of a series of weights hung from the force sensor hook. Now is probably a good time to get in the habit of labeling the columns of tables with descriptive labels *and appropriate units*, as shown in Fig. 0.2. Since you will be converting mass to force using $F = mg$, it is a good idea to leave a blank column next to the column where masses are recorded so that we can make Excel do the work of filling in the force column.

To have excel fill in the force column with the calculated force in N, highlight the top cell of the new column (right next to the cell with your first mass value entered) and enter the formula you want Excel to execute. Formulas in Excel begin with an = sign, followed by the mathematical expression you want, where variables can be entered either manually, or through reference to the cell address in which the variable value has been entered.

For instance, for the data shown in Fig. 0.2, to make cell B3 display the gravitational force (in N) acting on the mass entered in cell A3, one could type in “=A3*0.001*9.80” and hit enter. In this case, the factor of 0.001 comes from converting g into kg and the factor of 9.80 is for $g = 9.80 \text{ m/s}^2$. The formula can now be copied down the column by highlighting the cell with the formula, grabbing the bottom right corner of the cell, and dragging it down the column. Excel will recognize that “A3” should be changed to “A4” in the formula for cell B4 and so forth.

Once you have two columns recording the applied force and the output voltage, you can plot your data. Excel calls this a “chart” (because Excel is made for businesspeople) and you can create one by highlighting the two columns with your data and choosing **Scatter**

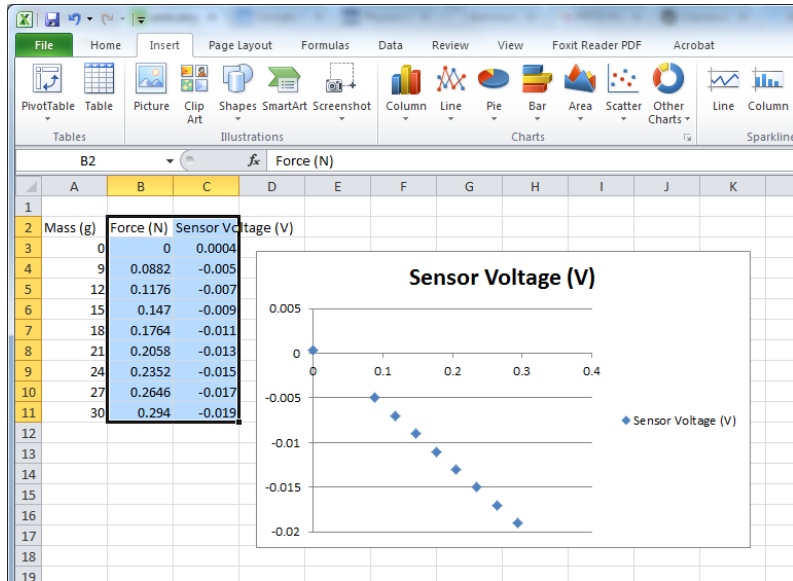


Figure 0.3: Excel has created a terrible-looking plot. In the opinion of your author, what Excel lacks in the appearance of its plots it makes up for in ease-of-use for students, which is why it is recommended here. If you have other programs you prefer to do your own data analysis, feel free to use them.

from the **Insert → Charts** menu or something similar in whatever version of Excel you are using.

If you had Excel make a scatter chart for you in this way, your workbook probably looks similar to that in Fig. 0.3. This plot has no axis labels, so it takes a little looking to even figure out which column was used for the y -axis and which for the x -axis. I would recommend that the first thing you do when creating a plot in Excel is to label the axes and units for those axes. How this is done will depend upon your version of Excel, but you're probably looking for something like **Chart Tools → Layout**. Using the features you have at your disposal and a bit of web searching, you can hopefully figure out how to make a reasonably clear plot of your data, such as that shown in Fig. 0.4. All plots that end up in your report must have axis labels and appropriate units, as well as a figure caption with a title, description of what is displayed, and possibly a fit line equation. Instructions for how to incorporate plots into your reports can be found in Appendix B.

0.2.4 Linear Fit to Numerical Data

Next, we would like to have Excel calculate the equation of the best fit line to our data. To do this, you will have Excel “add a trendline” to your data. Since we expect the voltage to be linear in the applied force, we are looking for an expression in the form

$$V = aF + b \quad (0.1)$$

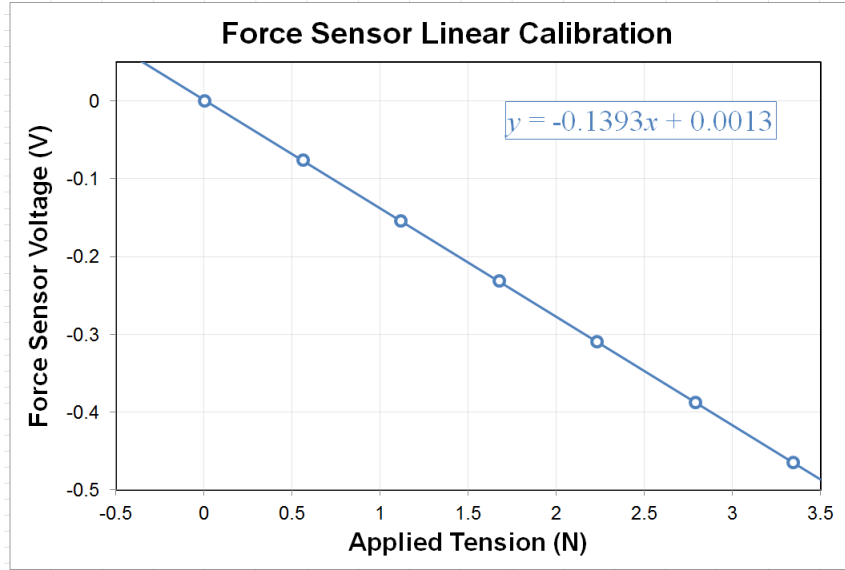


Figure 0.4: A fairly clear plot of some data shown with a linear fit line. Note the title, axis labels, units, and fit line equation are all clearly visible, and none of the tick labels or text is overlapped with anything that makes it difficult to read.

to relate the measured voltage V to the applied tension F in terms of the slope a and offset b of our sensor. Note that a and b will have units, that they constitute the results of a measurement, and that they need to have a quantitative uncertainty associated with them.

We will use Excel to calculate a and b for us by having it add a linear trendline (a.k.a. a linear best fit) to the data and display its equation on the chart, as shown in Fig. 0.4. The procedure for adding a trendline will vary from version to version of Excel, but right-clicking on one of the data points or going to **Chart Tools → Layout** are likely places for this option to be hiding. In the trendline options, remember that we want a linear trendline, we do not want the offset set to a particular value (so it will remain a fitting parameter; your sensor may still have an offset despite the tare procedure), and we want the equation displayed on the chart.

A guide to making figures and captioning them using Word and Excel by Julio S. Rodriguez, Jr. and Anthony Ransford can be found in Appendix B.

0.2.5 Calculating Uncertainties in a Linear Fit with Excel

For the example data of Fig. 0.4, we find that the linear fit line is described by the equation $y = -0.1393x + 0.0013$. Comparing this to Eq. 0.1, we are tempted to identify $a = -0.1393 \text{ V/N}$ and $b = 0.0013 \text{ V}$ and declare victory. However, we still need the uncertainty in the measured values (δa and δb) used to generate this fit before we can report the results of a measurement. As is always the case, we cannot claim we measured something (in this case, the sensor calibration) without also describing the uncertainty associated with

this measurement.

One question that we can ask ourselves is “why is there an uncertainty at all? After all, there is a single, unique fit line that is the very best fit to these data. Why would that have an uncertainty?” This is a very good question. The answer is that the scatter in the data will effectively permit a series of different lines that all essentially model the data to the same degree. For data with a lot of scatter, the “goodness of fit” of the best fit line is only a very tiny amount “more good” than a whole collection of lines with similar slopes and offsets, so the uncertainty will be large. For data with very little scatter, a small change in the slope or offset will substantially degrade the “goodness of fit,” and the uncertainty is correspondingly small. Excel provides you with the quantitative tools to evaluate statements like this in a scientific manner, and we will use this throughout the term.

The trendline feature in Excel was a quick and easy way to get the best-fit slope and intercept from a least-squares fit, but it gives us no quantitative way to determine the uncertainty in the slope and intercept that it found. There are two ways your author knows of to get the uncertainties in linear fits in Excel. The first is to use an Excel function called **LINEST** that returns an array and is powerful, but not incredibly user-friendly. The other way is to use the **Regression** tool.

The regression analysis tool will take as its input your two columns of data and give you lots of information about how well your data can be described by a linear relationship. For instance, it will calculate the same equation for the best fit line that we got from the **Add Trendline** feature, but it will provide more digits, and (most importantly) it will provide the uncertainties in the fit parameters. These uncertainties are based entirely on the scatter in your data points around the fit line and therefore do not contain any information about systematic uncertainties. If your data span a range much larger than the resolution of your measurement tool (probably true in this case), the scatter in your data points already reflects this resolution limit implicitly.¹

To perform a linear regression analysis in Excel, look for the regression tool somewhere like **Data → Data Analysis** or **Tools → Data Analysis**. One of the data analysis tools should be **Regression**. You will enter the location of your x and y data, and I would recommend having the output option set to new worksheet, such as shown in Fig. 0.5.

Figure 0.6 shows the results of the linear regression analysis, along with some highlighting of the parameters we were interested in calculating. The regression tool gives the uncertainties in the slope and intercept in the column called *Standard Error*.

At this point, it would again be tempting to think we are done and write $a = (-0.139320505 \pm 0.0000776577)$ V/N and $b = (0.001334872 \pm 0.000181541)$ V and call it a day. After all, we’ve got the uncertainties and the units, right? The problem with this is that the *precision* of these reported numbers is much, much better than the uncertainty indicates it should be. The statistical uncertainty given by, for instance, $\delta b = 0.000181541$ V tells us immediately that the last four or five digits of this number are meaningless. The data itself fluctuates at

¹If your data do not span a range larger than your instrument resolution, all of your data points are probably identical, and the instrument resolution is likely the largest source of statistical uncertainty in this case.

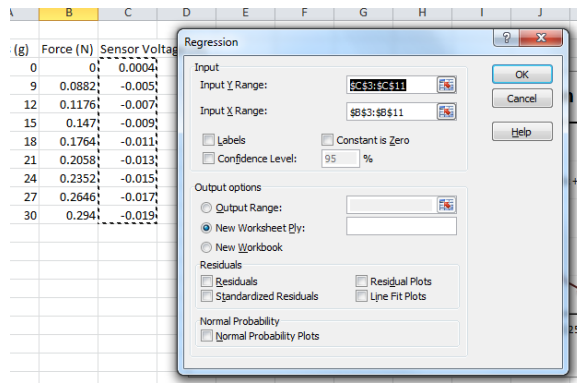


Figure 0.5: The linear regression tool in some version of Excel. Your version may look a little different, but the basics will be the same.

A	B	C	D	E	F	G	H	I
1 SUMMARY OUTPUT								
2								
3 Regression Statistics								
4 Multiple R	0.999999068							
5 R Square	0.999998136							
6 Adjusted R Square	0.999997825							
7 Standard Error	0.000280235							
8 Observations	8							
9								
10 ANOVA								
11	df	SS	MS	F	Significance F			
12 Regression	1	0.252758744	0.252758744	3218554.999	2.0245E-18			
13 Residual	6	4.7119E-07	7.85317E-08					
14 Total	7	0.252759215						
15								
16	Coefficients	Standard Error	t Stat	P-value	Lower 95%	Upper 95%	Lower 95.0%	Upper 95.0%
17 Intercept	0.001334872	0.000181541	7.352994048	0.000323882	0.000890656	0.001779087	0.000890656	0.001779087
18 X Variable 1	0.139320505	7.76577E-05	-1794.033166	2.0245E-18	-0.139510527	-0.139130484	-0.139510527	-0.139130484

intercept intercept uncertainty
linear slope slope uncertainty

Figure 0.6: The results of using the linear regression tool in Excel. The best-fit line slope and intercept are highlighted, along with their uncertainties.

a level that is way too large for us to say anything about b on the 10^{-9} V scale. You can always keep just one nonzero digit on an uncertainty and not get yourself into any trouble in this course, so that would give us $\delta b = 0.0002$ V and $\delta a = 0.00008$ V/N. The best values should then be written with the same absolute precision, and we have our final result for the measured calibration of this force sensor:

$$V = aF + b \quad (0.2)$$

$$\begin{aligned} a &= (-139.32 \pm 0.08) \text{ mV/N} \\ b &= (1.3 \pm 0.2) \text{ mV} \end{aligned} \quad (0.3)$$

As a quick sanity check on these measured results, we note that the last digit of a_{best} is in the 0.01 mV/N place, which is the same position as the last digit in δa , as it should be. The same is true for b : the last digit we quote for b is in the 0.1 mV place, as is the last digit of δb .

0.3 Homework 0

Read through these problems before you leave the lab to ensure that you have saved all of the data you will need. This short exercise is designed to prepare you for your first real experiment, Experiment 1. Your completed homework must be a short document that is typed and formatted using a computer. During your lab section for Experiment 0, your TA will give you a due date and instructions for how to turn in your completed homework. You may find that the information in Appendix B is useful for completing your homework, so be sure to take a look at Appendix B.

1. You will need a cover page for your reports in this course, so now is a good time to make a template for yourself you can reuse later. Make a cover sheet that includes the following information:
 - Experiment number and title. This week, this will be something like “Experiment 0: Sensor Calibration and Linear Regression”
 - your name and UID
 - the date the lab was performed
 - your lab section (for instance, “Wednesday 9am.”)
 - your TA’s name
 - your lab partners’ names
2. A student is trying to measure the constant acceleration of some object in the lab by measuring the change in velocity of the object over some fixed time interval. Repetition of the experiment many times and careful error analysis has resulted in a measurement

of the velocity change ($\Delta v = \Delta v_{\text{best}} \pm \delta \Delta v$) and the time duration ($\Delta t = \Delta t_{\text{best}} \pm \delta \Delta t$) with uncertainties. Knowing that the measured acceleration is given by $a = \Delta v / \Delta t$, what is the proper expression for the uncertainty in the measured acceleration, δa ?

3. What is the maximum number of digits Capstone will display (recall §0.2.2)? If the sensor precision is exactly 4 digits and you take data with 10 displayed digits, describe what your actual measurement precision is and what you would expect to see in digits 5 through 10. If the display precision is turned down far enough, it may be possible to completely eliminate sensor fluctuations. Describe why doing this might not be the best idea for taking good data.
4. Present your final plotted results of the calibration procedure as a figure (include the data, the fit line, and the fit line equation on the plot). You should take the time to make the plot look clear and have all of the axes labeled. Present a brief line or two of text that could be used as a figure caption for this plot.
5. State the results of your calibration (with uncertainty from your fit). This may require a sentence or two of explanation to clearly define your parameters, but you do not need to describe the whole procedure of the experiment. Your fit should have included a possible nonzero y -intercept. What does your value for this intercept tell you about the effectiveness of the taring procedure (§0.2.1)?
6. Equations 0.1 and 0.3 tell us how to convert a known tension F into a predicted output voltage of the sensor V (including the uncertainty in this conversion), but to use this as a “force sensor,” we really want to know how to convert V into F , right? Use the measured values of $a_{\text{best}} \pm \delta a$ and $b_{\text{best}} \pm \delta b$ that you presented in your response to the previous question to rewrite your calibration curve in the form $F = cV + d$, including the appropriate uncertainties in c and d . Hint: look at Eq. ii.23.
7. You have been provided with information on how to access the syllabus for this course. Read the syllabus, paying special attention to the text in red. Consider a case where two students, Frankie Fivefingers and Avril Armstrong are in different sections of Physics 4AL this quarter. At the end of the quarter, they both have an average numerical score of 84, but Frankie gets a B+ in the course while Avril gets a C+. How is this possible? What can you conclude about the mean numerical scores of the other students in their sections?

Experiment 1: Uniform Acceleration

Experiment 1 is the first experiment for which you will be expected to submit a full-credit report. Your report is due about a week from now, and your TA or instructor will give you specific instructions on how to submit your report as well as when the due date is.

In Experiment 1, you will be measuring the acceleration of a composite system composed of some masses connected by a string passing over a pulley. The position of the accelerating masses and string will be monitored as a function of time by the DAQ system, and these data will be recorded for a series of 5 different masses. A bit of data analysis is required to produce a plot that can be fit to a straight line to obtain a measurement of the acceleration. You should already have experience working with the DAQ (chapter i), producing linear fits with uncertainties (§0.2.4 & §0.2.5) and doing a proper uncertainty analysis of your complete measurement (chapter ii), so you may find those sections to be helpful references for Experiment 1.

In order to measure constant acceleration, the friction between the accelerating object and everything that is stationary must be kept to a minimum. While there will still be some residual friction (as well as drag forces), the air track setup depicted in Fig. 1.1 does a good job of minimizing its effect. A “glider” placed on this track will float along on a cushion of air when the pump is pressurizing the track, exhibiting nearly-ideal linear motion. The glider and air track setup will be used for many experiments in this course.

Fig. 1.2 shows the air track set up for Experiment 1. A glider with total mass M is supported on a cushion of air on a level air track and is attached to a hanging weight (mass m) by a string that passes over a pulley.

The equation of motion for this system is given by:

$$a = \frac{gm}{m + M} \quad (1.1)$$

where a is the acceleration of the glider-string-weight system and g is the earth’s gravitational acceleration for a free-falling body.

In this lab, you will be measuring the acceleration for 5 different values of m (do not exceed $m = 50$ g). Feel free to vary M as well for any of these runs. The acceleration measurement will require that you convert position vs. time data into a measured value for acceleration (with uncertainty, of course!). These position vs. time data will be recorded by the DAQ using a “smart pulley.”

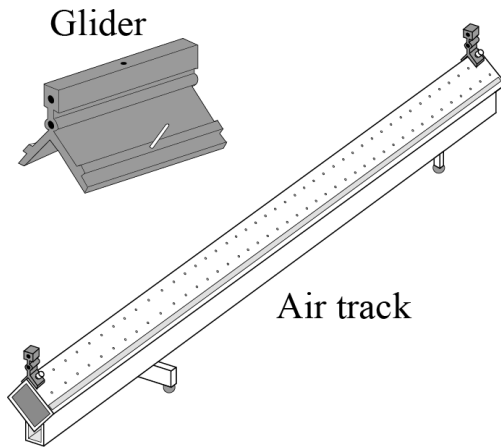


Figure 1.1: Apparatus for linear motion with very low friction. The air track is pressurized by a continuously-flowing pump, causing air to flow out through the array of holes on the surface. When a glider is placed on this track, it moves freely in 1D with very little friction, just like an air-hockey puck.

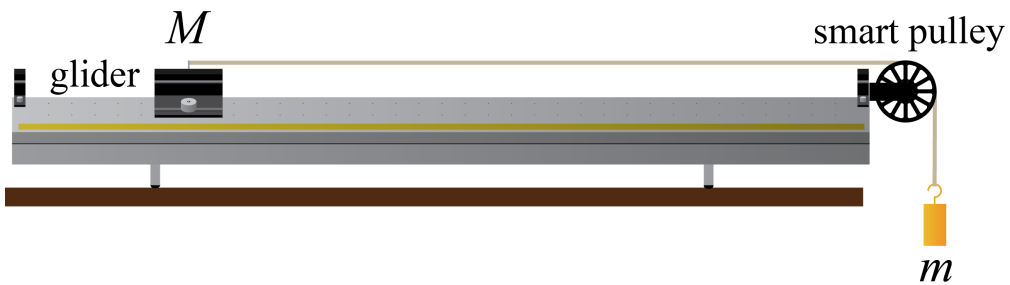


Figure 1.2: Experiment 1 setup. The glider mass can be changed by putting different amounts of weight on its sides, and the hanging mass can be changed by adding more weights with hooks. The smart pulley is attached to the DAQ and records the timing as the spokes pass by a sensor.

1.1 Procedure

In order for Eq. 1.1 to be valid, we have assumed that the air track is level. This is generally not the case, and there will be multiple experiments in this course that use the air track. Your first task is to level the air track. You can accomplish this by placing a glider on the track and turning on the blower. The track itself is not completely flat, so there is really no such thing as “perfectly level” over the whole length of the track, so do the best you can. You will find that the two feet under the cross-bar of the air track (one is visible sticking out from the bottom of Fig. 1.1) can be turned to change their height. Your goal is to get to the point where a free glider won’t move either direction with the blower on.

You will also need to set up your DAQ to work with the smart pulley, so plug the smart pulley cord into a digital channel on the 850, turn it on, and start Capstone. Configure the appropriate channel for **Photogate with Pulley**.

The smart pulley really only has the ability to measure whether or not a wheel spoke is blocking a little infrared LED from shining into a photodiode. The LED and photodiode are set up with a gap between them, which is called a photogate. Every time the photogate goes from being unblocked by a spoke to being blocked by it, the 850 tells Capstone the time stamp for that event, so the raw data in this case is really the time stamp for each time when the photodiode detects a “falling edge.” Therefore, no data is collected if the pulley isn’t moving, or during the time when the spoke is moving but hasn’t yet blocked the photogate. Furthermore, the photogate has no idea which direction the pulley is moving, so you should be careful when interpreting results. You may assume that the linear distance the perimeter of the pulley moves between successive times when the photogate goes from being unblocked to blocked is given by

$$\kappa_{\text{SP}} = (1.50 \pm 0.05) \text{ cm/block.} \quad (1.2)$$

You may notice that Equation 1.2 is given in the form $\kappa_{\text{SP}} = \kappa_{\text{SP,best}} \pm \delta\kappa_{\text{SP}}$, but you are not told whether the uncertainty $\delta\kappa_{\text{SP}}$ should be treated as systematic or statistical in nature. You may take this uncertainty to be statistical for the purposes of your analysis, in which case it will already be taken into account when you do your regression analysis, because this effect will show up as scatter of your data points.

Capstone has the ability to perform some computational tasks on the data and to use its own algorithms and calibration of the hardware to display position, velocity, acceleration, etc. This will be useful for future tasks, but for Experiment 1, you should save the raw data (**Block Count () vs. Time (s)**) and use your own data analysis to convert this into 5 acceleration measurements (with uncertainties, of course!). This is designed to help you understand how to turn raw experimental data into a measured value with uncertainties, where you have full knowledge and control over the algorithms being applied to the raw data.

Fig. 1.3 shows an example with some fake data. It is always helpful to have a visual representation of the data you are collecting in real-time, because this can give you a quick feel for whether something is not set up properly. For this, it might be a good idea to open a **Scope** or **Graph** display to show, for instance, **Linear Speed (m/s) vs. Time (s)**. Since

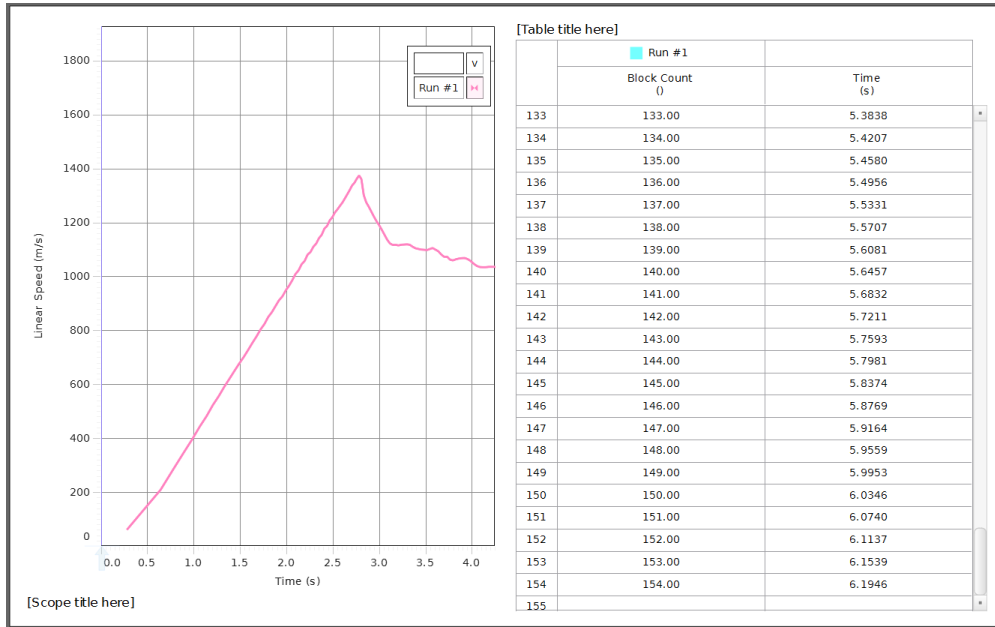


Figure 1.3: Example data from Capstone showing the simultaneous generation of a **Scope** plot qualitatively showing the portion of the data that will be useful and the **Table** that can be used to cut-and-paste your data into Excel for saving and analysis. Note that the **Scope** plot shown here is showing a glider moving at about Mach 4, so don't trust it! It is only a qualitative tool to help you view your data in real-time.

you do not know how Capstone calculates linear speed, you will not use this. The only data you should use will be Block Count () vs. Time (s). The display of speed is only to give you a visual cue of your data. Since you will also be saving your data to analyze it , you will also need to open (simultaneously) a **Table** for collecting your data. Remember, the two columns you will need to generate are Block Count () and Time (s). Do not save a column for Position, Linear Speed, Linear Acceleration, or any other pre-processed quantity. **Continuous Mode** in the **Controls** palette should work for gathering your data. The sample rate seems to have no effect for this hardware.

With your lab partner, you will be saving 5 data sets (each with a different set of masses). Keep in mind that you will need to measure the mass of the glider, so don't forget! Once the DAQ is set up, you should be able to generate a plot something like that shown in Fig. 1.3. The **Scope** plot in that figure shows the point where the velocity stops increasing linearly, which is when the weight hits the floor or the glider hits the pulley, whichever comes first. You may use this plot to decide which data to save (you are only interested in the linear portion). Be sure to increase the number of displayed digits in the table until you are no longer precision limited before exporting your data (look at the Time (s) column in Fig. 1.3). Highlight the data you want to save in the **Table** and copy and paste it into Excel. You should then save it somewhere safe. Each person should get 5 data sets with different masses for m and/or M that are unique. You may use the same masses as your lab partners, but the raw data should be unique for each person.

1.2 Analysis

The data you saved is in the form of something called “Block Number” vs. time. Using Eq. 1.2, you can create a new column for position by simply multiplying block number by $\kappa_{SP,best}$. Remember, you have been instructed to ignore $\delta\kappa_{SP}$ for this analysis since your regression analysis will automatically take this effect into account, so you will really only be using $\kappa_{SP,best}$. Next, you will need to numerically differentiate the position data. To do this, you may calculate a single average velocity for every two position vs. time points using

$$\bar{v}_i = \frac{\Delta x}{\Delta t} = \frac{x_{i+1} - x_i}{t_{i+1} - t_i}. \quad (1.3)$$

Note that since each velocity measurement requires *two* position data points, you will have one fewer data points for velocity than position. The column of velocities you generate now needs a column of times associated with them. Since the formula in Eq. 1.3 gives you the *average* velocity in the time interval between t_i and t_{i+1} , the best time to associate with velocity \bar{v}_i is the average of t_i and t_{i+1} ,

$$\bar{t}_i = \frac{t_i + t_{i+1}}{2}. \quad (1.4)$$

Armed with your two new columns, velocity and time, you can now generate a scatter plot of your data. Be sure to truncate your data to only show the linear portion of your plot.

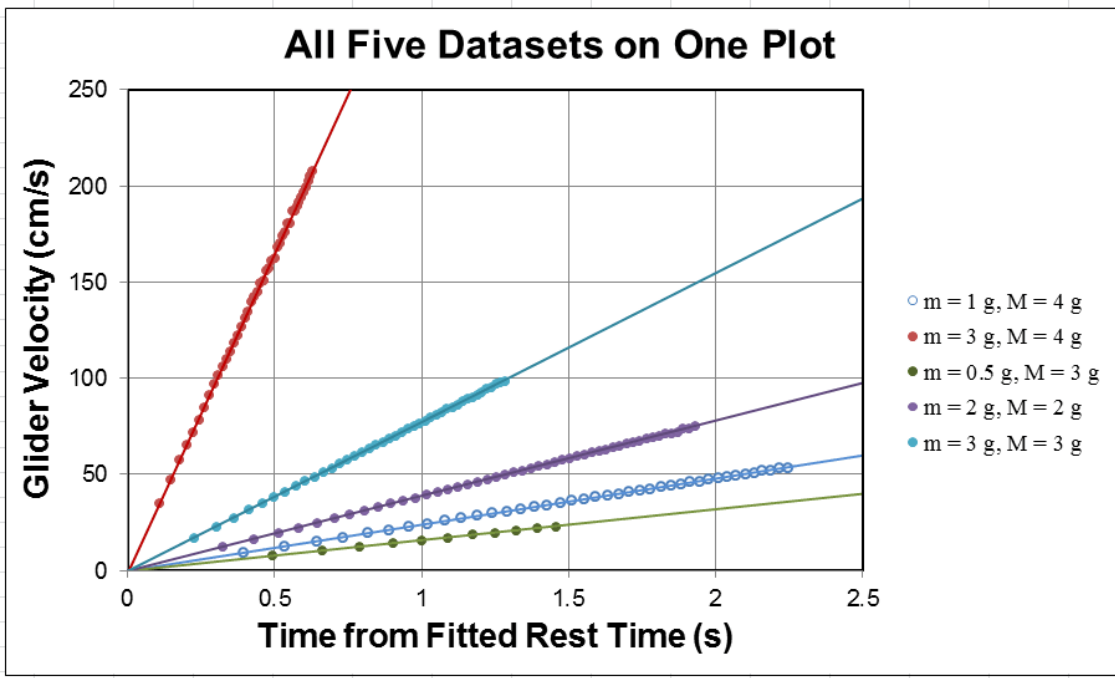


Figure 1.4: An example of five different data sets on one Excel scatter chart. Making the fit lines the same color as the data points lends clarity to what would otherwise be an incredibly cluttered plot. This is fake data with fake units, so please do not try to make your plot look just like this one! The important thing is to make your results as clear as possible.

Using the techniques that were discussed in chapter 0, fit a line to the velocity vs. time for each of your 5 data sets to produce 5 measurements of the acceleration (with uncertainties obtained from the fits). Keep in mind that the reason we are obtaining uncertainties from the fits here is that we expect the uncertainty to be dominated by the *scatter* of the individual data points, not the *systematic* uncertainty of each data points. The fit line uncertainty captures this effect beautifully. Note that since you are only interested in the slope, it is probably best to leave the intercept as a free fitting parameter and then to ignore it since the initial velocity may not have been zero when the spoke crossed the photogate. Compare these measured accelerations to your predicted values.

1.3 Report guidelines

For experiments 1 through 5, your reports will be a single document but will have two sections. The first section will be called the *worksheet*, the second will be called the *presentation mini-report*. The worksheet will contain your main results presented as numbered items. The worksheet section is intended to be a basic report of what you did in the lab and how you analyzed your data to draw conclusions, but does not need to be a self-contained, full lab report (you will be writing full lab reports for experiments 5, 6, and 7 in later weeks). Most of your grade for the worksheet section of your report will be based on your data taking, analysis, and conclusions.

Each week until experiment 5 we will focus on one aspect of a formal written lab report (such as the abstract, or figures, or citations), and you will be asked to produce some example of this aspect for the presentation mini-report section of your assignment. The details of this section will change from week to week and may or may not involve your data. Most of your grade for this section will be based on the degree to which your presentation mini-report is on par with high-quality published scientific presentations in physics journal articles.

This week, the worksheet will be worth 40% of your grade and the presentation mini-report will be worth 60%.

1.3.1 Worksheet guidelines

Your worksheet should contain the following sections

1. Cover Sheet

- experiment number and title
- your name and UID
- the date the lab was performed
- your lab section (for instance, “Monday 3pm”)
- your TA’s name
- your lab partners’ names

2. Plots

Include plots of all five of your data runs showing velocity vs. time and the fit lines. This could be a single plot with five data sets on it or five plots with one data set on each. Report the slope of the fit line for each (with its uncertainty, units, etc.) in a figure caption.

3. Data Table

Report the main results from your experiment in a table such as the one below, where your entries will be from your measurements and analysis. Your table does not need to be exactly like this one, but should contain essentially the same information.

Trial	Hanging mass m_{best} (g)	Glider mass M_{best} (g)	Fit acceleration a_{fit} (m/s ²)	Predicted acceleration a_{predict} (m/s ²)
1	5.0	15.0	0.23 ± 0.01	0.25 ± 0.08
2	4.0	20.0	0.19 ± 0.01	0.20 ± 0.07
3	3.0	25.0	0.100 ± 0.005	0.08 ± 0.07
4	2.0	35.0	0.300 ± 0.006	0.29 ± 0.05
5	1.0	45.0	0.200 ± 0.002	0.30 ± 0.06

4. Derivations

Derive equation 1.1 in this manual as well as your propagation of uncertainties used in the table above.

5. Conclusions

Write a brief discussion of your results. Compare the accelerations you measure from fitting your velocity vs. time data sets to what you would predict from Eq. 1.1 with your measurements for the masses. Do they agree? If not, try to convince your reader that the reason for the disagreement is understood and suggest a way to improve the agreement in a future experiment.

6. Extra Credit (always optional)

Instead of obtaining a measurement of the acceleration by fitting a slope to the calculated velocity vs. time, which only works in the case of constant acceleration, we could have differentiated the data once more to obtain a direct measure of acceleration vs. time. Try this with just one of your data runs and present a plot of your results. Discuss your results and explain why the noise looks the way it does. Obtain a measurement of the acceleration by using the mean of your calculated accelerations and an uncertainty based on the procedure outlined in §ii.1.6. Compare the results of the two methods and use this to draw a conclusion of which measure you believe is better.

1.3.2 Presentation Mini-Report Guidelines

Credit where credit is due

Formal scientific writing contains proper citation of the works whose ideas and results are used. In a highly interconnected world, students (and professors alike, I might add) have a vast wealth of material available to them that can occasionally find its way into their work without appropriate citation of the person who deserves credit. Any time you use material that has been generated by somebody else, you will be expected to either give appropriate credit to that person's work or to be able to successfully argue that it is common knowledge that does not require citation.

For instance, if a student were to take a figure from the lab manual and to use it in their report without giving credit to the author(s), a person reading the report will see the figure and assume the student made this themselves. The student would be implicitly claiming credit for something somebody else did and passing it off as their own. Claiming credit for another person's work is probably the second biggest "no-no" in science (behind fabricating results). Furthermore, whether on North campus or South, a student's turning in another person's work as their own is a clear violation of the UCLA standard for academic honesty, and can carry with it fairly severe consequences. We will therefore be particularly diligent about giving credit where credit is due in Physics 4AL, which is the main focus of this week's presentation mini-report.

A word of caution

It is easy to find many lab reports for Physics 4AL written by former and current students. As discussed in the syllabus, your lab report must represent your own work. This includes the logical presentation of the report, which is often the most difficult part of writing. If a student uses another person's work as source material for their own (even if they re-word everything), they are using another person's presentation and passing it off as their own, which is a violation of academic and scientific ethics.

The same thing is true of figures (and their captions). You must generate all of the figures in your reports on your own (the only exception to this is pictures from the lab manual that depict the apparatus, as discussed below in §1.3.5). It is not okay to have, for instance, the same figures as your lab partners, even if you cite them in an effort to give them credit; the entirety of your reports must be generated by you.

verbatim text

It will almost certainly not be appropriate for you to include verbatim text from any source in your work for this course (please see the syllabus if you are confused as to why this is). It is important to understand that one cannot pull verbatim text from a source and just drop a reference number and the end of the sentence or paragraph with a bibliography citation – the reader deserves to know where the quotation *started*, as well as whether or not you are taking someone else's words. If you need to use verbatim text in a scientific paper, it should probably have quotation marks around it and the full author's name (in addition to a reference designator and bibliography entry), or maybe even be its own paragraph, probably with different indentation and font (italics are standard) than the rest of the paper. The point is that the reader needs to be able to clearly identify when another person's words are

being used.

Presentation mini-report on a current topic in physics research

For this week's presentation mini-report you are tasked with writing a short review (no more than 700 words) about a topic of your choice in contemporary physics research. This will be a review-style paper where you can discuss the basics of some result in physics in the past decade or so and what the likely next steps may be in the field. Your target readers are scientifically-literate non-specialists; your goal is to inform them of the main points driving the field and the likely directions it will go in the future. This should be written as if it were to be published in a scientific journal, which means you will need to properly cite research and review articles in scientific and engineering journals, with full citations in a bibliography (the bibliography does not count toward the word count). Please do not cite any source that is not either a journal article or a book. Websites, patents, overpass graffiti, and the like are not appropriate as they typically raise questions about source permanence and whether the name of the author is the one who really deserves credit (highly questionable for patents).

You are not expected to be responsible for understanding the technical details of the physics topic you choose, which is beyond the scope of this course. Your grade will primarily be based on how well you are able to produce a short review that covers the main topics and cites relevant and important sources properly. Your writing will be graded, and should be concise, objective, scientific prose. Please state the word count of your review paragraph below the last sentence.

1.3.3 How to write a bibliography

Scientific bibliographies and citation styles differ from journal to journal. In physics 4AL, for your reports you will use the format from the journal Nature. The full format guide for Nature citations can be found at <http://www.nature.com>, but since we only care about a subset of those instructions, the important points are as follows.

- References are each numbered in the order in which they are first cited in the text, tables, and figure legends of the document that references them.
- When cited in the text, reference numbers are superscript with no space between the superscript numeral and the word, not in brackets unless they are likely to be confused with a superscript number. Multiple citations are separated by commas in the superscript, unless they are part of three or more consecutive bibliography items, in which case the range of citation numbers may be indicated by a dash between the first and last citation numbers.
- The bibliography will follow the text of your review and is a list of the articles cited in order of the citation numbers.
- Each entry starts with its number on a new line, followed by the authors' names, the article title, journal name, volume, starting page (or full page range) of the article, and then the year of publication.

- All authors should be included in reference lists unless there are more than five, in which case only the first author should be given, followed by “*et al.*”. Authors should be listed surname (typically their last name) first, followed by a comma and initials of given names (typically their first name or first and middle names), in the order in which the names appeared on the paper.
- Titles of articles should be in upright (not italic) text. The first word of the title is capitalized, followed by the rest of the title written exactly as it appears in the work cited (aside from capitalization), ending with a full stop. If there are words or symbols in the title whose capitalization is necessary to properly convey their meaning, they may be capitalized as needed.
- Journal titles are italic and either abbreviated according to common usage or written in full. Volume numbers are bold, upright font, followed by a bold comma and then the page numbers (or at least the number of the first page) in regular (not bold), upright font. This is followed by a space and then the year of publication in parentheses in regular, upright font. The entire entry is terminated by a full stop.
- Citations of whole books begin with the authors’ or editors’ names (subject to the same formatting as journal article authors). The book title follows in italic font with all main words capitalized. Next, the publisher, city of publication, and publication year appear parentheses and upright font. The entire entry is terminated by a full stop.

1.3.4 Resources

Nature Format Guidelines

<http://www.nature.com/nature/authors/gta/#a5.4>

Scientific typesetting guidelines from NIST

<http://physics.nist.gov/cuu/pdf/typefaces.pdf>

<http://physics.nist.gov/cuu/pdf/sp811.pdf>

Appendix C shows an example bibliography (a very long one!) from a Nature paper [2]. You are expected to use the formatting found in this bibliography. This bibliography is a good example of how to format entries, but is also a good example because of its makeup. Almost all (> 99%) of the entries are published journal articles or published books, which is what is expected in scientific writing. Citation of another student’s lab report, for instance, would be entirely inappropriate. Cited material needs to be static, available to the readers of your paper, have clear authorship, and should ideally be peer-reviewed (such as is true for scientific journals, and is generally close to being true for published books). Sources that are published only online are in almost no cases appropriate. This is because online content changes with time and often has unknown authorship, which explains why citing Wikipedia is not appropriate. An author of a scientific paper needs to make sure that somebody reading

their writing 70 years from now will be able to read the exact source they are citing in their writing.

1.3.5 Exception: Citing this lab manual for reproduced figures

Students in 4AL are welcome to use the images from this lab manual that depict the Physics 4AL equipment in their reports if they properly cite the lab manual as the source of these figures. This is an exception to the rules for citations given above (the lab manual is not actually appropriate, strictly speaking, but I have decided to allow students to use the figures of the apparatus unless they are specifically requested not to). The rest of the content of the lab report should probably not appear in your lab reports and therefore should probably not be cited. Copying text from this lab manual (which includes figure captions, even for figures that are borrowed and properly cited) is not appropriate for a report in physics 4AL, since the syllabus clearly indicates that each student should be writing their reports in their own words.

If you use an image of a piece of scientific apparatus from this lab manual in your report, that is considered a sufficiently direct re-use of material as to warrant a mention of the authors' names in the figure caption, followed by a citation number and of course a bibliography item. For instance, if Figure 1.1 is reproduced in a student's lab report (whether they modify it or not), the figure caption should say something like "Figure reproduced (with permission) from Fig. 1.1 by Campbell, W. C. *et al.*⁴" and then there would be a bibliography item following the format below:

4. Campbell, W. C. *et al.* Physics 4AL: Mechanics Lab Manual (ver. August 31, 2017). (Univ. California Los Angeles, Los Angeles, California).

1.4 Epilogue

Experiment 2 will be a measurement of the free-fall acceleration due to earth's gravity, g . However, it should be possible for you to use your results from Experiment 1 (along with a little bit of theory) to produce a measurement of g . A measurement of this type would be considered somewhat more "indirect" than what you will do in Experiment 2 to measure the acceleration due to gravity, but it is worthwhile thinking about this and considering the advantages of each method as you perform Experiment 2 next week.

Experiment 2: Measurement of g

In the previous experiment, you measured the uniform acceleration of a mechanical system subjected to a constant force. Since the force in Experiment 1 was produced by gravity acting on a measured mass m , you should be able to turn your results into a measurement of the gravitational acceleration g . However, the actual acceleration (a) that was measured in Experiment 1 was much less than g because the system was not in free-fall. This week, you will be directly measuring a free-falling body to determine (a) if the acceleration due to gravity is a constant during free fall and, (b) what is the value of the acceleration g .

Experiment 2 will involve making a few choices about how you set up the experiment. Consider, for instance, a single photogate, similar to that used on the smart pulley in Experiment 1. If the gap between the LED and the photodiode is large enough to permit a falling object to occult the LED, this device can be used with the 850 to record the arrival time of the object at the photogate. One way to look at this is that a single photogate can be used to determine the *position* of the object at that arrival time, which we can write as (x_1, t_1) . This does not even give us enough information to measure the average velocity, much less the acceleration of the ball. Just like your data analysis from Experiment 1, we need at least two points, (x_1, t_1) and (x_2, t_2) to measure a velocity, and at least two velocities to measure an acceleration, etc.

We therefore imagine that we now have two such photogates, vertically separated by some distance d . If we drop, say, a plastic ball from above so that it goes through one and then the other photogate as it accelerates in free-fall, the difference between the arrival times at each photogate (recorded by the DAQ) should permit us to measure the average velocity between the gates, essentially given by Eq. 1.3. But we still only have a single velocity measurement, which is not enough information for us to measure the acceleration.

One could imagine measuring a series of velocities as a function of the height above the top photogate from which the ball is dropped, but this would not necessarily allow you to determine if the acceleration is independent of the height from which the ball is dropped. Another approach would be to take many measurements from a given height while changing the spacing between the photogates, then repeating this process for a series of different heights to see if the acceleration is dependent upon the initial height.

We would, however, prefer a method that can provide a measured acceleration in a single trial, and that does not require us to drop a ball from a well-calibrated height and particular initial velocity, which would be difficult to perform. In this experiment, you will be using

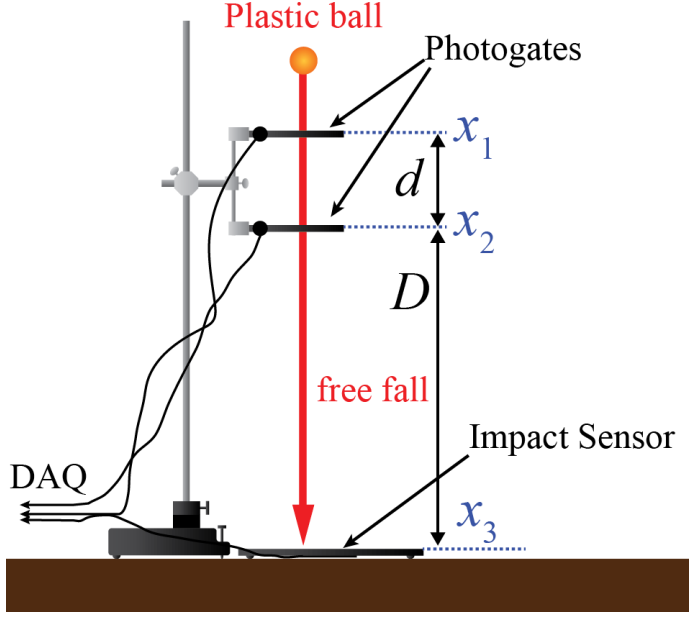


Figure 2.1: Apparatus for measuring acceleration of a ball in free-fall. A plastic ball passes through two photogates before striking an impact sensor mat. The DAQ should be able to measure the arrival time of the ball at all three transducers. Measured values for $x_2 - x_1$ and $x_3 - x_2$ can then be used to determine the acceleration. By changing the height of the pair of photogates above the impact sensor, one can test if the acceleration depends upon initial height.

two different arrangements to measure g : multiple sensors that record the arrival of a simple object (a ball), and a single sensor that records the arrival of various different parts of a complex object (a photogate comb).

First, you will be using a set of three transducers to measure the acceleration of a falling ball (as shown in Fig. 2.1). The first two transducers are photogates, with the last transducer being an impact sensor mat. You will show through derivation in your report that if the gravitational acceleration is constant (independent of initial height or velocity), your measurement method does not require knowledge of the initial height or velocity, which makes it robust against these difficult to control systematics. You will also vary the height of the pair of photogates above the impact sensor to test this claim.

Second, you will be using a single photogate to record the arrival time of each slot edge in a slotted bar called a *photogate comb* (Fig. 2.3). By measuring the distance between successive slot edges, the arrival time of each at the photogate can be used to track the overall position of the comb vs. time. A polynomial fit to the data will have a quadratic term that is proportional to g .

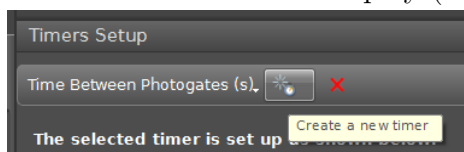
2.1 Procedure

2.1.1 Multi-sensor Method

An example apparatus configuration for the first method of determining g is shown in Fig. 2.1. Each photogate is fitted with a slotted mask that the light must pass through to hit the photodiode. When the bottom of the ball blocks this slit, the DAQ will record the time of this event, so the relevant height that corresponds to, say, x_1 in Fig. 2.1 is the height of this slit. You will need to measure the distances $x_2 - x_1 \equiv d$ and $x_3 - x_2 \equiv D$ and record your measurements, along with your best estimate of the systematic error in these measurements (note that the slit has some width).

To setup the DAQ, we will actually be recording the time between photogate triggers (T_1) and the time between the second photogate trigger and the impact sensor trigger (T_2). Plug the three transducers into three digital channels on the 850. Choose Photogate and Time Of Flight Accessory for the appropriate channels in Capstone **Hardware Setup**.

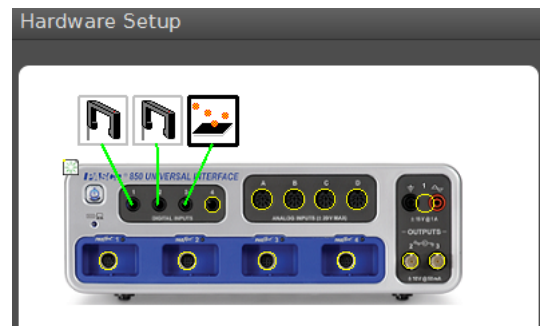
The two measurements we want will be prepared in **Timer Setup**, which can be found in the **Tools** palette. Your first measurement to set up is to have the DAQ record the time between when the ball blocks the first photogate to when it blocks the second photogate. Set up a <New Timer>, choose Build your own timer in step 1, and select your two photogates in step 2. By clicking on the little drop-down menu next to each photogate in step 3, you can select Blocked for each photogate (as shown in Fig. 2.2a.). You can then give your timer a descriptive name (this will appear as a column header) and click Finish. Capstone will automatically identify the units it uses for this display (seconds, normally).



To configure your second timing measurement (the time between when the ball reaches the second photogate and when it hits the impact sensor), click the **Create a new timer** button at the top of the **Timer Setup** area. Your second timer will measure the time between when the second photogate is blocked to when the ball hits the impact sensor (which Capstone calls Blocked for the Time Of Flight Accessory), as shown in Fig. 2.2b.

Once your timers are prepared, you can start a **Table** from the **Displays** palette with your two timer measurements in the table. You may now record data in **Continuous Mode**. Capstone will put the two measured times in the table every time the ball is dropped through the sensor setup. You should set the number of displayed digits on the text in the columns to one or two more digits than you think you need so that you do not limit your precision.

One thing to keep in mind is that the impact sensors tend to work best and have the fastest response when the ball lands right above the position of the sensor on the bottom of



To configure your second timing measurement (the time between when the ball reaches the second photogate and when it hits the impact sensor), click the **Create a new timer** button at the top of the **Timer Setup** area. Your second timer will measure the time between when the second photogate is blocked to when the ball hits the impact sensor (which Capstone calls Blocked for the Time Of Flight Accessory), as shown in Fig. 2.2b.

Once your timers are prepared, you can start a **Table** from the **Displays** palette with your two timer measurements in the table. You may now record data in **Continuous Mode**. Capstone will put the two measured times in the table every time the ball is dropped through the sensor setup. You should set the number of displayed digits on the text in the columns to one or two more digits than you think you need so that you do not limit your precision.

One thing to keep in mind is that the impact sensors tend to work best and have the fastest response when the ball lands right above the position of the sensor on the bottom of

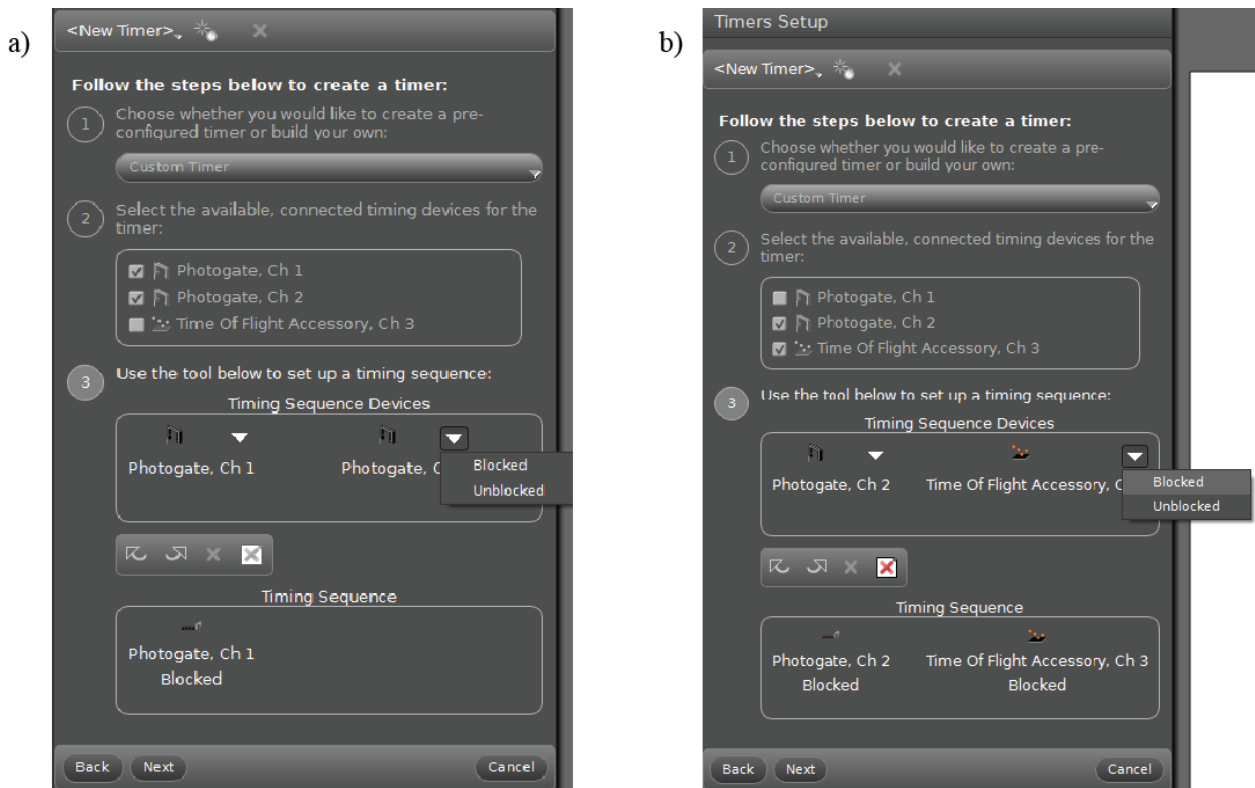


Figure 2.2: Setting up the two timers for Experiment 2. a) Example parameters to have the DAQ measure the time between when the ball reaches the upper and lower photogates. b) Same idea, but for the DAQ to measure the time between when the ball reaches the second photogate and hits the impact sensor. Note that the software refers to this as producing a **Blocked** state for the impact sensor.

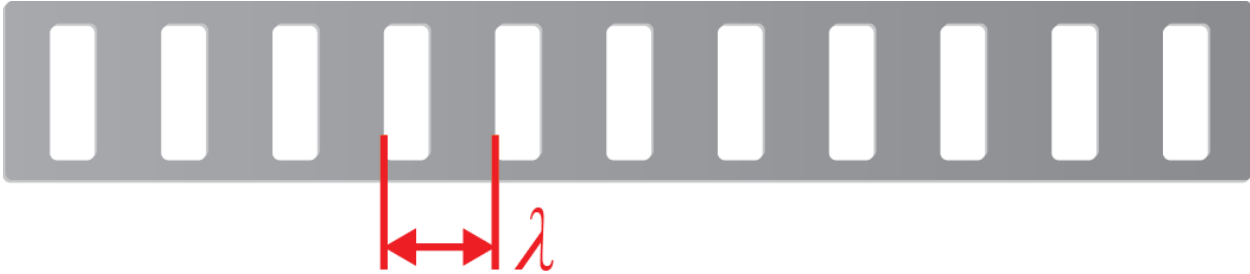


Figure 2.3: A photogate comb with uniformly-spaced through-slots. By dropping this vertically through a photogate, the position of the comb can be tracked as it accelerates in free fall by monitoring the slots passing through the photogate as a function of time. The spacing between successive leading (or trailing) slot edges is shown as λ .

the pad. The pads tend to be marked with a little circle on the top where this is, but you may want to aim for that spot to reduce your systematic uncertainty associated with the transit time of the acoustic wave between where the ball hits and the sensor location.

Each person should record at least 10 drops for each of 5 different heights of the pair of photogates above the impact sensor D for a total of at least 50 data points. Do not share data points, but feel free to use the same values of D as your lab partners. Try to spread these heights out over a wide range to really provide a stringent test of whether the acceleration is independent of height. Be sure to record your measured values for D with uncertainties.

2.1.2 Photogate Comb Method

Now we will attempt the same measurement with a different apparatus. Remove the impact sensor and one of the photogates from the ring stand and the 850 so that you have just one photogate. You will be dropping a fairly long photogate comb through the gap, so be sure to set the height of the remaining photogate high enough that the comb can fall all the way through it before hitting the table. Please feel free to move the whole setup to the floor if you like since it takes a good bit of vertical space to measure g with this method.

An example photogate comb is shown in Fig. 2.3. First, measure the spacing between successive edges of the slots in your comb (shown as λ in Fig. 2.3). You may assume that the placement of the slot edges is uniform across the whole length of the comb to 0.1 mm, so the best way to determine λ is probably not by measuring λ , but rather by measuring $n\lambda$ (for some integer n) and dividing by n . If you do this, the uncertainty in your measured value for $n\lambda$ will clearly be a *systematic uncertainty*, since it will apply to all of your data points. You should take this into account when you think about assigning an uncertainty to your measurement.

Next, set up the DAQ to record the arrival time of each slot edge. In **Timer Setup**, make a new **Pre-Configured Timer**. For timer type, select **Picket Fence**. You will record **Block**

Event Times in a table. This means you may need to throw out your first data point (since the bottom edge of the comb is not a slot), so it is worth thinking about this a little bit. The flag spacing field does not matter for your data since you will be recording times. You will use your measurement of λ when you perform your analysis, which will allow you to account for your uncertainty in that measurement.

One person can hold the photogate comb above the photogate and the other can use a **Table** to record the **Block Event Times** by clicking **Fast Monitor Mode** a little before their partner lets go of the photogate comb. Each person should use unique data set for their report (do not share these data with your partners). Take at least 5 data sets each. You can experiment with the starting height above the photogate to maximize your chances that you get at least one data set with as small an uncertainty as possible.

2.2 Analysis

2.2.1 Multi-sensor Method

For the ball drop experiments, you will have sets of data for 5 different values of D . The data the DAQ has recorded for each trial is T_1 and T_2 , the time between the photogates and the time between the second photogate and the impact sensor. These data points can be combined with your measured values for the distances D and d to measure the acceleration

$$g = \frac{2}{T_1 + T_2} \left(\frac{D}{T_2} - \frac{d}{T_1} \right). \quad (2.1)$$

You will need to derive this expression in your worksheet, but you will find that it corresponds to the difference between the average velocities in both regions divided by the travel time between the middle of the upper region to the middle of the lower one.

You will have two contributions (*statistical* and *systematic*) to the uncertainty in your measurement of g for each distance D , which you may add together to get your total uncertainty. Since we have to this point not spent a lot of time dealing with systematic uncertainties, we will start by discussing this rather dicey topic.

Unlike statistical uncertainties, for which there are provably reliable methods for estimation and combination, there are no generally-applicable rules for systematic uncertainties. Recall from §ii.1.5 that systematic uncertainties can generally not be quantified by repeating measurements, and are therefore typically estimated by using logical arguments about the influence of various effects on the measurement. If there is more than one source of systematic uncertainty in a measurement, you, the scientist, must decide how to combine them. An aggressive method that is applicable in the case that the uncertainties are uncorrelated and normally distributed, is to add the uncertainties in quadrature, which produces a relatively small uncertainty in the measured value and a danger that the true value does not fall within this uncertainty about a third of the time. A more conservative method that is often used is to add the uncertainties directly, which produces a larger uncertainty in the final measurement, but a stronger guarantee that the true value falls within this uncertainty. We will use

a very conservative method in this case by estimating the total influence of the systematic uncertainties and stating a large uncertainty that is almost guaranteed to contain the true value.

You may estimate the *systematic* uncertainty in your measured value of g for a particular value of D due to uncertainty in D and d by using their upper and lower limits (for instance, using $d = d_{\text{best}} + \delta d$ and $d = d_{\text{best}} - \delta d$) in your calculation of g . Plugging the upper and lower limits for d and D into Excel with your best values for T_1 and T_2 for each height is a good way to see how these affect your measured value for g . You can then take $(g_{\text{max}} - g_{\text{min}})/2$ as your systematic contribution to δg for each D .

There is also a *statistical* contribution to δg for each D due to the spread in your 10 measured values. Use the method of §ii.1.6 to calculate your statistical contribution to δg . Compare the size of these two contributions. If they are of comparable size, add them together to make your final estimate of δg . If either the statistical or systematic contribution to δg is more than 10 times smaller than the other, you may ignore it, in which case your value for δg is just equal to the larger one. If you think about this, there is no difference between these two methods since you will almost certainly be stating your uncertainty with only one significant digit. You will be asked to discuss the process by which you determined δg in your worksheet.

After determining a measured value for g (with uncertainty) for each value of D , plot your measured best values g_{best} vs. D . Is there a trend? One way to determine if there is a trend in a collection of data is to try to fit your data to a line and see if the slope is consistent with zero. For our purposes in this course, “consistent with zero” would mean that the uncertainty in the slope overlaps with zero.

2.2.2 Photogate Comb Method

For each data set, you will now have a table of time stamps for when the photogate was blocked by the edge of a slot. Using your measured value of λ , construct a table of position vs. time. It is not necessarily clear what object’s position is being tracked (it’s probably the top edge of the first slot, though this depends upon your definition of $x = 0$), but that’s not important for your measurement; what you care about is the quadratic part of the curve, not the offset in x (or t).

For each of your data sets, make a plot of position vs. time. Does this look like (part of) a parabola? If not, you may have something amiss with your data. Remember to think about the first data point and whether or not to include it.

Excel provides an easy way to fit your data to a quadratic through the **Add Trendline** option. You can choose **Polynomial** and make it of **order 2**, and even display the resulting equation on the chart to get g_{best} . The problem with this is that it doesn’t provide you with an uncertainty in g ! In order to do that, we will need to do a full regression analysis for a 2nd order polynomial, which is not as easy to implement as the Add Trendline option.

A	B	C	D	E	F	G	H	I	
1	SUMMARY OUTPUT								
2									
3	Regression Statistics								
4	Multiple R	0.999998457							
5	R Square	0.999996914							
6	Adjusted R Square	0.999996657							
7	Standard Error	0.000145125							
8	Observations	27							
9									
10	ANOVA								
11		df	SS	MS	F	Significance F			
12	Regression	2	0.163799495	0.081899747	3888668.682	7.45672E-67			
13	Residual	24	5.05467E-07	2.10611E-08					
14	Total	26	0.1638						
15									
16		Coefficients	Standard Error	t Stat	P-value	Lower 95%	Upper 95%	Lower 95.0%	Upper 95.0%
17	Intercept	6.03752E-05	0.000101206	0.596558733	0.556387934	-0.000148503	0.000269254	-0.000148503	0.000269254
18	X Variable 1	-0.436780206	0.002123098	-205.7277817	1.77001E-40	-0.441162065	-0.432398348	-0.441162065	-0.432398348
19	X Variable 2	-4.899809228	0.010003731	-489.7981671	1.61783E-49	-4.920455915	-4.879162542	-4.920455915	-4.879162542
20									

quadratic coefficient uncertainty in quadratic coefficient

Figure 2.4: The results of a quadratic regression in Excel. The third row of results shows the best value and uncertainty of the quadratic term. See Fig. 0.6 for a description of the constant and linear terms.

2.2.3 Quadratic Regression Analysis

When we introduced the linear regression analysis in Excel in §0.2.5, the **LINEST** function was mentioned as an alternative way to calculate linear fit parameters, and the same is true for a quadratic fit. However, in the interest of ease-of-use, we will again choose to describe how to do this using the **Regression** tool, but feel free to research how to do this with **LINEST** if you like.

The trick to making a quadratic regression is to make a third column of data that has the square of the original horizontal-axis data in it. In our case, if our time data is in cells A1:A100, we can make another column right next to this one whose first entry is =A1^2 and copy that down the rest of the column by, *e.g* dragging its corner down to row 100. Assuming that A1:A100 has our measured **Block Times**, B1:B100 has the squares of these block times, and C1:C100 has the distance data, we start a quadratic regression analysis the same way as was explained for a linear fit in §0.2.5, but enter the range \$A\$1:\$B\$100 for the **Input X Range**. This can be easily accomplished by highlighting both columns.

An example quadratic regression result is shown in Fig. 2.4. Comparing this to Fig. 0.6, we can immediately see the constant and linear terms and their uncertainties in the same places, but there is a third row beneath them now. This row contains the information about the quadratic term, with the best value and uncertainty shown in Fig. 2.4.

Using quadratic regression on your data, extract a measured value for g from your data. Remember, the uncertainty given by the regression is only the *statistical* uncertainty. If you have a *systematic* uncertainty in, for instance, the distance column due to uncertainty in

λ , you may want to perform separate regressions for different values of $n\lambda$ at the top and bottom of your range of uncertainty in $n\lambda$ and compare the resulting range in measurements of g_{best} to the statistical uncertainty in g given by the regression.

2.3 Report Guidelines

Last week, we covered citations. From this point forward in 4AL, if you need to reference prior work by somebody, you will be expected to do so using the rules from last week (even in your worksheet). If you cite somebody's work, you will of course need to include a bibliography at the end of your report in Nature format, and this bibliography will never be counted toward a word count if there is a limit for that section of that week's report.

This week's worksheet will be worth 30% of your grade and the presentation mini-report will be worth 70%.

2.3.1 Worksheet Guidelines

Your worksheet should contain the following sections

1. **Cover Sheet**

- experiment number and title
- your name and UID
- the date the lab was performed
- your lab section (for instance, "Wednesday 12pm.")
- your TA's name
- your lab partners' names

2. **Derivation** Derive Eq. 2.1. Please include just enough detail to demonstrate how this equation describes what you care about, no more than that.

3. **Plots** The focus of this week's presentation mini-report is plots, but the plots you are asked to include in your worksheet this week do not have to meet the same standard as the one you will make for your presentation mini-report.

Include a plot of g vs. D for the ball drop method. Do you expect that g should depend upon D ? Briefly discuss this and what your data tell you. Can you find a way to quantitatively confirm or rule out a linear dependence on D ?

You will include a plot of your best dataset of photogate comb results in your presentation mini-report, so decide which set is your best and then include your four other data sets as a plot (or plots) in your worksheet. Include the fit curves on your plots.

4. Data Tables

Include a table of your ball drop results from different heights. An example is shown below. If an entire column shares the same systematic uncertainty, this should be stated in the table caption. If the uncertainty differs row-by-row, it is best to state the uncertainty explicitly in each entry.

Trial	Photogate spacing d (cm)	Gap to impact sensor D (cm)	Measured acceleration g (m/s 2)
1	1.1	3.0	9.6 ± 0.7
2	1.1	5.0	9.8 ± 0.3
3	1.1	15.1	10.1 ± 1.3
4	1.1	20.3	8.6 ± 1.8
5	1.1	30.7	9.843 ± 0.004

Include a table of your five photogate-method measured values of g . Briefly describe your uncertainty analysis and whether the uncertainty is dominated by statistical or systematic uncertainties.

5. Conclusion

Write a brief discussion of your uncertainty analysis and results. Compare the accelerations you measured with the expected value of g . Which method (ball drop or photogate comb) do you think is the most accurate? Which do you think is the most precise? Did you choose to use a combination of systematic and statistical error or did you just use one? Explain why.

6. Extra Credit (optional)

One of the main challenges associated with getting an accurate measurement of g with the photogate comb method is keeping the comb vertical as it drops. You will find some string and other things around the lab that you can use to experiment with ways to make sure the comb doesn't swing or tip once it has been released. For instance, some students have experimented with using paper strips, tape, string, and other tools they have constructed to try to get the best measurement.

Design and perform your own experimental test comparing a couple of methods, and analyze the data to draw conclusions about whether there are methods that perform better than others.

2.3.2 Presentation Mini-Report Guidelines

Many people reading a journal article will immediately jump to the figures before deciding to read the article. The figures will often give a quick visual representation of the content of the paper. It is important for an author to use this knowledge to guide the reader through what they are presenting by laying out the figures in a logical and possibly chronological way.

Make a figure showing your best photogate comb measurement (the distance vs. time) to the standards of a scientific journal (see below) and write a paragraph with fewer than 400 words of body text introducing the figure and discussing what it shows. This does not need to be a completely self-explanatory paragraph, but should instead resemble a paragraph taken verbatim from a (non-existent) longer paper that you would have written about this experiment. Your figure should be referenced in your paragraph and will need a caption. The quadratic fit should be shown, and its results should be described. The caption does not count toward the word count, and should probably not exceed 200 words or so. Please write the number of words used in your figure caption and the number used in your body text on a separate line at the end of your presentation mini-report.

2.3.3 Plots in scientific papers

All figures in well-written scientific journal articles are both clear and necessary. Along with the guidelines below, an important part of clarity is that the text in the figure must be as large or larger than the font of the body text. This usually means that the figure itself is formatted with very large font sizes for its labels since the figure is typically reduced in size when inserted into the text. A guide for how to insert Microsoft Excel figures into Microsoft word documents with captions and figure labels can be found in Appendix B.

In Physics 4AL, it should be possible for students to complete their assignments with only two different types of figures: linear-axis scatter or line plots and apparatus diagrams. We will focus on the former, though many of the points discussed below regarding the caption will apply to diagrams as well.

1. Plots should include the following items unless there is a good reason to omit any of them:
 - axes and a bounding box with tick marks pointing inward
 - axis labels (see below)
 - tick labels (these are the numbers)
 - data points and possibly lines joining subsequent points (when needed for clarity)
 - a fit or theory curve may be included
 - If multiple related data sets can be plotted on the same axes without creating confusion, they should share the same axes. If multiple plots or figures are closely related, they should be combined into one figure if doing so does not come at the expense of clarity.
2. Every figure (and table) needs a caption directly below the item it describes, and plot captions should include the following items:
 - “Figure XX.” or some other appropriate designator with a unique number that is referenced in the body text, followed by

- a descriptive title, followed by
- a description of all lines and symbols on the plot and what they mean
- a brief discussion of what the data (and curves) show

Typically, about five labeled tick marks will be sufficient for fully-specifying an axis. Tick labels should have an appropriate number of digits for the range they describe. Though you are unlikely to encounter this in physics 4AL, if the plot range covers a small fraction of some large absolute scale, you can subtract an overall offset from the tick labels and explain what this is in the axis label. For instance, if frequency is being plotted from $f_{\min} = 12.642\ 808$ GHz to $f_{\max} = 12.642\ 816$ GHz, the tick labels should probably be every 2 kHz, so the tick labels would be the numbers 8, 10, 12, 14, and 16 and then the axis label would say something like “Oscillator frequency, f (kHz) –12 642 800 kHz.”

3. Common mistakes to avoid:

- Do not include any lines or curves that are not well-defined (such as splines that are not fully described, etc.). All lines and curves must be completely specified.
- Do not put a title at the top, as the title is the first part of the caption. Note that this is one of many differences between a figure in a scientific journal and the figures in this lab manual, which is not a scientific journal article.
- If possible, avoid the use of yellow or light green (or any color that will be hard to see).

4. Plot Axis

The format for an axis label in physics 4AL will be “Quantity name, Symbolic Designation (Unit).” The quantity name should be plain English words (*e.g.* “Distance to stop,” “Delay between pulses,” “Glider speed,” “Number of events,” etc.). The symbolic designation is optional, and if used is the mathematical symbol you be use to represent this quantity in the body text and its equations (D , t , v , N , etc.). Last (and not optional), the units symbol for the tick mark labels should be written in parentheses. Though you are unlikely to encounter this in Physics 4AL, if the units of an axis (almost always the vertical axis) are suppressed because they are truly irrelevant and would be distracting, it is conventional to write “(arb.)” for the units.

Axis limits should be chosen to highlight the important points of the plotted material as well as possible. This may involve cutting off some of your data (typically on the far left or far right), so you will have to think about whether you can omit parts of your data set without changing what the data show. Omitting data to change conclusions is not okay – data may only be omitted if doing so improves clarity of presentation without altering the interpretation of what the data support.

5. Adding the caption

A good figure caption tells the reader not only what is on the plot, but *why* it is important and *what conclusions can be drawn from the results*. The first thing after the designation (*e.g.* “Figure 1.”) should be a short, *descriptive* title. The title should not simply be “(y-axis label) vs. (x-axis label)” – your reader will already know that from looking at your figure. Your goal is to give the reader a good idea of what it is you are presenting and why you are presenting it. For instance, for a figure from Experiment 0, instead of “Voltage vs. Weight,” a much more descriptive figure title would be “Calibration of the force sensor.”

Next, describe what is on the plot. The reader should be able to tell what every data point and curve on the plot is. If there is a fit curve on the plot, it needs to be discussed in the figure caption. In contrast to many of the figures you see in this lab manual (which is not a scientific paper), please do not put your fit line equation on the body of the plot; the fit line equation and the fit parameters need to either appear in the caption or the caption should clearly indicate to the reader where they can be found.

One good way to add a fitted curve’s equation to the caption is to write the equation using symbols, then to present the values for these symbols (and their associated units and uncertainties). For instance, “The solid red curve is a fit of the data to an exponential decay, $J(t) = Ae^{-t/\tau}$ with fit parameters $A = (43 \pm 4)$ km and $\tau = (22.60 \pm 0.06)$ fs.” Alternatively, this can be accomplished by referencing specific equations in the body text instead (see, *e.g.* Eqs. 0.2 and 0.3 of this manual).

6. Final notes

A guide to graphing in Excel and adding captions in Word by Julio S. Rodriguez, Jr. and Anthony Ransford can be found in Appendix B of this lab manual.

2.4 Epilogue

2.4.1 Specialized defined units for gravitational acceleration

The “law of falling bodies” is usually attributed to Galileo, by which we mean that he is often described as the first to discover that gravitational acceleration is constant and independent of mass. In recognition for this achievement, he has been given the highest honor in physics (even higher than the Nobel prize!): a unit named after him. Naturally, it is a unit of acceleration, the “Galileo.” $1 \text{ Gal} \equiv 1 \text{ cm/s}^2$. Gravimetric maps often display their gravity anomaly data in units of mGal, or “milli-Galileos.” There is also a defined unit called *Standard Gravity* [8] that is given by $g_0 \equiv 9.806\,65 \text{ m/s}^2$.

2.4.2 g in Knudsen 1-238¹

¹This analysis and section were contributed by Chandler Schlupf (2015).

Standard Gravity (g_o) is some sort of average of the apparent gravitational acceleration over the surface of the earth, but the gravitational acceleration at any given point can change by up to about a percent depending where the point is due to several factors. The first is that the Earth is not perfectly round, but rather an oblate spheroid (shaped like an onion), so its radius is not constant and the surface is not equidistant from the geometric center. Second, since the Earth is spinning, a centrifugal pseudo-potential that varies with latitude is produced, decreasing the *apparent* gravitational acceleration near the equator compared to the poles.

Furthermore, local variations in the makeup of the Earth's crust can influence the value of g by changing the average density of the ground below, as well as the distance from the center of the earth. For example, a pocket of low-density material such as a liquid or gas underneath the Earth's surface can cause a tiny decrease in the measured gravitational acceleration right above it. Gravimetric measurements are therefore sometimes used to locate petroleum deposits.

All of this means that the value of g in a given location is not, in general, equal to Standard Gravity g_o . In fact, these effects (and others) essentially guarantee that g_o is actually the gravitational acceleration *almost nowhere on the surface of the earth* (look how many digits there are on g_o)! Luckily, the only important thing for Experiment 2 is knowing the value in our lab room.

Measured data of variations in the Earth's gravitational field are collected on gravimetric maps. One such map for our location created by the Southern California Areal Mapping Project can be found at <http://pubs.usgs.gov/of/2003/0269/>. Unfortunately, there is not a data point on UCLA's campus (to obtain accurate measurements, they only take data points on solid bedrock). However, we can use surrounding points to get a good estimate. Averaging the three closest points to UCLA and taking their standard deviation as an estimate of the systematic uncertainty gives us a value for gravity in Knudsen 1-238 of $g = (9.7955 \pm 0.0003) \text{ m/s}^2$.

Experiment 3: Conservation of Mechanical Energy

Conservation of energy is a powerful conceptual and computational tool that is useful in essentially every field of science and engineering. Dissipation of energy into random thermal motion still obeys conservation of energy, but it is sometimes difficult to keep track of the dissipated energy, so we will be focusing here on the conservation of mechanical energy. In this experiment, you will measure the kinetic and potential energy of a harmonic oscillator during half of an oscillation cycle, where you will try to determine to what degree the initial potential energy is converted entirely into kinetic energy and then back into potential energy. The experiment has been designed in a way to try to minimize dissipation, but you will be able to analyze your data to quantify how much energy is being dissipated from the mechanical energies.

A glider is provided that has a comb of photogate flags mounted to the top. You will be using a photogate to measure the passing of each flag, which will enable you to determine the position and velocity of the glider. Two springs are also provided to produce a restoring force on the glider to some point on the air track. By measuring the spring constant of this restoring system, you will be able calculate potential energy as a function of position

$$U = \frac{1}{2}kx^2. \quad (3.1)$$

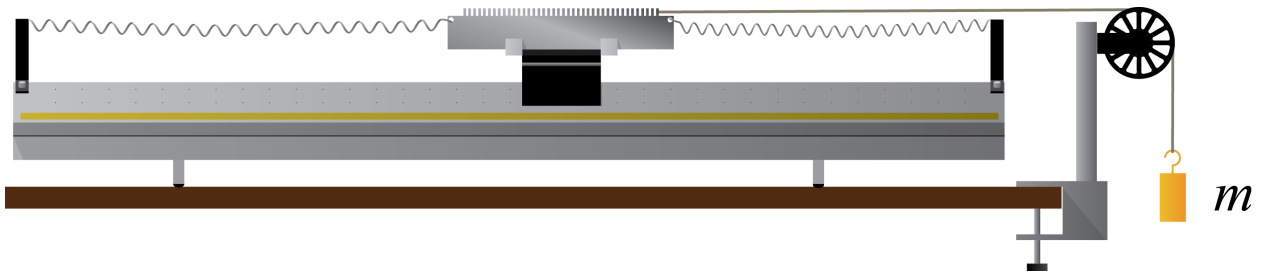


Figure 3.1: Apparatus for measuring the effective spring constant providing the restoring force for your glider. Once the spring constant has been determined, the hanging mass, string, and pulley should be removed.

You will also measure the mass of the glider (with photogate comb attached!), which will enable you to determine the kinetic energy as a function of velocity:

$$K = \frac{1}{2} M v^2. \quad (3.2)$$

The tricky part of Experiment 3 will be the data analysis, where you will need to figure out how to interpret your raw data (a series of time stamps for when the photogate goes from being unblocked to blocked) to calculate these quantities. You will need to determine how to find the kinetic energy as a function of *position* so that for every data point where you calculate the potential energy, you can also calculate the kinetic energy. By plotting these together, you can also plot their sum, which should be constant in the absence of dissipation. You will find that despite the fact that the amount of energy of each type changes drastically over the course of half an oscillation, their sum is remarkably flat. The slight decrease in total energy over your measurement will enable you (through fitting) to determine the coefficient of friction of your nearly-lossless air track setup.

3.1 Procedure

The first experimental task to complete is to determine the mass of the glider with its photogate comb and record this for your analysis. You will then need to determine the spring constant associated with the restoring force of your spring setup, as shown in Fig. 3.1. The spring constant measurement does not utilize the DAQ at all, and will require you to write down a series of measurements for your analysis and report.

Figures 3.1 and 3.3 show the basic idea. By measuring the position of the glider for a series of different masses m , a plot of applied force (mg) vs. displacement can be fit to determine the slope of this trend, which has units of force per displacement and is the effective spring constant of your system. Be sure to get data for at least 5 different masses. Once you have gathered enough data for your spring constant measurement, you may disconnect the pulley system and hanging mass from the glider and move it out of the way. You may share data for the spring constant measurement with your lab partners, but will be expected to use your own data sets for the rest of Experiment 3.

To measure the position and velocity of the glider for your analysis and report, we will be using a photogate to tell us when each tooth first blocks the photogate. This is a tricky business, and you will want to be very careful that you describe your procedure in your own notes so that you can use them to interpret your data later.

The teeth on the photogate comb are 2 mm wide, as are the spaces between teeth, both to an uncertainty of 30 μm . You will only be using half of a single oscillation of the glider for Experiment 3, so you may pick a direction for the glider to be moving when it passes the photogate. Remember, the photogate cannot tell the difference between the glider moving left or right, so this will simplify your analysis by confining the movement to one direction only. You will pull the glider back just beyond the photogate, start the DAQ recording, then release the glider. You may stop recording as soon as the glider stops to reverse its direction.

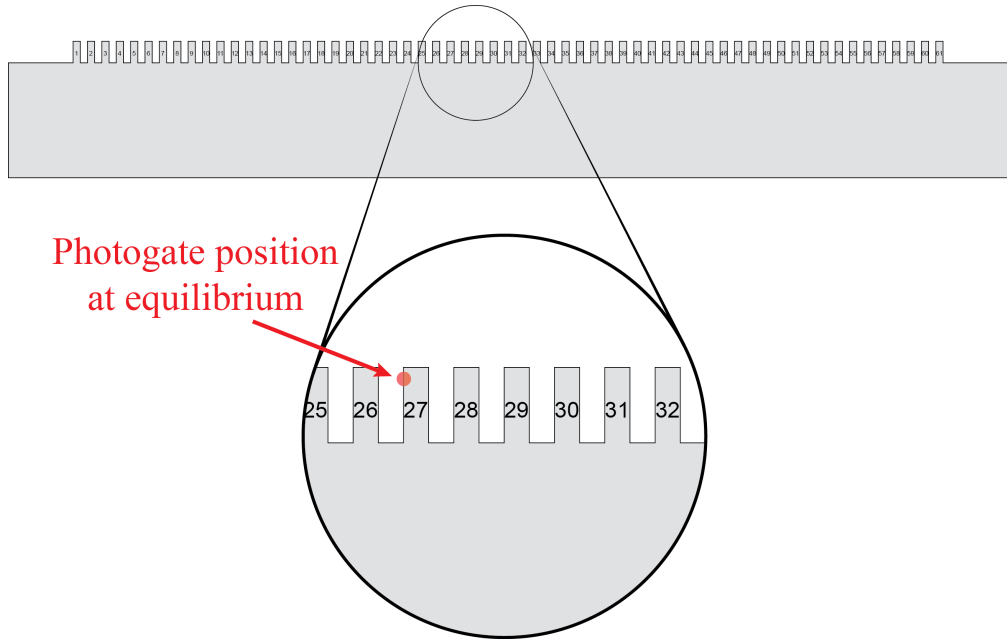


Figure 3.2: An example photogate comb shown with an example for a position of the photogate when the glider is in its equilibrium position. In this case, it is probably easiest to analyze the data if one chooses to pull the glider back to the right instead of the left.

First, it is important to set and record the equilibrium position of the glider relative to the photogate beam. A good choice is to put the photogate so that a tooth near the center of the comb is just on the verge of blocking it (the light on the top of the photogate turns on when it is blocked). You will thank yourself later if you are very careful about recording (a) which tooth that is and (b) which direction the glider needs to move to block the beam when it is at equilibrium. Beware that the teeth may have marks on them that are meaningless; be sure to do your own counting to determine which tooth number you are using.

Figure 3.2 shows an example configuration where the photogate is set up to trigger on the 27th tooth if the glider is displaced to the left a tiny amount from equilibrium. In this example, pulling the glider all the way to the right so that tooth number 1 is just past the photogate position and then letting go and having the DAQ record the time stamps every time the photogate goes from being unblocked to blocked means that the 27th time stamp happens at exactly the equilibrium position, which one could define as being $x \equiv 0$. This would mean that the first time stamp happened at a displacement from equilibrium of $x = -104$ mm. Likewise, if for the same configuration the glider had been pulled off to the left and then let go for recording data, the equilibrium position would be reached about halfway between time stamp 35 and 36, because the photogate triggers when it goes from being unblocked to being blocked. In this case, the first time stamp indicates the glider is at a position of $x = -138$ mm from equilibrium.

To set up the DAQ for recording these time stamps, connect your photogate to a digital

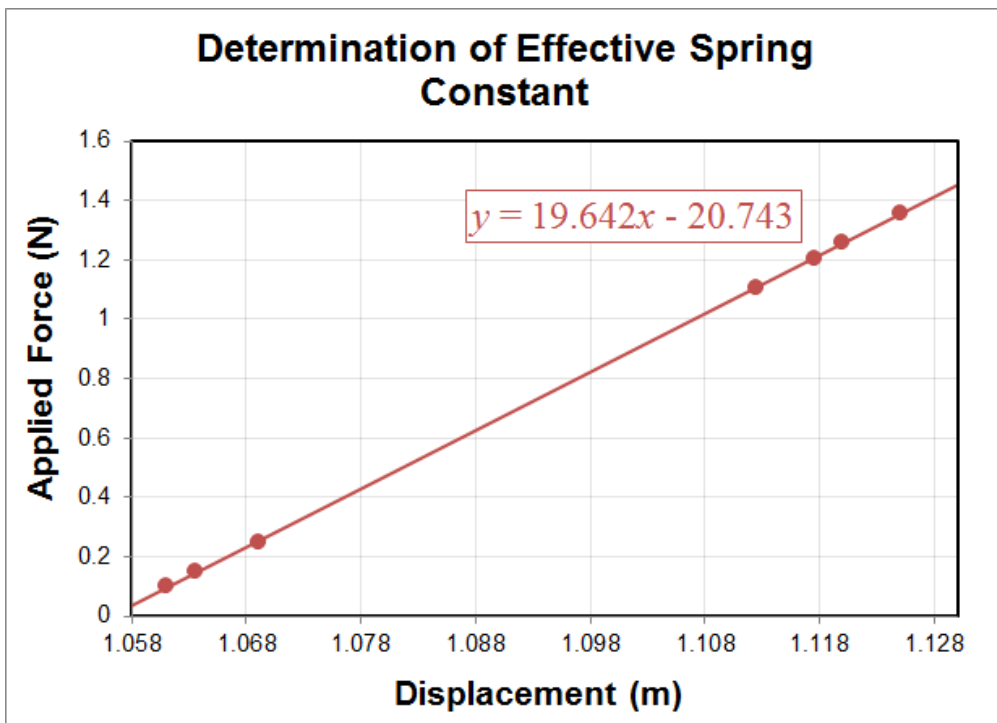


Figure 3.3: Determination of a spring constant by fitting a line to measured values of force vs. displacement. In this case, the spring constant was determined to be $k = (19.64 \pm 0.04)$ N/m.

channel and select Photogate in **Hardware Setup**. In **Timer Setup**, you should make a new **Pre-Configured Timer** based on your photogate channel that is of the **Picket Fence** type. You will record **Block Event Times** in a table. The flag spacing field does not matter for your data since you will be recording time stamps. Once this timer has been created, you may create a **Table** and use **Fast Monitor Mode**. One person can pull the glider back in the chosen direction past the photogate, then their lab partner can click fast monitor mode. The glider can then be released. Once the glider reverses its direction, stop the DAQ and you may copy and paste your data into Excel to save for your analysis. Each person needs their own data set, but all three may be recorded in a row using the same apparatus setup.

3.2 Analysis

For your measurement of the spring constant of the restoring force, plot your force vs. displacement data. You will need to make sure your plot has the appropriate data as x and y , because it is easy to get these mixed up, especially in Excel. Figure 3.3 shows an example with some fake data. The y -intercept is of no interest here as we are only concerned with determining the slope of the fit line. Remember, the SI units for spring constant are N/m, so be sure to convert your masses into applied force correctly (remember the difference between

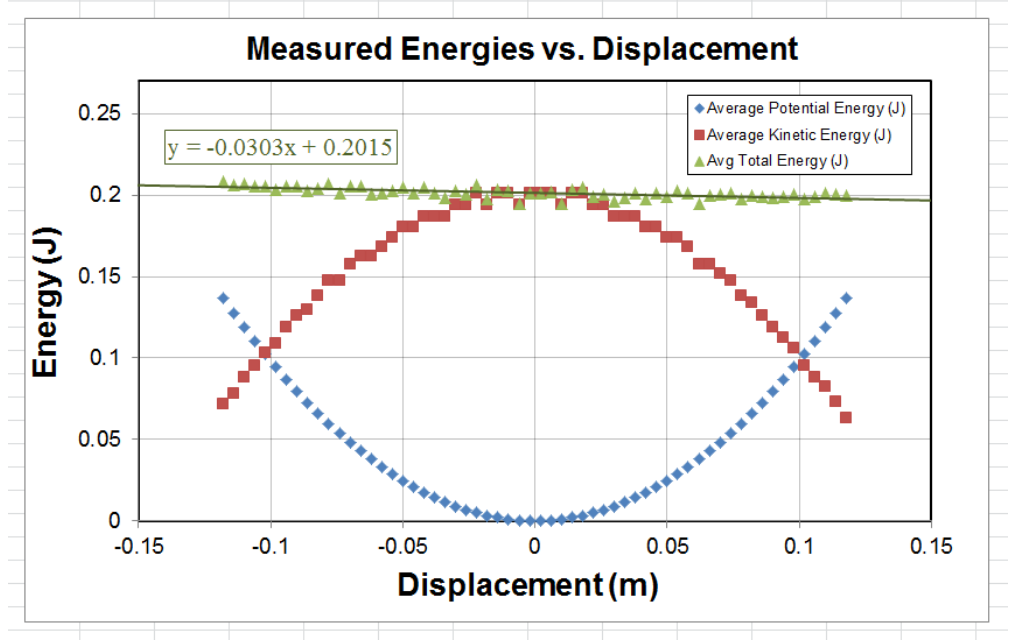


Figure 3.4: Mechanical energy of a glider vs. position. The potential energy shows the harmonic well for this oscillator. The kinetic energy is based on differentiating the same data that was used to calculate the potential energy, so it is more noisy, as expected when differentiating data.

grams and kilograms), and you hopefully found in Experiment 2 that $g = 9.8 \text{ m/s}^2$ (you may of course use this value even if you got a different answer in Expt. 2).

Your data for the moving glider should consist of a column of time stamps. Using your knowledge of where the photogate was relative to the comb when the glider was at equilibrium, you should be able to convert these time stamps into positions, where you should define the equilibrium position to be $x = 0$. This is important because you will be calculating the potential energy using Eq. 3.1, so $x = 0$ should correspond to $U = 0$.

It is certainly true that we could calculate the potential energy as a function of distance based on these data (since you now have a value for the spring constant k). However, we will be calculating velocity by numerically differentiating your data, which is the same as saying we will be using the following expression (as in previous experiments)

$$v(\bar{x}(i)) = \frac{\Delta x}{\Delta t} = \frac{x_{i+1} - x_i}{t_{i+1} - t_i} \quad (3.3)$$

where $\bar{x}(i)$ is the average position in this interval,

$$\bar{x}(i) \equiv \frac{1}{2} (x_{i+1} + x_i). \quad (3.4)$$

So we will have a value of U at every x_i , but a value for K only halfway between every x_i and x_{i+1} (which we call $\bar{x}(i)$). Since we want to calculate the potential, kinetic, and total

energy at the same place, we can, for instance, determine the potential energy for each value of $\bar{x}(i)$. To do this, create a new column for the average positions $\bar{x}(i)$ that is the average of each successive pair of points in the x_i column. You can then create a column that calculates the potential energy $U(\bar{x}(i)) = \frac{1}{2}k\bar{x}(i)^2$ at each value of $\bar{x}(i)$ using Eq. 3.1. Create another column and fill it with calculated values of the kinetic energy

$$K(\bar{x}(i)) = \frac{1}{2}M \left(\frac{x_{i+1} - x_i}{t_{i+1} - t_i} \right)^2 \quad (3.5)$$

using your measured value for the mass of the glider with its comb on top. Last, create a third column that calculates the total mechanical energy for each position $\bar{x}(i)$.

Create a plot that shows kinetic energy, potential energy, and the total energy as a function of displacement $\bar{x}(i)$. An example is shown in Fig. 3.4. Your potential energy should look like a parabola, characteristic of a harmonic oscillator. The kinetic energy will be more noisy than the potential energy since it is based on numerical differentiation of data, which magnifies noise in the data. The total energy should be very linear. If your calculated total energy does not look linear, it is likely that you have set your zero point in the wrong place when trying to convert between time stamps and displacement from equilibrium. Fit a line to the total energy vs. distance and determine its slope (with uncertainty). The slope of this line has units of $J/m = N$, and represents a constant force that dissipates energy from your oscillator, probably due to friction. Using your known value for the glider mass, calculate the coefficient of friction needed to produce this slope.

3.3 Report Guidelines

For both the worksheet and the presentation mini-report for Experiment 3, you will be expected to apply what you learned in the previous experiments about citations and plots. For instance, your worksheet for Experiment 3 will contain two plots, and those plots should conform to all of the guidelines from §2.3.3 (aside from the body text, which will often not be necessary on a worksheet).

This experiment's worksheet will be worth 30% of your grade, with the presentation mini-report worth 70%.

3.3.1 Worksheet Guidelines

Your worksheet should contain the following sections

1. Cover Sheet

- experiment number and title
- your name and UID
- the date the lab was performed

- your lab section (for instance, “Monday 9am.”)
- your TA’s name
- your lab partners’ names

2. Discussion

- Include a description of which direction your glider moved and where the photogate was compared to which tooth.
- Describe how you calculated the potential energy and kinetic energy at the same positions in space.

3. Plots and Tables

- State your measured value for the mass of the glider with its photogate comb.
- Make a table of your data used to calculate the spring constant.
- Include your plot showing the fit line for determining the spring constant. State your measured value for the spring constant (as always, with its uncertainty and units).
- Include your plot of the three energies vs. position, along with a linear fit to the total energy vs. position.
- Present your calculated value for the coefficient of friction of the glider on the air track (with its uncertainty, of course!).

4. Extra Credit

Since the photogate does not distinguish between movement of the glider in the $+x$ and $-x$ directions, we confined our analysis to half of an oscillation. However, by appropriately converting the measured times stamps into displacement (warning: *this step is very tricky!*), it is possible to generate a plot with multiple oscillations. Save data for at least two full oscillations of your glider and use this to plot the two types of energy vs. *time* (as opposed to plotting them vs. distance). Estimate how long it would take your glider to decrease its oscillation amplitude by a factor of e (one digit of precision is okay for this). Fig. 3.5 shows the results of doing something like this, where the decay of the energy in the mechanical degrees of freedom is clearly visible.

3.3.2 Presentation Mini-Report Guidelines

The first page of a scientific paper will almost always contain the title, author list, and an abstract for the paper. The title and abstract are where you will tell your story to the largest audience. The title and abstract must stand alone and the main points should be able to be understood without the bulk of the report. An emphasis on clear, specific, and minimalist

writing will be important not only to communicate what you have done and why it is important but also to convince the reader that the rest of your paper is worth their time. In Physics 4AL, we will follow the guideline that no abstract is to contain more than 200 words. Please always write the number of words contained in your abstracts on a separate line below the last sentence. For this week's presentation mini-report, please write a title, author list, and abstract for your work on experiment 3. Please put this mini-report on a single, new page, with the title at the top, followed by the author list (centered), followed by the abstract.

Abstract

An abstract is a recap of all the information of a scientific article, conference, presentation or research update. The abstract should be a standalone document where the reader could broadly understand all major points (including the conclusions) of the research without reading further. You are tasked with writing an abstract for Experiment 3 (the one you have just performed) with fewer than 200 words. In this abstract you will describe what was done and why. Were you testing some model or another for the behavior of some physical system? Were you testing a fundamental principle of physics, or measuring a property of something? Were you investigating the degree to which a system exhibits some desired effect?

In this course, we will depart somewhat from the Nature style in that your abstracts should not include citations or background. An abstract should be succinct with no unneeded words. Scrutinize every word and use the minimum number of words required to express your ideas. Remove words that are ambiguous or imprecise. Even though an abstract is short, it is worth your while as a scientist to make sure you put the time in to make something you are proud of, as many times it is the only published evidence of conference talks, presentations or research updates.

Title

Above your abstract you will include a title. The title is sometimes the single most important thing in a paper. By the pigeonhole principle it is at least the most read part of a paper. The title should be explicit and understood by the most general of your target audiences. You need to tie yourself to the similar research out there while distinguishing what you have done as something different. Like the abstract it is of utmost importance to scrutinize every word with a focus on clarity. The title should not be an English sentence.

Author List

We will follow the standard U.S. author list convention of initials followed by surname. You will be the only author on your Physics 4AL papers. At the end of your name include a superscript that indicates a footnote with your affiliation. For example “*F. D. Roosevelt¹*”. On the bottom of your abstract you would note the affiliation, for example “¹*Department of Physics Port Chester University*”. Your lab partners' names will be on your cover sheet, so there is no need to worry about giving them credit for helping you to take data. Since all of the analysis, figures, text, and so forth for your report have to be entirely generated by you, we will let the cover page suffice for crediting lab partners.

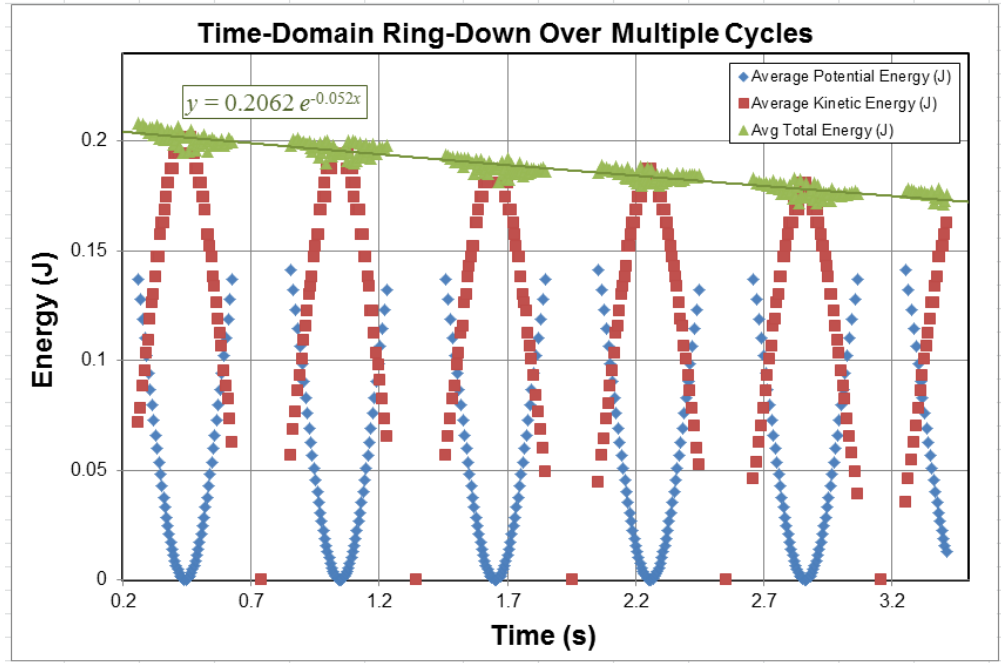


Figure 3.5: The total mechanical energy of a glider slowly decreases due to dissipation (see Extra Credit). In Experiments 5 & 6, you will be measuring properties of harmonic oscillators that have similarities to this one.

3.4 Epilogue

A plot of the potential energy vs. position (such as shown in Fig. 3.4) gives a visual representation of the “potential well” in which the glider oscillates. The frequency of a mass m oscillating in a parabolic well ($U = \frac{1}{2}kx^2$) is given by

$$\omega = \sqrt{\frac{k}{m}}. \quad (3.6)$$

Using the measured value for k associated with the data in Fig. 3.3 and the measured mass gives a prediction for the oscillation frequency that matches the frequency shown in Fig. 3.5 at the 10^{-2} level, demonstrating that this system is well-modeled as a simple harmonic oscillator.

Experiment 4: Momentum and Impulse

In the previous experiment, you investigated conservation of energy by monitoring the trade-off between kinetic and potential energy in a harmonic oscillator. However, as you were able to quantitatively verify in Experiment 3, mechanical energy can be dissipated into heat in a number of ways. It is often fairly difficult to keep track of these dissipation mechanisms, and so the conservation of energy balance sheet can end up with a kind of catch-all entry for “dissipation” that limits its usefulness as a predictive tool in all but the most well-controlled environments.

Compared to conservation of energy, conservation of momentum is often said to be more “fundamental.” There are a few reasons why you may hear this claim, but for our purposes it should suffice that it’s often easier to keep track of and predict the flow of momentum in real-world situations than energy. For instance, both elastic and inelastic collisions are required to conserve linear momentum with respect to the movement of the colliding objects, while conservation of energy allows kinetic energy to be converted into, for example, heat during the collision.

In Experiment 4, you will be investigating the relationship between two different ways of measuring an *impulse*, which is a momentum change (and therefore has units of momentum). You will measure the initial and final velocities of a glider on an air track that impacts a rigidly-mounted force sensor, which will give you a first method for measuring impulse:

$$\Delta P = P_f - P_i. \quad (4.1)$$

You will also record the reading on the force sensor during the collision as a function of time, allowing you to integrate the force to provide you with your second method for measuring the impulse:

$$\Delta P = \int dt F(t). \quad (4.2)$$

It is interesting to note that we expect the two measurements, Eq. 4.1 and Eq. 4.2 to be equal to each other no matter how inelastic the collision with the force sensor is. It should not matter if this collision conserves the kinetic energy of the glider, increases it, or decreases it; we should always expect to be able to use Eq. 4.2 to predict P_f based on P_i , regardless of

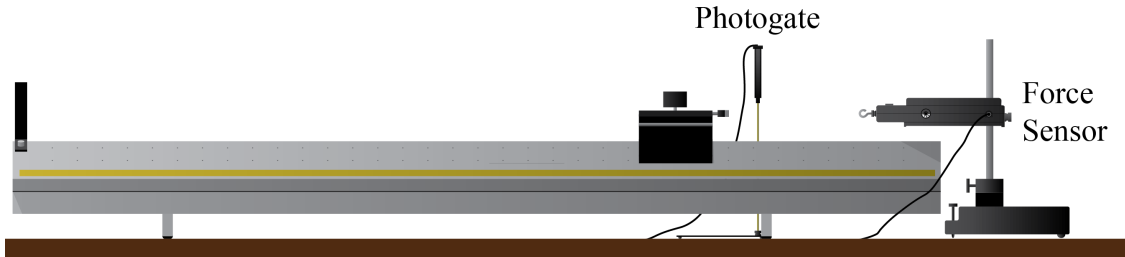
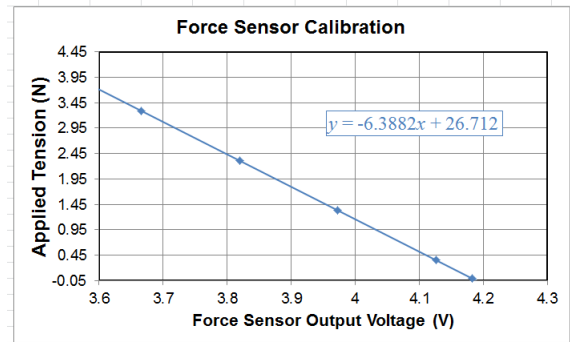


Figure 4.1: Apparatus for measuring the impulse of a glider colliding with a force sensor. The flag on the glider passes through the photogate both before and after the collision, providing a means to measure the initial and final momentum. The force sensor allows you to record $F(t)$, which can be integrated numerically to obtain an independent measure of the impulse.

whether there is a piece of bubble gum or a diamond on the end of the glider that hits the force sensor¹.

4.1 Procedure



Your first step will be to calibrate your force sensor, whose internal calibration is not trustworthy on the level needed for this experiment. You will essentially follow the same procedure as that used in Chapter 0. You will set up your force sensor as a **User Defined Sensor** whose output will be in volts. You should record the voltage reading for at least 5 different weights hanging from the force sensor hook spanning the range from 0 to not more than 1 kg. You may assume that the calibration slope found by measuring tension is also appropriate for compression.

You should be sufficiently familiar with the hardware at this point to be able to do this step without detailed instructions, but you may want to take a look back at Chapter 0 if you have questions. You may share your sensor calibration data with your lab partners, but you should perform the analysis and fitting on your own.

Figure 4.1 shows the experimental setup for producing your two, independent measurements of the impulse of the collision between the glider and the hook of the force sensor. The photogate flag on top of the glider allows you to use the photogate to measure the speed of the glider both before and after the collision. For this, you will need to know the mass of the glider (with all of its attached flags and bumpers) and the length of the photogate flag.

¹Please do not put gum on the lab equipment. However, please do feel free to leave diamonds all over it.

		X Run #1	● Run #1
	Time (s)	User Defined (V)	Speed (m/s)
907	0.4530	0.0798	
908	0.4535	0.0787	
909	0.4540	0.0783	
910	0.4545	0.0792	
911	0.4550	0.0781	
912	0.4555	0.0802	
913	0.4560	0.0787	
914	0.4565	0.0781	
915	0.4567		0.1925
916	0.4570	0.0781	
917	0.4575	0.0799	
918	0.4580	0.0786	
919	0.4585	0.0787	

Figure 4.2: The DAQ will rapidly fill in the first two columns of your table once you tell it to record. By scrolling through the table while watching the speed column, you should be able to find your measured initial and final speeds, which will be the two entries in this column.

You will use the **Speed** function of the photogate timer, so you will need to enter the length of the flag into Capstone during setup.

To configure the photogate, select **Photogate** for the appropriate channel and then move on to **Timer Setup**. Choose a **Pre-Configured Timer** for one photogate with a single flag. In Step 4, you will choose **Speed** as the measurement that will be visible, at which point you will need to type in the length of the flag (in meters) to complete your timer setup. The **Speed** measurement that Capstone uses is simply the entered flag length divided by **Time in Gate**, so feel free to use either, keeping in mind that the important thing is that the fractional uncertainty in flag length will be the same as the fractional uncertainty in the speed measurement (assuming the timing has a much smaller fractional uncertainty).

For the force sensor, you should keep the same settings you had for the calibration, which is to call it a **User Defined Sensor** on an analog channel.

Your data will consist of three columns in a **Table**, which will be filled in **Continuous Mode** once you hit **Record**. You will want a column for **Time (s)**, **User Defined (V)**, and **Speed (m/s)**. The first two columns will start getting filled in as soon as you hit **Record**, where the **Speed** column will only get two entries, which will show up only at the time the glider has passed through the photogate. In the **Controls** palette, be sure the sample rate for the **User Defined Sensor** is set fast enough to generate enough samples to give you good results without creating an excess of data. Capstone has been known to have sporadic problems on this experiment for high sample rates (≥ 10 kHz), so you may want to stick to sample rates of a few kHz and fairly gentle collisions to get good data for this experiment.

To take your data, start the glider moving toward to photogate and start recording just

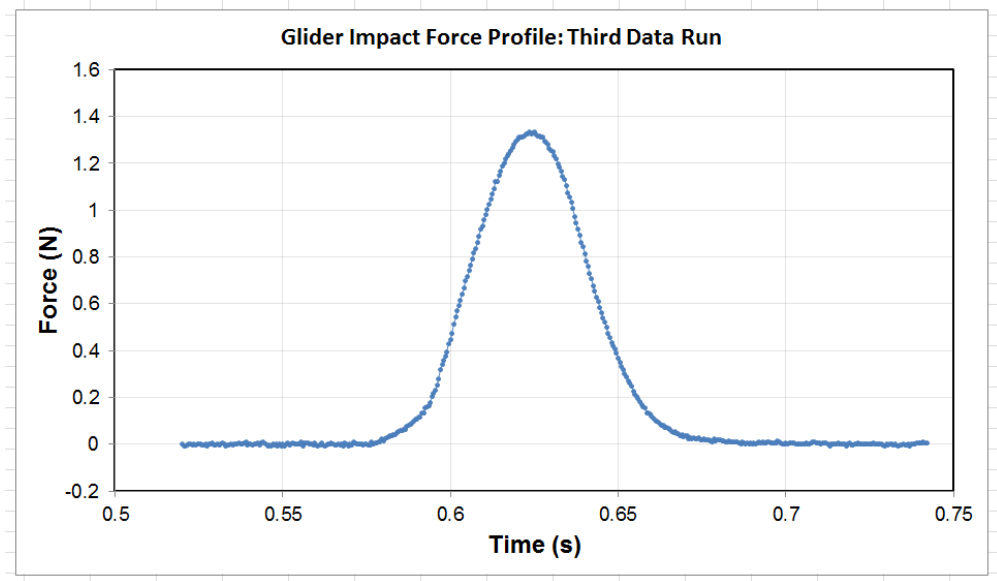


Figure 4.3: Force sensor reading before, during, and after the collision. The first 100 ms or so of data was averaged to provide a measurement of the force sensor baseline, which was subtracted from the data before creating this plot. The area under this curve is a measurement of the impulse of the collision.

before it reaches it. As soon as the glider has passed through the photogate on its way back the second time, you may stop recording. You will now have three columns of data, two of which are very full with the third one almost completely empty. Be sure to increase the number of displayed digits on your table to high enough precision so that you are not limited by this. Figure 4.2 shows an example of what part of your data might look like. You should be able to find two entries in the **Speed (m/s)** column. Write these down somewhere for your analysis, and be sure to think about whether or not to enter a minus sign on one of them (remember, the photogate does not know which direction your glider is moving).

Your two remaining columns of data may be quite long. If there are more than about 5000 rows, you should probably try re-taking your data with a faster trigger-finger on the record button so that you only get the part of the data you really need. You may find that you need to move the photogate closer to the force sensor to minimize the dead time, but be sure your photogate measures the glider speed when it is freely moving, not while it is impacting the sensor. By scrolling through your data, you should be able to find a section that shows lots of changes in the **User Defined (V)** section. That section is what you will need for your report, so copy and paste it (both columns) into Excel for saving. Be sure to get enough data before and after the collision to give you a good feel for your baseline (see Fig. 4.3). **Each person will need two data sets of their own for their analysis.** Try to get two different speeds to compare them to one another.



Figure 4.4: Force sensor reading before, during, and after a fast collision. The reading shows oscillations, or “ringing” after the collision that can be ignored for your integration.

4.2 Analysis

For your determination of the calibration of the force sensor, plot your data and run a regression fit to determine the slope (with uncertainty). You will probably want your slope to have units of N/V so that you can just multiply it by your column of recorded voltages to get force. Remember to flip the sign appropriately to convert between tension and compression.

Your first measurement of the impulse comes from your two speed measurements given by the photogate. Multiply your measured velocities by the mass of the glider to create a measured value of the initial and final momentum, then use Eq. 4.1 to convert this into a measurement of the impulse.

Using your calibration of the force sensor, you can create a new column in Excel that converts your measured voltages into force. Create a scatter plot of your measured force vs. time. Even if you tared the force sensor before taking your data, you will want to choose a big group of data points at the beginning to average to define your baseline, so use your scatter plot to choose an appropriate range to average for this and create a new column of forces that have the background subtracted. You can now create a new scatter plot of your results, as shown in Fig. 4.3.

You may notice that your plot shows some “ringing” in the reading after the collision,

such as is shown in Fig. 4.4. For your numerical integration of your data, this can be safely ignored as long as the amplitude of the oscillations is much smaller than your impact (such as is shown in Fig. 4.4), and your integration really only needs to include the big peak from when it starts to rise to about the point where it crosses zero again.

To complete your analysis, you will want to integrate your data to find the area under the big peak of your force vs. time plot (Eq. 4.2). To do this integral numerically, simply find the sum of all of the force measurements during the big peak and multiply this by the duration of the small time step Δt between successive points. This method of numerical integration is called a Riemann sum, and we have assumed that the force measurements are all equally spaced in time by Δt . Mathematically, we are using

$$\Delta P = \int_{t_1}^{t_n} dt F(t) \approx \Delta t \sum_{i=1}^n F(t_i) \quad (4.3)$$

where $\Delta t \equiv t_{i+1} - t_i$. You should compare your impulse measured with both methods. If they are off by a large factor, make sure you got all your units correct and that you subtracted the background force reading appropriately.

4.3 Report Guidelines

As usual, you will be expected to use what you learned from the presentation mini-reports of Experiments 1 and 2 to format your report (citations and plot guidelines). However, you will not be called upon to produce an abstract, etc. (covered in Experiment 3's presentation mini-report) again until you begin writing full lab reports in Experiment 5.

This week's worksheet will be worth 40% of your grade, with the presentation mini-report representing the remaining 60%.

4.3.1 Worksheet Guidelines

Your worksheet should contain the following sections

1. Cover Sheet

- experiment number and title
- your name and UID
- the date the lab was performed
- your lab section (for instance, “Wednesday 9am”)
- your TA’s name
- your lab partners’ names

2. Discussion

- Present your measured values for the mass of the glider (with all its accessories on it) and the width of the photogate flag, with uncertainties.

- Present a plot of your calibration of the force sensor. You do not need to make a table, but be sure to include the fit line on your plot.
- Be sure to state your calibration constant for converting the force sensor voltage into newtons with the uncertainty you found for this constant. This can either be in the plot caption or can be written as body text and referenced in the plot caption.
- Present your two calculated impulses that were based on the photogate speed measurements, one for each data run.
- Include a plot of each of your two measured force vs. time curves with the background subtracted from the force sensor.
- Describe how you used the force vs. time data to determine the impulse, *i.e.* how you performed the numerical integration.
- Present your two measured values for the impulses based on numerical integration of the force profiles. To assign an uncertainty, you may estimate this by assuming the fractional uncertainty of your integral is the same as the fractional uncertainty of your force sensor calibration coefficient.
- State the results of the two different methods for both runs in a table (with uncertainties).

3. Extra Credit (optional, as always)

The inelasticity of a collision can be quantified through a unitless number called the *coefficient of restitution*, C_R . When two objects collide, C_R is defined as the ratio of the final relative speed of the colliding objects to the initial relative speed. As such, it tells you something about how elastic the collision was, where $C_R = 1$ for perfectly elastic collisions and $C_R = 0$ for completely inelastic collisions. Team up with another table and use two gliders and two photogates on the same setup to measure C_R for two gliders colliding with different bumpers (including one collision with no bumpers). Compare the degree to which energy and momentum have been conserved for each collision.

4.3.2 Presentation Mini-Report Guidelines

For this week's presentation mini-report, please write an introduction and a methods section for your work on Experiment 4. Please write the word count for your introduction on a new line below its last sentence.

Introduction

The introduction section explains, in your own words, the purpose of your experiment and how you will demonstrate this purpose. Try to be as brief as possible while getting your point across. The main idea is to leave the reader with a good idea of what you were trying to measure and how you went about it without going into painfully extreme detail.

According to Nature letters this should be less than 300 words so we will stick to that. The introduction should give historical background, explain what problem you are trying to solve, motivate how this work solves that problem and briefly explain what you did.

Methods

The methods section should outline in full technical detail how you set up the experiment, what equipment you used and how you avoided systematic errors. How you analyze your data is normally included in the analysis section that is not required this week. This means you may reference analysis techniques in your methods section even if though the analysis section does not exist! The methods section should have enough detail that a student with the same equipment should be able to reproduce your results – after all, science demands reproducibility. You do not need to describe the details of the software or DAQ to the reader, who can be assumed to know what a DAQ is and may use a different one to perform the same experiment. But they should know what the DAQ is doing (what is it driving, measuring, triggered on, etc.). Be sure that any images of equipment, charts or graphs are properly cited unless explicitly created by you.

4.4 Epilogue

Smart phones these days are amazing. Your author could go on about this for days, but one of the neat features available is the vector accelerometer. By attaching a smart phone to the glider and performing the same experiment you did this week, your author was able to take data at the same time with the smart phone and the PASCO force sensor. By multiplying the measured acceleration by the mass of the smart phone and glider system, very good agreement between these two methods was achieved (see Fig. 4.5).

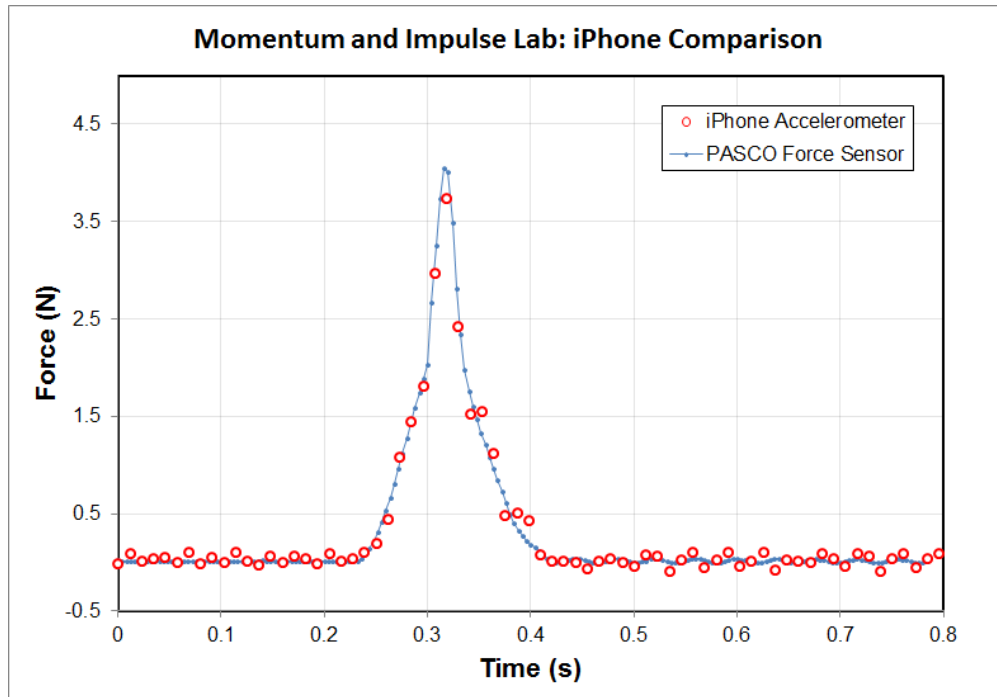


Figure 4.5: Comparison between the PASCO force sensor reading and the accelerometer from an iPhone 4 that was riding along with the glider. The only free parameter for simultaneously plotting the two data sets was the time offset.

Experiment 5: Harmonic Oscillator

Part I. Spring Oscillator.

The career of a young theoretical physicist consists of treating the harmonic oscillator in ever-increasing levels of abstraction. -Sidney Coleman

You have already briefly encountered a harmonic oscillator in Experiment 3, where a glider was held between two springs on an air track. The next three experiments in this course are spent going into greater detail in the study of oscillating systems. You will study the effects of damping, resonance, driving, superposition, normal modes, and phase shifts in these systems. Here, in Experiment 5, you will be measuring the resonant frequency of an undamped and damped harmonic oscillator. You will measure the damping term and compare your results to predicted values based on a simple model. You will want to keep your calculations from this experiment handy because you will need to apply some of these techniques in your analysis of Experiment 6.

The oscillator for Experiment 5 is a mass hanging from a spring, shown in Fig. 5.1. You will measure the mass and the spring constant, which will allow you to make a prediction for the resonant frequency (f_o , the cyclic frequency in Hz) of this undamped harmonic oscillator:

$$f_o = \frac{1}{2\pi} \sqrt{\frac{k}{m}}. \quad (5.1)$$

The spring will hang from a force sensor, providing you with a means to monitor the oscillations of the hanging mass as a function of time using the DAQ. In your analysis, you will be able to produce a measurement of f_o and compare it to your predicted value based on Eq. 5.1.

We will then add a damping force $F = -bv$ that is proportional to the velocity v of the oscillating mass. We can model this system by an equation of motion of the form

$$m\ddot{x} = -kx - b\dot{x} \quad (5.2)$$

where k is the spring constant and x is the position of the mass in the vertical direction¹. The damping term, b , has units of mass/time, and tells you something about how much

¹If you are not familiar with the dotted notation, each dot is a shorthand for a derivative with respect to time. So $\dot{x} \equiv dx/dt$ and $\ddot{x} \equiv d^2x/dt^2$, etc.

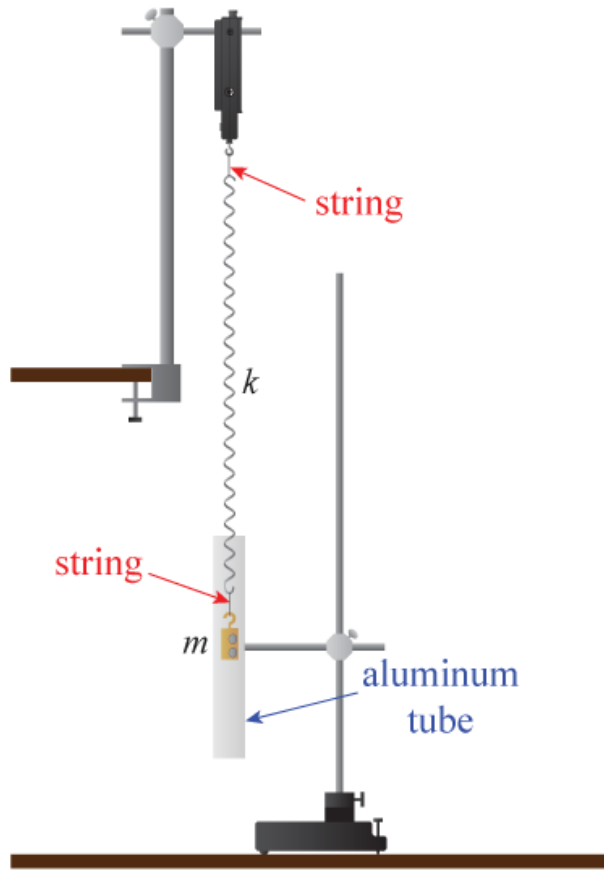


Figure 5.1: A weight hanging from a spring can exhibit oscillatory motion that is well-described as being a simple harmonic oscillator. The force sensor from which the weight hangs provides readout of the oscillatory motion. The weight has strong magnets attached so that when the motion occurs inside a hollow aluminum tube, eddy-current heating provides a dissipative force that is proportional to velocity. It is important to decouple the rotation of the spring from the mass by using thin strings to attach the spring at both ends.

time it takes to damp out oscillations of some given mass. We will typically be concerned not with b itself, but with combinations of b , m , f_o , and k that are more straightforward to interpret.

Experimentally, it is a little bit challenging to come up with a method for producing a pure damping term of this form without, for instance, adding a friction term (which would not depend upon velocity). Your hanging mass for this experiment has some strong magnets embedded in it, which we will use to produce the necessary damping force. The hanging, oscillating mass will be surrounded by a vertical conducting tube that is made from aluminum, a “nonmagnetic” material.

The effect of this tube on a magnet that is not moving will be very small and we will neglect it here. However, when the magnetic field is *changing in time* due to the motion of your oscillating mass, it causes eddy currents in the aluminum to be created due to the tube’s inductance. The induced current is proportional to the velocity of the hanging mass. Since aluminum has some finite resistivity, these currents are dissipated into heat. You will not be required to derive these effects, but it is useful for you to have some idea why a non-magnetic material might have a profound effect on the motion of a magnet.

By monitoring the amplitude of oscillations as a function of time, you will be able to test whether the damping really is well-described by Eq. 5.2, and to provide a measured value for $2m/b$, which is the characteristic “damping time” of your damped oscillator. This will also permit you to measure the Q -factor (or, simply the Q) of your resonance, which allows you to complete your simple model of this system.

5.1 Theoretical Background

Your TA will probably cover this in more detail before you begin your experiment, but this section is a brief discussion of how to derive the relationships needed for your analysis. Given Equation 5.2:

$$m\ddot{x} = -kx - b\dot{x},$$

we want to find the form of the solutions for $x(t)$. As is often the case when dealing with differential equations, we can resort to a method of guess-and-check to find solutions. We will use complex notation for our oscillator to make the algebra easier, choosing to try the following form for our solution

$$x(t) = Ae^{i\omega t}. \quad (5.3)$$

We are in this case only interested in finding the (possibly complex) frequency ω , which characterizes the time-dependence of the oscillator’s behavior. To find ω , we can simply plug this into 5.2 to get

$$\begin{aligned} -\omega^2 m A e^{i\omega t} &= -k A e^{i\omega t} - i\omega b A e^{i\omega t} \\ m\omega^2 &= k + i\omega b. \end{aligned} \quad (5.4)$$

We can solve this quadratic equation for ω using the quadratic formula to get

$$\omega = \frac{ib}{2m} \pm \sqrt{\frac{k}{m} - \frac{b^2}{4m^2}}. \quad (5.5)$$

Exercise 5.1 Sanity check: what does Eq. 5.5 give us if we remove the damping? This should make some sense given what you know about oscillating spring-and-mass systems. Also, how should we interpret the \pm in Eq. 5.5? As a hint, consider the fact that we chose a solution of the form $x(t) = Ae^{i\omega t}$ instead of $x(t) = Ae^{i\omega t} + Be^{-i\omega t}$.

We will take the plus sign of the \pm for concreteness, but all of this analysis works just as well if we chose the minus sign. Since this frequency has a nonzero imaginary part, we would like to interpret what this means. Consider what happens if we plug Eq. 5.5 back into Eq. 5.3:

$$\begin{aligned} x(t) &= Ae^{i\left(\frac{ib}{2m} + \sqrt{\frac{k}{m} - \frac{b^2}{4m^2}}\right)t} \\ &= Ae^{i\sqrt{\frac{k}{m} - \frac{b^2}{4m^2}}t} \times e^{-bt/2m}. \end{aligned} \quad (5.6)$$

The second term in Eq. 5.6 is a pure exponential decay and does not contain any oscillating terms. This comes from the imaginary part of Eq. 5.5, and demonstrates that imaginary frequencies are usually used to express dissipative terms. We can therefore introduce the *damping time* τ , defined as

$$\tau \equiv \frac{2m}{b}. \quad (5.7)$$

The damping time is the amount of time it takes this undriven, damped oscillator to have its amplitude decrease by a factor of $1/e$.

The first term in Eq. 5.6 is oscillatory and suggests that we adopt the following definition:

$$f_{\text{damped}} = \frac{\omega_{\text{damped}}}{2\pi} \equiv \frac{1}{2\pi} \sqrt{\frac{k}{m} - \frac{b^2}{4m^2}} = f_0 \sqrt{1 - \frac{b^2}{4km}} \quad (5.8)$$

where f_0 is given by Eq. 5.1. It is helpful to look back at Eq. 5.6 with these new definitions, giving us

$$x(t) = Ae^{i\omega_{\text{damped}}t} \times e^{-t/\tau}. \quad (5.9)$$

The real part of this expression is clearly a sinusoidal oscillation at frequency ω_{damped} that has an exponentially-decaying amplitude with time constant τ .

Last, we will define something called the *Q-factor* (also known as the “quality factor” or simply as “the *Q*”) of this resonance, which is 2π times the ratio of the total mechanical energy to the amount of energy that is dissipated in a single cycle. Without proof, we will define Q to satisfy

$$f_{\text{damped}} \equiv f_0 \sqrt{1 - \frac{1}{4Q^2}}, \quad (5.10)$$

which gives us

$$Q = \frac{\sqrt{km}}{b}. \quad (5.11)$$

In the limit of $Q \gg 1$, the Q of a resonance is also the ratio of the resonant frequency (f_{damped}) to Δf , the full-width-at-half-maximum (FWHM) of the (power) resonance curve. The power resonance curve would be a plot of, for instance, energy dissipated per cycle vs. frequency. You will explore this in more detail in Experiment 6.

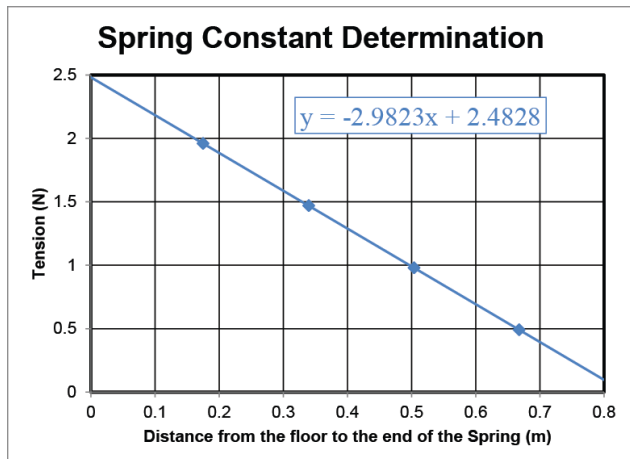
5.2 Procedure

Since you will be measuring the frequency of a weight hanging from a spring, you will need to measure the mass of the weight and the spring constant to provide something against which to compare your direct time-domain measurement. While it may not be important for your measurement of the spring constant, make sure that the spring is attached to the hook of the force sensor via a string instead of being attached directly (and likewise for the weight on the bottom of the spring), as shown in Fig. 5.1. Using a string to decouple the rotation of the spring as it stretches from the mass and hook is important for making sure your system is well-modeled by the simple equations above.

Measure the spring constant by hanging at least 5 different masses from the spring and recording its length. You may find it is easiest to record the distance from the end of the spring to the floor, because this removes the need to hold the meter stick up in the air. Since this distance is linearly related to the length of the spring, the spring constant is still the slope, but there will be an overall minus sign (the spring constant is positive for these springs). You will perform the usual fitting in your analysis to turn these measurements into a measurement of the spring constant.

Next, you will set up the DAQ to measure the tension applied to the hook on the force sensor as a function of time. For Experiment 5, you do not need to know the *value* of the force, so feel free to set up the force sensor to display voltage or (uncalibrated) force units as you see fit. For this discussion, we will assume the output is being recorded in volts.

In order to measure the frequency of oscillations, you will start the mass oscillating freely and record the force sensor reading vs. time, as shown in Fig. 5.2. Be sure to keep the oscillation amplitude small enough that the spring stays linear, which means the coils should not touch one another and the spring should not be anywhere close to being plastically deformed, etc. For this measurement, it is good to have both a **Table** and a **Scope** display running simultaneously. You will want a sample rate that is high enough to really capture



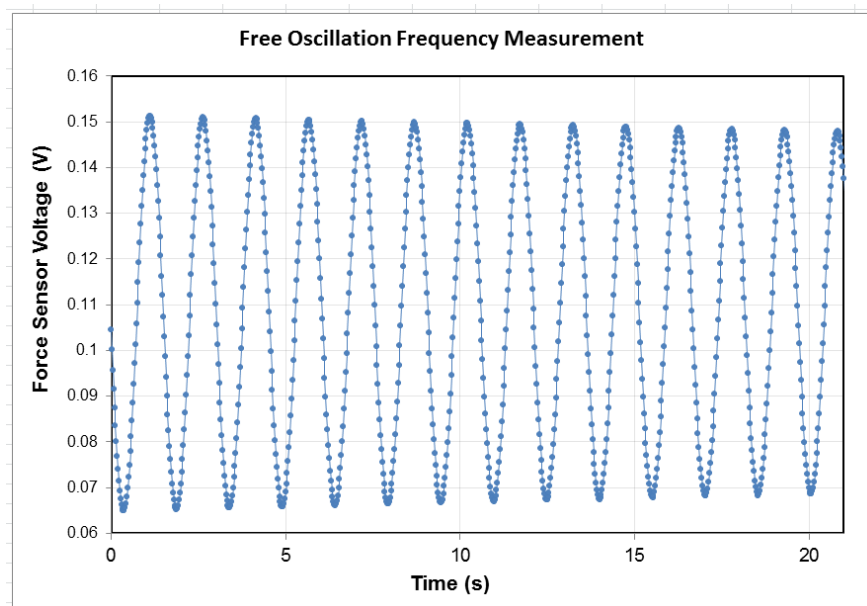


Figure 5.2: Free oscillation of a mass hanging from a spring. The oscillation frequency can be obtained by, for instance, zooming in on the first and 14th oscillation minima and dividing 13 by the difference between these two times. Note the subtle decay of the oscillation amplitude due to dissipation; this oscillator has a Q of more than 500.

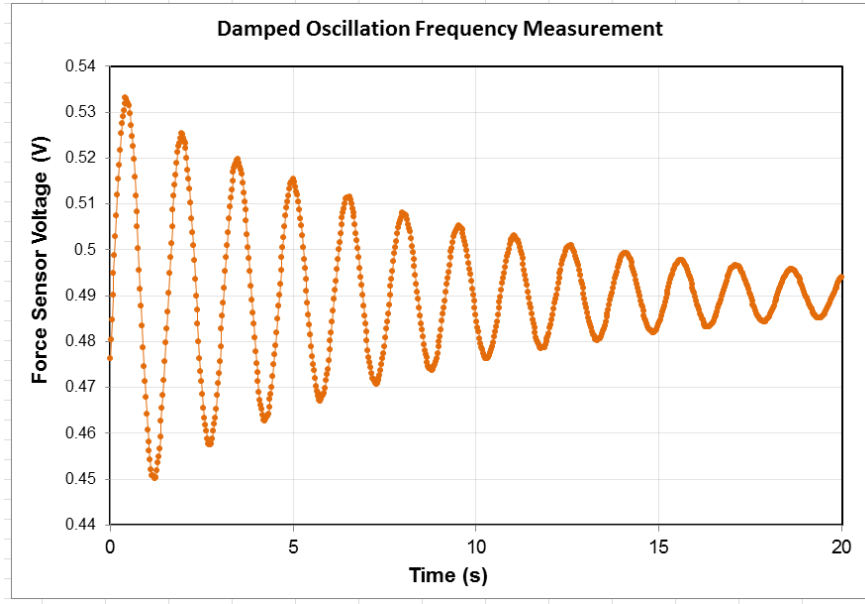


Figure 5.3: Damped harmonic motion. The characteristic damping time in this case is about 9.5 seconds, which corresponds to a Q of about 20.

the force maxima and minima (the “extrema”), so be sure your sample rate is at least 20 Hz in the **Controls** palette. If you exceed 50 Hz sample rate, it is likely that the amount of data you generate will be large enough to be a headache for you and you will not get a better measurement, so try something in the middle. Record oscillations for at least 20 seconds and up to 1 minute and then copy your voltage vs. time data into Excel for your records. Sometimes the force sensors show a significant drift in their mean value over the course of 20 seconds, so you may want to write down an estimate for this drift or to “warm up” the sensor by letting your weight oscillate on the force sensor for a few minutes. This effect is more important for the damped motion, so be sure to keep an eye on it and to either quantify the drift or find a way to remove it for the next part.

Next, you will record the same time-domain data with the damping term added. Arrange the aluminum tube to surround the oscillating weight without touching it. The magnets in the weight will produce a damping force when the tube surrounds the moving weight. Record the force sensor reading vs. time again and save your data. You will notice a significant decay in the oscillation amplitude as a function of time, as shown in Fig. 5.3.

5.3 Analysis

Plot your displacement vs. weight data and fit a line to determine the spring constant. Use a regression analysis to get an uncertainty on the slope, as usual. Combine this with your measured mass of the weight with embedded magnets to come up with a prediction for the

free oscillation frequency f_o using Eq. 5.1.

Next, you will measure the frequency of free oscillations directly from your time-domain voltage vs. time data. Plot your data and use the positions of the extrema to determine the oscillation frequency. You can do this by, for instance, zooming in on the first maximum to determine the time when this occurred, doing the same for the n th maximum, then dividing $n - 1$ by the time difference, which will yield f_o . You should estimate uncertainty by using some reasonable method, such as repeated measurements with different extrema or estimating your uncertainty in identifying exactly when each extremum occurred.

Do the same for your damped motion data. You will find that it is more difficult to determine the damped motion frequency (f_{damped}) than the free oscillation frequency since the signal-to-noise ratio gets worse as the signal amplitude decays, so your uncertainty is likely to be quite a bit larger for the damped motion than the free oscillations. Nonetheless, it should be possible to obtain a pretty good measurement of the damped oscillation frequency.

Next, you will see if the damping is well described by a velocity-dependent force and estimate the damping time τ (see Eq. 5.7). τ is the $1/e$ decay time of the amplitude of the oscillations, and the amplitude will only decay exponentially in time if the damping is indeed caused by a velocity-dependent damping force (as opposed to, say, a friction force). To do this, your first step will be to find the voltage that corresponds to the midpoint in the oscillations, as there is almost certainly a significant offset in your measurement. You need to subtract this offset from the peak voltages to measure the amplitude.

For instance, consider the data shown in Fig. 5.3. These oscillations are clearly not centered around 0 volts, and it looks like there is an offset of about 0.49 V. Try to find the proper offset voltage to subtract from your data to give you oscillations that are centered around zero. You may find that the force sensor reading drifted *during* your data run, in which case you may need to choose a sort of mean value or try subtracting a linear drift from the data. If your data includes points after essentially all of the oscillations died out, that may provide you will a good measure of the offset voltage. Subtract your offset from your data to produce oscillations that are centered around zero.

One of the things about an exponential decay is that the ratio of the heights of all pairs of successive maxima should be the same since the maxima are separated by the same time interval ($T = 1/f$). Record the heights of at least 6 successive maxima (more if you have good data). Calculate the ratio of the height of peak 1 to peak 2, then peak 2 to peak 3, and so forth for your data set. If the damping is indeed proportional to the velocity, these ratios should all give the same result.

Plot your ratios as a function of which extrema were being used as shown in Fig. 5.4. If the damping force is proportional to velocity, there should not be a discernible nonzero slope to the data in the plot and the scatter will be centered around some mean value. If you do detect a systematic trend upward or downward, be sure that you subtracted your offset voltage correctly, as doing this improperly will also result in a drift of the peak hight ratios with extremum number.

If you recorded amplitudes once per oscillation period T , the ratio of successive amplitude

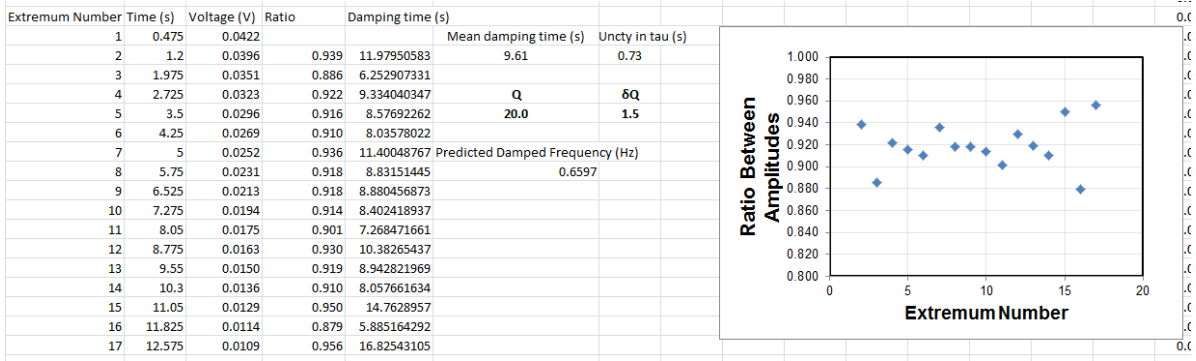


Figure 5.4: Analysis of the damped motion shown in Fig. 5.3. The peak height ratios are all centered around 0.92. Notice that the scatter seems to increase with extremum number, as expected since the peak height uncertainty increases.

measurements in an exponentially-decaying oscillation will be given by

$$\frac{V(t+T)}{V(t)} = \frac{e^{-(t+T)/\tau}}{e^{-t/\tau}} = e^{-T/\tau}. \quad (5.12)$$

Since you already have a measurement of $T = 1/f_{\text{damped}}$, you can convert each ratio measurement into a measurement of τ by solving for the amplitude damping time

$$\tau = -\frac{T}{\ln \left[\frac{V(t+T)}{V(t)} \right]}. \quad (5.13)$$

If your individual data points for the amplitude ratio did not show a trend (such as shown in Fig. 5.4), you can use your first and last measured amplitude to determine the damping time. Alternatively, you may combine all of your data points into a measurement of the damping time with uncertainty, $\tau = \tau_{\text{best}} \pm \delta\tau$. For this, you may use the procedure outlined in §ii.1.6 to help you come up with an uncertainty in your mean value of τ .

Next, determine Q from your measurements. There are a couple of ways to do this, so find a method that makes sense to you. Last, using your measured Q , predict the frequency of damped oscillations based on your measured frequency of free oscillations f_o . Is your measurement of f_{damped} consistent with this? Is the difference between your best value for f_o and f_{damped} statistically significant, or is the difference smaller than their uncertainties?

5.4 Report guidelines

This week, you will turn in your first full lab report. There will not be a worksheet this week. If you do the extra credit, include it in your lab report as if it were a normal part of your experiment. Your lab report should contain the following items.

1. Cover Sheet

- experiment number and title
- your name and UID
- the date the lab was performed
- your lab section (for instance, “Tuesday 3pm”)
- your TA’s name
- your lab partners’ names
- the word counts for your abstract and for the body text of your whole report

2. Full Lab Report

This week you will write a full lab report including abstract, introduction, methods, analysis and conclusions sections. Your completed lab report should look like an article submitted to a scientific journal. All guidelines from all of the previous weeks’ presentation mini-reports apply to this report, with the exception of reporting word counts, which are to be reported in the cover page as described above. Since you will be adding the analysis and conclusions sections, we will discuss some of the important points of these parts of a journal article.

Analysis

This section should contain an explanation of how the data were analyzed to test the experimental results against theoretical models. The methods section should have explained how the data were obtained, but the analysis section presents the data itself to communicate what the data show about the relevant physics. This section will also typically include the discussion of uncertainty analysis, including any relevant derivations of error propagation equations that were used.

The analysis section is typically where you would put your “main plot” for the paper. The methods section can have plots, but the point of those is to describe how the data were taken, whereas the goal of a plot in the analysis section is to show how the data illustrate some point about physics.

Conclusions

Briefly restate the goals of the experiment and describe how your results demonstrate (or fail to demonstrate) these objectives. Briefly describe at least one possible source of systematic uncertainty that could affect your measurement (and which direction the effect would tend to systematically shift your observations) and suggest a future measurement to eliminate it.

Suggested content

Your report should be a fully self-contained description of your work this week. If you performed a derivation or a measurement as part of this, it should probably find its way into your report. While this is probably all the instructions you need at this point to write a high-quality report, the following is a list of some of the specific things from this experiment that you should probably include in your report in one form or another. That said, anything that is needed to communicate to the reader what was done and what it showed should be included.

- A derivation of two or three equations that show how the quantities f_o , Q , τ , and b are related to one another. You may take Eq. 5.10 to be a definition of Q .
- A description of how you determined the frequency of oscillations and how you measured the decay time in the damped case.
- Your measured mass of the hanging weight.
- A plot of the spring constant measurement and a statement of the result, with uncertainty.
- Your predicted value for the free oscillation frequency.
- A plot of the free oscillatory motion vs. time. You do not need to worry about calibrating the y -axis and may simply plot it as being the force sensor reading in volts.
- How did you determine the free oscillation frequency from the data in this plot? What was your result?
- Compare your predicted free oscillation period and your measured value. Do they agree? If not, try to explain what is the cause of the mismatch.
- A plot of the damped oscillatory motion in the same manner as your previous plot. Use these data to measure the damped oscillation frequency.
- A plot of the measured ratios of successive extrema in your damped oscillation measurement. Is there a trend? If so, what does this mean? If not, what does this tell you?
- Present your measured value for the damping time with uncertainty.
- State your measured value for Q (with uncertainty) and use this to make a prediction of the damped oscillation frequency.
- Compare your measured damped oscillation frequency to this prediction. Do they agree? Are the two oscillation frequencies distinguishable given their uncertainties?

3. Extra Credit

It is possible to determine the frequency response of this system to any periodic driving force using the data you obtained. One way that this frequency response may be obtained is by taking the Fourier transform of the time-domain signal, which is called

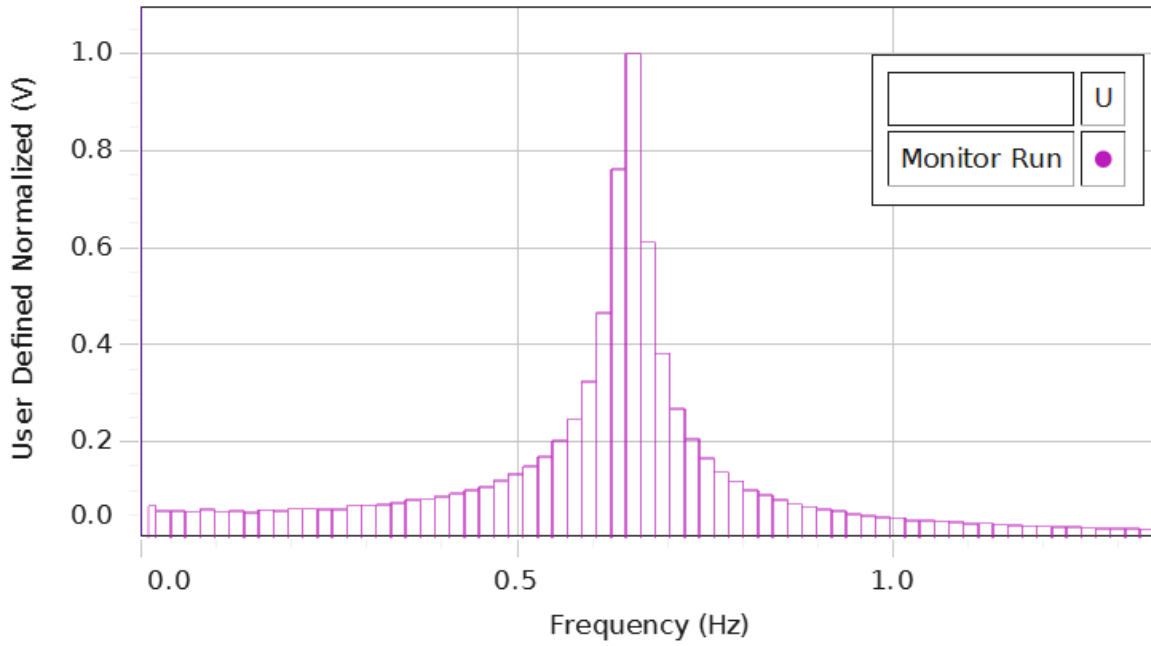


Figure 5.5: Fast Fourier Transform (FFT) of the data from Fig. 5.3. Based on the analysis, we would predict this *amplitude* spectrum to have a full width at $1/\sqrt{2}$ of its maximum of about $f_o/Q \approx 33$ Hz, which would be about two frequency bins wide on this plot, consistent with the spectrum shown.

the step response of your system. In Experiment 6, you will be looking at the amplitude response of another oscillator in the frequency domain, but it may be instructive to see what this would look like for the oscillator in Experiment 5. Capstone provides an algorithm for showing the frequency content in a time-domain signal called a Fast Fourier Transform (or FFT). Figure 5.5 shows the results of using this tool, which shows a very nice resonance curve.

Use the Capstone **FFT** tool in the **Displays** palette to see if you can generate a frequency-domain representation of your data such as that shown in Fig. 5.5. Estimate the width of the resonance (Δf), defined as the full width of this peak at a height of $1/\sqrt{2}$ of its maximum value. If Q is large, one way to calculate Q is as the ratio of the resonance frequency to the resonance width:

$$Q = \frac{f_o}{\Delta f}. \quad (5.14)$$

Use this to calculate Q and compare your answer to that obtained from your time-domain analysis.

5.5 Epilogue

Q-factors for resonators span a large range of values. The highest Q of which your author is aware for a man-made oscillator is an optical cavity that is made out of a single crystal of silicon [3]. This oscillator has a center frequency of $f_0 = 200$ THz and a frequency width of $\Delta f < 40$ mHz, which gives us $Q > 5 \times 10^{15}$. It is by using cavities such as these that researchers are able to obtain the passive stability required to make measurements such as those reported in [7] (Eq. ii.2).

Experiment 6: Harmonic Oscillator

Part II. Physical Pendulum.¹

The harmonic motion you have studied in previous experiments in this course was typically analyzed in the *time domain*, meaning you acquired and studied data as a function of time. It is also possible to analyze the properties of a harmonic oscillator in the *frequency domain*, which you will begin to explore in Experiment 6. You will also study the effects of damping in more detail, allowing you to demonstrate *underdamped*, *overdamped*, and *critically-damped* motion by experimentally controlling the damping coefficient. These concepts are important in control systems for physics and engineering applications, where we are often concerned with trying to find the fastest way to bring a system to a desired state.

The spring-and-mass oscillator you used in Experiment 5 was very well modeled by Eq. 5.2. However, you were not able to adjust the damping coefficient in a well-controlled manner using the aluminum tube, so we will use a more flexible setup in Experiment 6, shown in Fig. 6.1. An aluminum pendulum shaped like an anchor will serve as your oscillator. The oscillation frequency of this pendulum will be approximately independent of amplitude so long as the amplitude is small, where we will say that “small” means the angular motion does not move the bottom further than the width of the curved bottom portion of the pendulum.

A “wave driver” will be coupled to the pendulum through a vee-shaped torsion spring. This will allow us to not only drive the oscillator with a periodic signal, but also to read out the instantaneous position of the oscillator via the rotation sensor. Even though the wave driver will not be used for your study of damping regimes, the spring that couples the wave driver to the pendulum will be a factor in determining the resonant frequency of the pendulum. Since you will apply your results from the damping study to your study of driven oscillations and resonance, you should leave the wave driver attached to the pulley for your damping study even though it is not in use.

The wave driver can be connected to the DAQ via the banana jacks on the upper right of the 850 interface (see Fig. i.1). The rotation sensor plugs into one of the four “Passport” sockets on the bottom row of the 850 interface. Capstone will automatically detect and configure the rotation sensor, but you should configure output channel 1 to be an **Output Voltage Current Sensor**, which will allow you to monitor the phase of the drive signal.

¹This chapter was contributed by Priscilla Yitong Zhao (2013).

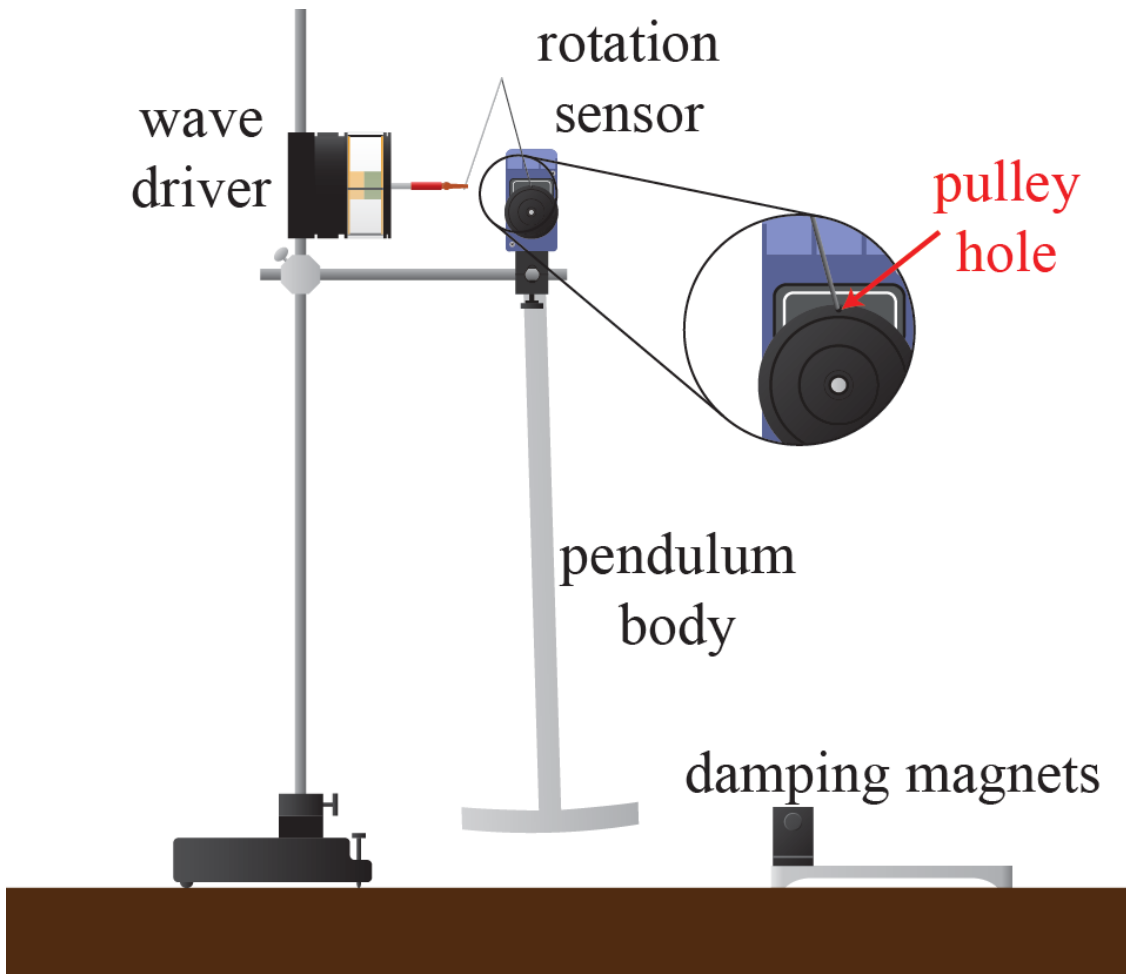


Figure 6.1: A physical pendulum for studying damping regimes and resonance. For small oscillations, the pendulum is a harmonic oscillator, and its angular position can be measured in real-time using a rotation sensor. A wave driver coupled to the pendulum by a torsion spring (shaped like a Λ , shown above) can be used to study damped, driven oscillations. The damping magnets can be moved into place and their spacing changed to provide a tunable velocity-dependent damping force.

Damping will once again be provided by eddy-current heating due to the motion of the oscillator. Unlike Experiment 5, however, this time it is the conductor that will be moving, and the magnets will be stationary. By moving the magnet stand so that the pendulum bottom passes midway between the two damping magnets, the amount of damping can be tuned by adjusting the spacing between the magnet poles and the bottom of the pendulum body.

You will acquire time traces for underdamped, overdamped, and critically-damped motion.

6.1 Theoretical Background

6.1.1 Undriven oscillations of a damped physical pendulum

A pendulum that is made of a rigid object (as opposed to a point-mass on an ideal flexible string) is known as a *physical pendulum*. It is no more or less physical than a ball on a rope, but this terminology is used nonetheless. The physical pendulum in this experiment is a sort of anchor-shaped piece of aluminum alloy cut from sheet metal, and will be characterized by a moment of inertia I about the rotation axis.

If we call the angular deviation of the pendulum from its equilibrium configuration θ , any nonzero value of θ will lift the center of mass of the pendulum above its equilibrium height. If the pendulum has a total mass M and the location of its center of mass is a distance l below the rotation axis, the restoring torque due to gravity will be given by $\tau_{\text{grav}} = -Mgl \sin(\theta)$.

The spring attached at the top also exerts a torque on the pendulum about its rotation axis. For an angular displacement θ , the spring's length is changed by an amount proportional to $\sin(\theta)$. The torque this exerts on the pendulum is proportional to this force times $\cos(\theta)$, resulting in a restoring torque that we may write as $\tau_{\text{spring}} = -B \sin(\theta) \cos(\theta)$.

Last, the magnet assembly at the bottom of the pendulum will exert a damping torque on the pendulum, turning the angular kinetic energy into heat via eddy-currents in the pendulum blade. This damping force is proportional to the tangential velocity of the blade, so the damping torque will be proportional to the angular velocity, which we will write as $\tau_{\text{damping}} = -b\dot{\theta}$. Putting these three terms together gives us an equation of motion for the pendulum that is rather complicated:

$$\begin{aligned} I\ddot{\theta} &= \sum_i \tau_i \\ &= -Mgl \sin(\theta) - B \sin(\theta) \cos(\theta) - b\dot{\theta} \end{aligned} \tag{6.1}$$

For small angular displacements ($\theta \ll 1$ rad), we may expand the trig functions and keep the first terms only, thereby invoking a *small angle approximation* ($\sin(\theta) \approx \theta$, $\cos(\theta) \approx 1$):

$$\begin{aligned} I\ddot{\theta} &\approx -(Mgl + B)\theta - b\dot{\theta} \\ &= -k\theta - b\dot{\theta} \end{aligned} \tag{6.2}$$

where we have defined a constant $k \equiv Mgl + B$.

If we compare Eq. 6.2 to Eq. 5.2, we see that this is exactly the same equation of motion as we had in Experiment 5 with the replacement $x \rightarrow \theta$, $m \rightarrow I$ and different physical definitions of k and b (with different dimensions). We may therefore write down the solutions directly by making these simple substitutions in Eq. 5.6

$$\theta(t) = Ae^{i\sqrt{\frac{k}{I} - \frac{b^2}{4I^2}}t} \times e^{-bt/2I} \quad (6.3)$$

$$= Ae^{i\omega_{\text{damped}} t} \times e^{-t/\tau}. \quad (6.4)$$

with the analogous definitions of the oscillatory frequency² and damping time:

$$\omega_{\text{damped}} \equiv \sqrt{\frac{k}{I} - \frac{b^2}{4I^2}} = \sqrt{\omega_0^2 - \frac{1}{\tau^2}} \quad (6.5)$$

and

$$\tau \equiv \frac{2I}{b} \quad (6.6)$$

with the undamped resonance frequency $\omega_0 \equiv \sqrt{k/I} > 0$.

The motion (described by the real part of θ) is again a sinusoidal oscillation at frequency ω_{damped} that has an amplitude that exponentially decays with time constant τ . We identify three regimes of damping in this system:

- *Underdamped motion* occurs when there is still oscillation of the pendulum for zero initial velocity, meaning θ changes sign at least once. This occurs when the oscillation frequency is faster than the damping rate: $\omega_0 > \frac{1}{\tau}$, which guarantees that ω_{damped} is purely real. A good example of underdamped motion can be seen in Fig. 5.3.
- *Overdamped motion* occurs when $\omega_0 < \frac{1}{\tau}$. Looking at Eq. 6.5 shows us that in this case, ω_{damped} will be purely imaginary, which means the angular displacement of the pendulum for zero initial velocity (Eq. 6.4) will be described by a pure exponential decay with no oscillations.
- *Critically-damped motion* is the crossover regime between these two cases, given by $\omega_0 = \frac{1}{\tau}$. For critical damping, the system will return to its equilibrium state faster than either overdamped or underdamped motion. Automobile suspension systems, the dash pots on the doors to the lab, and earthquake suppression systems are all examples of engineering tasks where one would want this feature of critical damping.

6.1.2 Driven oscillations

If the wave driver is driven by the analog output of the 850 interface, there will be a new term in the equation of motion for this physical pendulum that oscillates with the driving

²Here, as elsewhere in this manual, we use ω as a symbol for angular frequency (units of rad/s or just s⁻¹) and f as a symbol for cyclic frequency (units of Hz).

current, which we will assume is proportional to $\cos(\omega_d t)$ for drive frequency ω_d . In the small-angle approximation, we have

$$I\ddot{\theta} = -k\theta - b\dot{\theta} + C \cos(\omega_d t). \quad (6.7)$$

The solution to Eq. 6.7 consists of the sum of two terms, known as the *complimentary* and *particular* solutions:

$$\theta(t) = A_c \theta_c(t) + A_p \theta_p(t) \quad (6.8)$$

where the complimentary solution is the one we have from undriven oscillations

$$\theta_c(t) \equiv e^{i\omega_{\text{damped}} t} \times e^{-t/\tau} \quad (6.9)$$

and the particular solution is given by [4]

$$\theta_p(t) \equiv \frac{1}{\sqrt{(\omega_o^2 - \omega_d^2)^2 + \left(\frac{2\omega_d}{\tau}\right)^2}} \cos(\omega_d t - \phi(\omega_d)) \quad (6.10)$$

where

$$\phi(\omega_d) \equiv \arctan\left(\frac{2\omega_d}{\tau(\omega_o^2 - \omega_d^2)}\right). \quad (6.11)$$

The complimentary solution describes all of the *transient* behavior of the system, which depends upon things such as initial conditions but does not depend upon the driving term in any way. This behavior is called transient because as $t \rightarrow \infty$, $\theta_c \rightarrow 0$. The timescale over which the transient behavior dies out is τ for critical and underdamping. For this experiment, this means that when you make a change to the system by, for instance, changing the drive frequency, you must wait at least τ before interpreting the behavior of the system as being dominated by the particular solution. You should consider this when trying to decide how to set the damping rate for the second half of this experiment.

6.1.3 Resonance

The particular solution, on the other hand, describes the *steady-state* behavior of the system under a constant-amplitude, sinusoidal driving torque. The pendulum will oscillate at exactly the drive frequency ω_d , but with an amplitude and phase that depend upon the relationship between ω_d and ω_{damped} . Fig. 6.2 shows the calculated amplitude of the steady-state behavior for a series of oscillators with the same undamped resonance frequency but different levels of damping.

The drive frequency at which the amplitude is maximized is called the *resonant frequency* of the damped, driven system, ω_R . To find ω_R , we can differentiate the amplitude of the response in Eq. 6.10 with respect to ω_d and solve for ω_d such that this is zero, which gives us the resonant frequency of a damped and driven harmonic oscillator:

$$\omega_R = \sqrt{\omega_o^2 - 2\frac{1}{\tau^2}}. \quad (6.12)$$

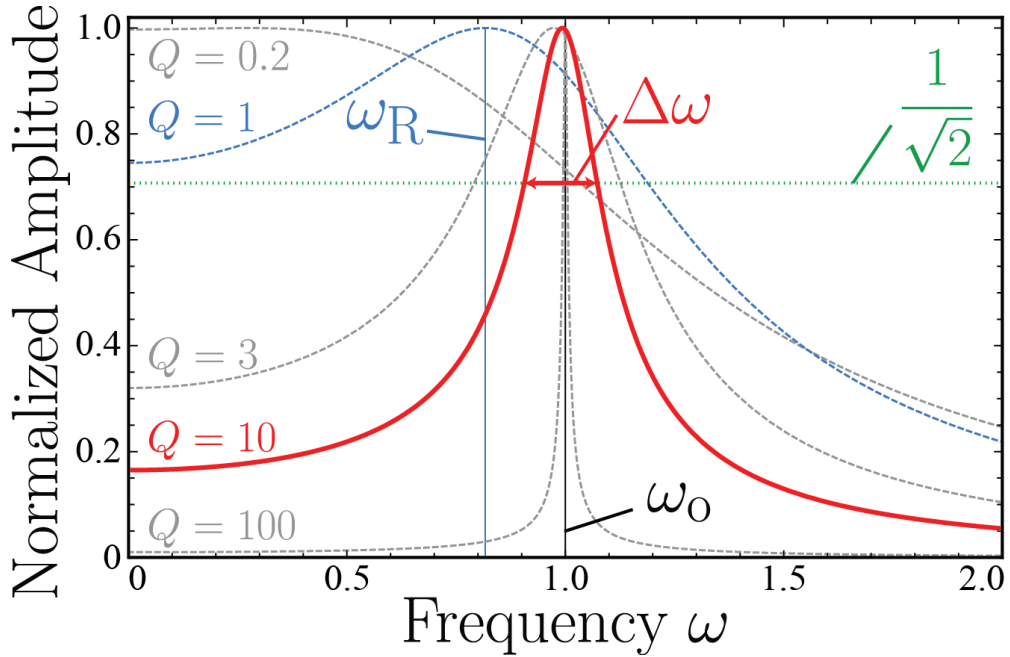


Figure 6.2: Amplitude response of damped resonators. The amplitudes are normalized to set the peak amplitude equal to 1, and the undamped resonance frequency for all curves is $\omega_o = 1$. Low- Q oscillators show resonant frequencies ω_R that are significantly different from ω_o . As the quality factor increases, the resonance position converges to $\omega_R = \omega_o$. The resonance width $\Delta\omega$ is shown for a $Q = 10$ resonance, where $\Delta\omega$ is the full width when the amplitude is $1/\sqrt{2}$ times its maximum value.

Comparing this to Eq. 6.5, we see that the resonant frequency can be close to ω_{damped} , and in many situations they are used interchangeably. In the limit $\tau \gg 1/\omega_o$, both of these resonant frequencies converge to ω_o , and you will find that they are often assumed to be equal (especially for $Q \geq 10$ or so, see below).

We can define the *quality factor* Q of this system to be

$$Q \equiv \frac{1}{2}\tau\omega_R \quad (6.13)$$

to rewrite our particular solution as

$$\theta_p(t) \equiv \frac{1}{\sqrt{(\omega_o^2 - \omega_d^2)^2 + \left(\frac{\omega_R \omega_d}{Q}\right)^2}} \cos(\omega_d t - \phi(\omega_d)) \quad (6.14)$$

For an oscillator with a high Q-factor ($Q \gg 1$), the damping time τ is many oscillation periods long. As discussed above, in this case we see that ω_R and ω_{damped} are both approximately equal to ω_o . In fact, we can rewrite Eq. 6.12 in terms of Q as

$$\frac{\omega_R}{\omega_o} = \frac{1}{\sqrt{1 + \frac{1}{2Q^2}}}. \quad (6.15)$$

This factor goes to 1 very quickly as Q is increased. For instance, an oscillator with a modest quality factor of $Q = 3$ has a resonance frequency that is only about 3% slower than the undamped case.

For these cases where the damping is very slight and the Q is therefore substantially greater than 1, it can be shown that the Q-factor is the ratio of the resonant frequency to the width of the resonance curve

$$Q \approx \frac{\omega_o}{\Delta\omega} \quad (6.16)$$

where $\Delta\omega$ is the full width of the resonance, defined to be the frequency range over which the amplitude response (the amplitude in Eq. 6.14) is greater than or equal to $1/\sqrt{2}$ of its maximum value. (This will be familiar to you if you did the Extra Credit from Experiment 5.)

Last, the phase term described in Eq. 6.11 is shown in Fig. 6.3 for the same oscillators as the amplitudes in Fig. 6.2. This plot has been constrained to positive values of ϕ to show that the phase changes smoothly through resonance, a general property of damped oscillators. Far below undamped resonance, the phase of the response is almost exactly the same as the drive, but begins to increase as undamped resonance is approached. Right on undamped resonance ($\omega_d = \omega_o$), the phase lag is exactly $\phi = \frac{\pi}{2}$, regardless of the quality factor. Past this point, the phase lag continues to increase, asymptotically approaching $\phi = \pi$ at infinite frequency.

From a practical perspective, if we are tasked with trying to locate the (undamped) resonant frequency ω_o (a common situation in physics and engineering), looking at the phase response is going to be far more sensitive than using the

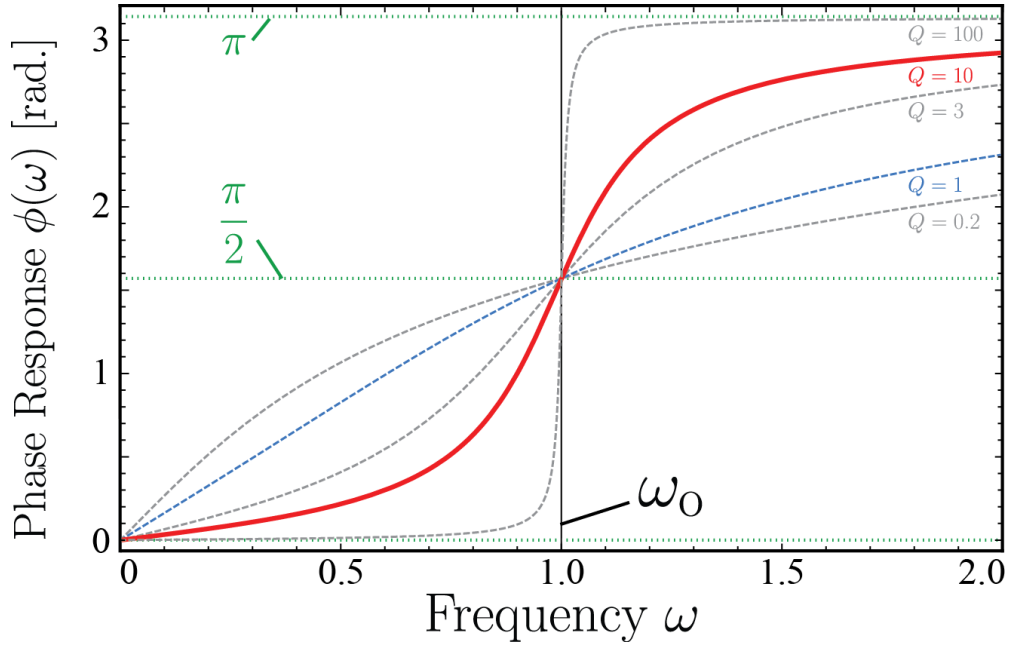


Figure 6.3: Phase response of damped resonators. The phase response is the difference between the phase of the driving force and that of the displacement. Curves are shown for the same parameters as Fig. 6.2. For driving frequencies below undamped resonance, the response is said to be “in phase with the drive,” with the lag increasing as the drive frequency increases. At the undamped resonant frequency, the response is out of phase from the drive by $\pi/2$, regardless of Q . Past this point, the response is said to be “out of phase with the drive” and the phase lag continues to increase with frequency, saturating at $\phi = \pi$.

amplitude response. The reason is that in the immediate neighborhood of resonance, the amplitude response levels out and does not depend sensitively on frequency, whereas the phase response has a maximum slope at this point. The amplitude response therefore becomes insensitive to frequency right where you need it the most, while the sensitivity of the phase to frequency is maximized here.

6.2 Procedure

To set up the apparatus, start by connecting the spring on the wave driver to the wheel on the pendulum rotation sensor as shown in Fig. 6.1. You will leave this connected for the entire experiment. To make sure the pendulum swings freely for all parts of the experiment, set the heights of the posts and clamps so that the pendulum blade can swing freely a couple of inches above the table so that the blade is well-centered at the height of the magnets. In order to center the angular readings about the equilibrium position, uncheck **Zero Sensor Measurements at Start** in the options for the rotary motion sensor and click **Zero Sensor Now** when the pendulum is in its equilibrium position.

6.2.1 Harmonic motion with damping

To investigate the various regimes of damping, you will be pulling back the pendulum to some starting position and letting it go, recording the angular displacement vs. time using the rotation sensor via the DAQ. Remember, the small-angle approximation we used in the theory section is only valid for angles right around $\theta = 0$, so be sure to set your starting position no more than one blade length from the equilibrium position.

You may find it useful to have a photogate attached to the 850 to record the starting condition when you let go of the pendulum. To do this, position the photogate such that the pendulum blade just unblocks it when motion begins.

The amplitude sampling rate should be set so that you get enough data points to clearly see which damping regime you are in without recording lots of points for the same value of the angle. You should play around with this in **Scope** mode to choose an appropriate sampling rate. You will be recording angle vs. time for different values of the spacing between the magnets.

Record traces of the pendulum angle vs. time for the case where the magnets are removed entirely, as well as 4 or five gaps between 50 mm and 10 mm. You will want to get a clear set of data for underdamped motion and a clear set for overdamped motion for your report.

Next, determine the magnet spacing to achieve critical damping. Remember, you are looking for the minimum damping such that the angular velocity of the pendulum does not change sign. Take steps at least as small as 1 mm for this, and save a good set of data showing critical damping for your report. Fig. 6.4 shows some example data for all three regimes. Note that you may need to record where $\theta = 0$ is for each data set to plot them on the same axes.

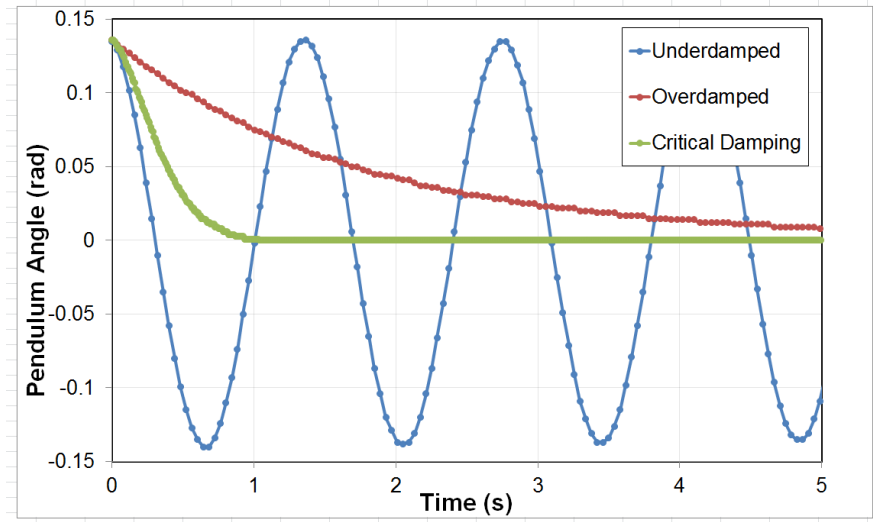


Figure 6.4: Illustration of damped motion in all three regimes of damping. All three plots were obtained with the same initial displacement and no initial velocity. The critically-damped trace clearly converges to $\theta = 0$ the fastest.

6.2.2 Harmonic motion with driving

For the second part of the experiment, you will be examining the amplitude and phase response of the driven, damped harmonic oscillator. For this whole section you will want to set the magnet gap to something with fairly low damping. Remember, you are looking to add just enough damping so that you don't have to wait too long for the system to reach steady state, but not so much that the oscillation amplitude is difficult to detect. You will benefit from trying to use your data from the previous section to set the magnet so that the free undriven oscillations damped out in about 5 to 10 seconds. Record a good trace of displacement vs. time for this setting of the magnet in undriven conditions just like you did for the previous part of the experiment.

You will be using the wave driver to produce a sinusoidal driving torque on the pendulum using the **Signal Generator** function. This is physically accomplished by attaching the banana plugs from the wave driver into **Output 1** of the 850. The drive function will be a Sine function, and you should probably keep the drive voltage below 5 V or so. The frequency range you will be exploring will be very near the frequency of the undriven, undamped oscillator, so take a look at your data from the first part with no damping magnets to estimate the undamped frequency.

First, you will locate the driven, damped oscillator resonance ω_R , which you may assume is equal to ω_0 since you are working with low damping. As discussed, the easiest way to do this is by looking at the *phase* response. To accomplish this, you will be making parametric plots known as *Lissajous figures*. What I mean by “parametric plot” is that you will be plotting two separate quantities that are related by a parameter, which in our case will be

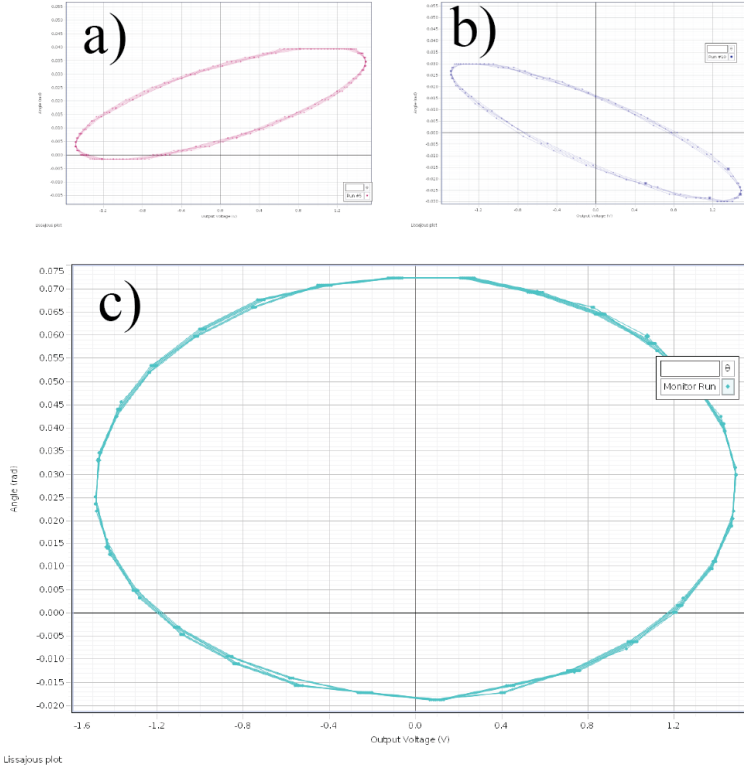


Figure 6.5: Parametric plots of the driving and response of a damped harmonic oscillator showing Lissajous figures. These screen shots from Capstone show the measured pendulum angle on the vertical axes and the drive voltage on the horizontal axes for drive frequencies (a) below, (b) above, and (c) right on resonance.

time. You will be plotting **Angle** on the *y*-axis and **Output Voltage** on the *x*-axis of a **Graph** display. You will also need to record data for several oscillations after the system reaches steady-state for your analysis, so now is a good time to set up a **Table** for doing that.

Your parametric plot will show both the drive voltage and the system response (the angle) on one set of axes. For steady-state behavior, this plot will look like a closed curve. You will need to play around with scaling the axes to try to make the extent of the shape on the *x*-axis be about the same distance as the extent on the *y*-axis so that you can clearly see the difference between a perfect circle and a slight ellipse. Fig. 6.5 shows an example screen shot of the parametric plot.

To find ω_R , you are looking for the drive frequency such that the steady-state behavior looks like a symmetric circle on the parametric plot, such as shown in Fig. 6.5(c). You will find that this technique is incredibly sensitive to the proximity to resonance, and even a small deviation from resonance will be visible as a slightly-tilted ellipse. The direction of the tilt tells you which direction you need to go to find resonance, as shown in Fig. 6.5(a) and

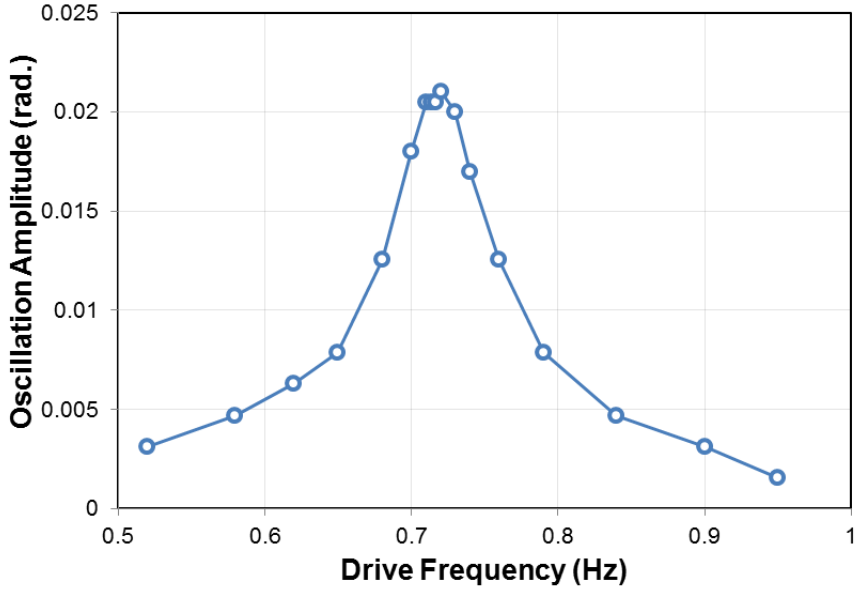


Figure 6.6: Measured oscillation amplitude spectrum of a damped, driven oscillator. The points are connected by straight lines, showing the Lorentzian shape of the resonance as predicted in Fig. 6.2.

(b). Estimate an uncertainty in your measurement of ω_R based on how small a deviation you think you can make without being able to tell a difference in the figure. You will need to save data for plotting Lissajous figures in your report for driving the system below, above, and right on resonance.

Last, you will examine the amplitude response of the oscillator as a function of frequency. It is by design that this lab manual is not going to provide you with detailed instructions for how to go about this; you are expected to come up with an appropriate experiment on your own (or with your lab partner) that you think makes sense. Record the amplitude of the pendulum oscillations in steady-state for at least 10 different drive frequencies. You are trying to make a figure that allows you to see the shape of the resonance curve, which will allow you to find its height and estimate its width. An example is shown in Fig. 6.6 with the data points connected by straight lines, which shows a Lorentzian shape similar to Fig. 6.2.

6.3 Analysis

For undriven damped motion, you recorded time traces of the angular displacement. From your trace that was taken with no magnets present, you should be able to determine the undamped oscillation frequency ω_0 . Make a plot clearly showing three time traces, one in each regime of damping. You can assign an uncertainty to the critical damping gap between the magnets based on how well you can measure the gap and how much change it would

take for you to say definitively that the damping has changed regimes.

For the driven, damped oscillator, plot your time trace of the undriven oscillator at the magnet gap you used for the rest of the lab. Using the same technique you employed in Experiment 5, find the damping time τ by analyzing how much the amplitude decreases as a function of time for undriven oscillations. Assign an uncertainty to your measurement of τ based on how well you think you were able to measure the change in amplitude.

You recorded a measurement of the driven resonant frequency ω_R that was obtained by looking at the Lissajous plots. Combine this with your measurement of τ to report a measured value for Q via Eq. 6.13. Plot three Lissajous figures for your report showing the shape below, on, and above resonance.

You have one more way to determine Q , which you will compare to this method. This second method to measure Q is to examine the amplitude response to apply Eq. 6.16. To do this, plot your amplitude spectrum and determine the peak height (which should occur at ω_R). It is sometimes helpful to connect the data points with straight lines for this analysis. Using your plot, come up with some way to estimate the full width of the resonance where the amplitude is $1/\sqrt{2}$ times its maximum ($\Delta\omega$), such as depicted in Fig. 6.2. You are unlikely to have two data points at exactly the right place, so you will need to make an educated guess about this width based on the plot and assign an uncertainty to it. You have been assigning uncertainties in this course for many labs now, and you should be able to come up with a way to do this that effectively reflects how well you really measured this quantity. Use your measurement of $\Delta\omega$ to calculate Q , and think about how much you trust this measurement compared to your other method for determining Q .

6.4 Report guidelines

This week you will NOT turn in a lab report, nor will there be a worksheet this week. Your presentation of this week's experiment will be part of a double credit lab report on resonance that will cover both Experiments 6 and 7. If you do the extra credit, please save it for your lab report next week and include it as if it were a normal part of your experiment. Even though there is no report due next week, students are encouraged to make sure they can be prepared to include everything they did this week.

1. **Some items to consider including in your next report:** It will be up to you to form a coherent story in the lab report due next week. You must decide what graphs, tables and other information should be included. Some general concepts for this lab are

- Regimes of damping
- Resonance
- Q-factor and line widths

2. Extra Credit In the driven resonance part of this experiment, you estimated $\Delta\omega$ by using a plot that probably did not have two data points right at $1/\sqrt{2}$ of the maximum amplitude. Find these two frequencies *experimentally* by moving the drive frequency around until the amplitude is at $1/\sqrt{2}$ of its maximum value. The difference between these two frequencies should be $\Delta\omega$. Plot Lissajous figures at both frequencies and describe what they have in common. Use your new measured value for $\Delta\omega$ to determine Q . Further, since the frequency of the peak of your amplitude spectrum is ω_R (even when ω_R and ω_o are not approximately equal), this gives you yet a *third* method for determining Q . The damped, driven resonance frequency ω_R must be halfway between the two frequencies you found for achieving $1/\sqrt{2}$ of the maximum amplitude. Combine this with Eq. 6.15 to get a third measurement of Q and compare all of your measurements and methods. Which do you believe is the most accurate, and why?

6.5 Epilogue

It is remarkable how much physics can be understood by modeling systems as harmonic oscillators. The Lorentzian line shape shows up in everything from nuclear scattering to molecular spectroscopy and plays an important role in almost every field of physics. Understanding the fundamentals, such as the phase change across resonance and how the shape changes with damping will be helpful for many advanced courses and research work in engineering and physics.

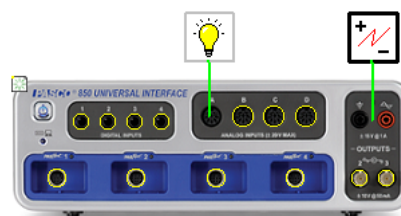
Experiment 7: Waves on a Vibrating String

In Experiments 3, 5, and 6 you studied systems that exhibited simple harmonic oscillations, where the part of the system that was oscillating was often modeled as being a single point-mass. Non-rigid, spatially-extensive systems can also exhibit simple harmonic motion, where each point in space has some property that oscillates periodically in time and is somehow related to the oscillations of its neighboring points. Phenomena such as these exhibit wave behavior, and wave phenomena show up in everything from light to sound to the quantum mechanical nature of probability amplitudes. In Experiment 7, you will be examining waves on a stretched, massive string with clamped boundary conditions. You will measure the group velocity of traveling waves on this string and predict and observe the behavior of many modes of standing-wave oscillation. Last, you will investigate one of the curious features of interference, where the addition of an intermediate boundary condition can be used to suppress certain modes while leaving others effectively unchanged. Information about laser safety can be found in Appendix A and should be read if you do not know how to safely use a low-power visible laser.

7.1 Procedure

To configure the DAQ for this experiment, you will need to be able to read the signal from a light sensor (analog channel) and to send a signal to the wave driver via output channel 1 (the red and black banana plugs). The polarity of the plugs does not matter.

In order to excite and monitor wave behavior, we will be using transverse motion of a thick, elastic string about a meter long. The tension in the string is an important parameter for us to control in a known way, so while one end of the string will be held in a clamp (shown in Fig. 7.1a and b), the other will pass over a pulley wheel (Fig. 7.1a and c) and weights can be hung from this end. The tension will be set by $T = (m_1 + m_2)g$, where m_1 and m_2 are the mass of the hanging weight and the portion of the string that is hanging from the pulley



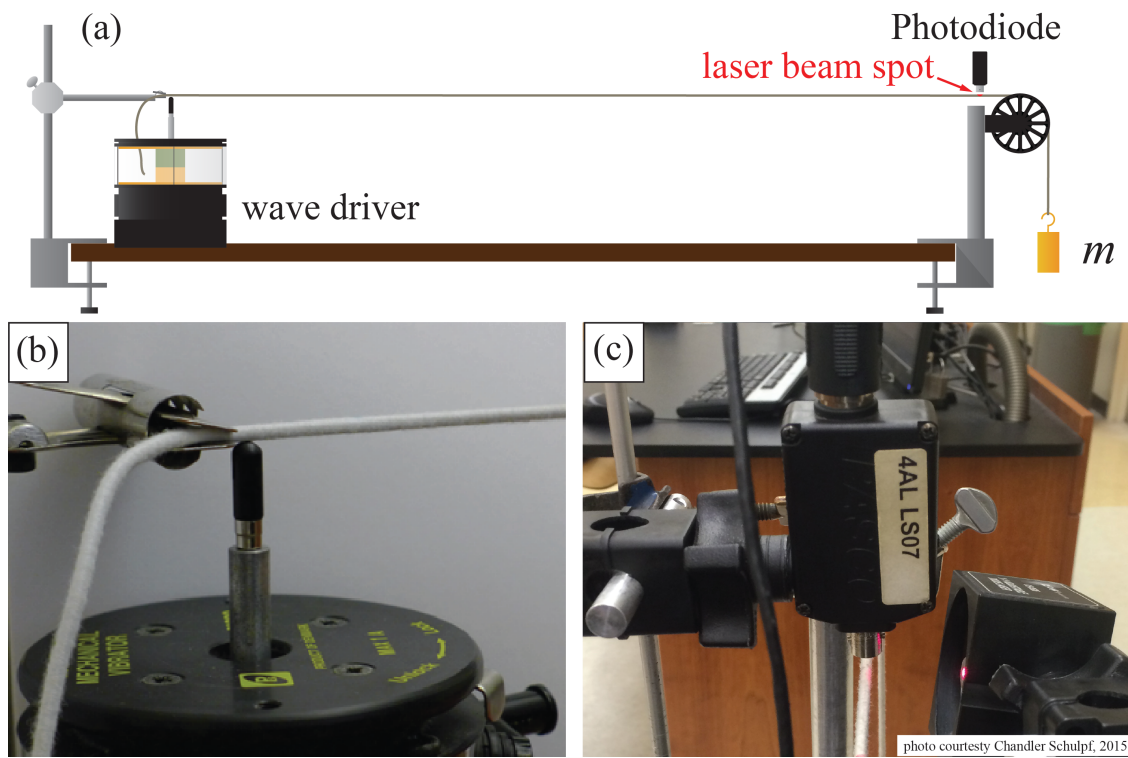


Figure 7.1: Apparatus for observing the vibrational motion of a massive string. (a,b) A wave driver excites vibrations near the clamp, which can be detected when (c) a laser beam scatters light into a photodetector at the other end. The tension in the string is controlled by hanging known masses from a pulley that defines the other boundary.

(which has a non-negligible mass!).

The wave driver will excite vibrations in the string by moving the actuator in the vertical direction. The actuator tip should just barely touch the string when the actuator is not running, and should be positioned 1-2 mm from the clamp, as shown in Fig. 7.1b. You may need to move the wave driver on the table until the driven waves are in the vertical plane and do not have a significant horizontal component. It is recommended that you do not put the string into the notch on the tip of the actuator, but rather just use the tip to push against the string.

You will be measuring the displacement of the string in the vertical direction by scattering laser light into a photodiode (also called a photodetector, light sensor, or simply “detector”). The laser spot should be positioned so that it illuminates the top third or so of the string when the string is not moving. The photodetector should be positioned directly above the laser spot very close to the string to minimize the effect of ambient light getting into the detector. In this way, if that section of the string moves downward, it scatters less of the laser light into the detector and the signal decreases, with the converse being true if this string moves upward. A photodiode gain setting of 10 seems to work well for this, but feel free to experiment.

The laser beam should illuminate the string fairly close to the pulley (see Fig. 7.1c). For Part 1 of this experiment (measuring the wave speed), it is recommended that you set the beam (and photodetector) 6-8 cm from the pulley apex. For Part 2 and Part 3 (standing waves), you will likely obtain the best results if the beam and photodiode detector are about 1 cm away from the pulley apex.

Setting the laser spot and detector positions correctly can be tricky, and it is worth your time to make sure you do this well to get high-quality data. It is recommended that you use **Scope** mode to monitor the **Light Sensor** while using **Signal Generator** to run the wave driver in a sinusoid at 4-10 Hz with 1-2 V of output. For measuring the wave speed (Part 1), adjust the laser beam and detector until the resulting signal is clearly visible above the background noise. For the standing waves sections of this experiment (Parts 2 and 3), you will also want to make sure that when you drive a standing wave on resonance with a sinusoidal drive, the output signal also looks like a nice, symmetric sinusoid, which indicates that the response is linear. Figure i.5 in Chapter i shows an example of non-sinusoidal response, where an asymmetry is clearly visible. By moving the laser spot, detector, and adjusting the drive amplitude, you should be able to get a signal that looks more like a sinusoid.

7.1.1 Part 1: wave speed

In the first part of this experiment, you will measure the wave speed for several values of the tension by hanging different weights from the string, but be sure to read below regarding length measurements before changing weights. The wave velocity is predicted by a simple model to be given by

$$v = \sqrt{\frac{T}{\mu}} \quad (7.1)$$

where T is the tension and μ is the linear mass density of the **stretched** string. Since the string stretches under tension, its linear mass density will change depending upon the amount of weight that is hung from the pulley.

As a first step to tackle this mass density issue, measure the mass M of the string, and be sure to subtract off the amount that will be hanging limply from the back of the clamp since this portion will not stretch when the weights are applied and plays no role in the experiment.

Example 7.1 A student has a string with total unstretched length of 2 m and total mass \mathcal{M} . After setting up the experiment, the student measures that there is 40 cm of excess string hanging off the backside of the clamp. The mass of the string involved in the experiment (this includes the portion hanging down to the weights since this section stretches as well) is therefore given by

$$M = \mathcal{M} \left(\frac{1.6 \text{ m}}{2 \text{ m}} \right), \quad (7.2)$$

which is $M = 0.8 \times \mathcal{M}$.

When tension is applied to the string, it will stretch, and the height of the knot holding the end of the string to the hanging masses will change. The linear mass density is therefore the mass M divided by total *stretched* length of the string from the clamp, over the pulley, all the way to the knot at the top of the weights. This length will change when the tension is changed, so be sure to keep track of it to note the changing linear mass density of the string. You should also try to estimate the mass of the portion of the string that hangs from the pulley to see if it needs to be included in your calculation of the tension, or if it is small enough to be neglected.

You will be measuring the wave speed for 3 different values of the tension T , so it is probably a good idea to go ahead and measure the stretched linear mass densities for 3 different values of the weight. For the second part of the experiment, you will want a good bit of tension on the string, so choose at least one of your 3 weights to have a mass of 350 g or more and then use this for Parts 2 and 3.

Conceptually, the wave speed measurement will proceed when you create a sharp rising edge with the **Signal Generator** driving the wave driver and measure the time it takes the resulting excitation to bounce back and forth between the pulley and the clamp. There will be a signal on the photodiode (some sort of wiggle) every time the pulse arrives at the photodiode. If the pulse travels down to the clamp and back in some time Δt , the speed will be the distance the wave traveled (call it $2L$) divided by Δt .

To take your wave speed measurement, select **Continuous** mode in the **Controls** palette. Figure 7.2 shows **Signal Generator** settings appropriate for measuring the wave speed. Set the signal generator to **Auto**, which will initiate the signal generator only when you start recording data. You can create a fast rising edge by changing the **Waveform** from **Sine** to **Square**. You will want the frequency to be quite low to give you lots of time to see the wave reflecting back and forth on the string, so it is recommended that you set the **Frequency** to

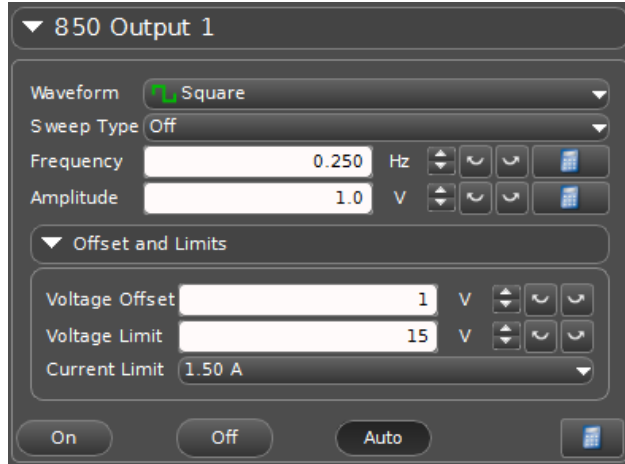


Figure 7.2: Capstone settings for creating a fast rising edge to measure the wave speed.

0.2 Hz or so (the exact frequency does not matter). The recommended **Amplitude** is about 1 V. Last, set the **Voltage Offset** to be the same voltage as you used for the **Amplitude** so that you don't excite a pulse before you can record a rising edge.

You can visualize your results by opening a **Graph** session from the **Displays** palette. You will be plotting two signals simultaneously (the wave driver voltage and the photodiode signal) to see when the pulse is launched. To set this up, select **Light Intensity (%)** for the *y*-axis and plot **Time (s)** on the *x*-axis. To add another *y*-axis, mouse over the plot area to wake up the menu bar and click on the “Add new *y*-axis to active plot area” button . The new axis will appear on the right side of the plot, and you can set it to plot **Output Voltage, Ch01 (V)**, as shown in Fig. 7.3. When you click **Record** on the **Controls** palette, the photodiode signal will be fairly flat and the voltage should be zero until the rising edge, at which point the voltage will jump to twice the amplitude setting and there will be a series of peaks on the photodiode signal for each time the wave gets near the laser beam spot. Click **Stop** once the voltage goes back to zero. Figure 7.3 shows a screen shot from Capstone with an example signal.

The size and shape of the wiggles you get will probably look very different from everyone else's, but the only thing that matters is that you see some sort of signal that repeats itself a few times. You can open a **Table** and save your data in Excel for your analysis and plotting. This may involve quite a bit of data, but hopefully not too much to take home with you. As always, be sure the table is displaying enough digits for you to get your data without introducing nasty rounding errors. Save data for all 3 values of the tension so that you can determine the wave speed during your analysis. Remember to measure the length between the pulley and the clamp so that you know how far the pulse travels between successive arrivals at the laser spot.

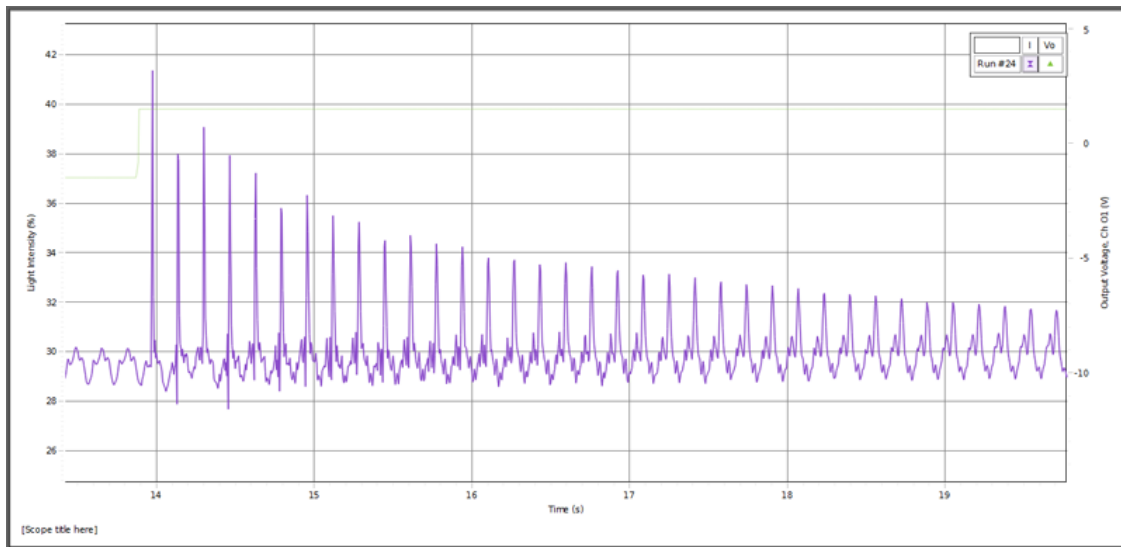


Figure 7.3: Capstone screen shot showing the launch of a pulse that makes many round-trips along the string.

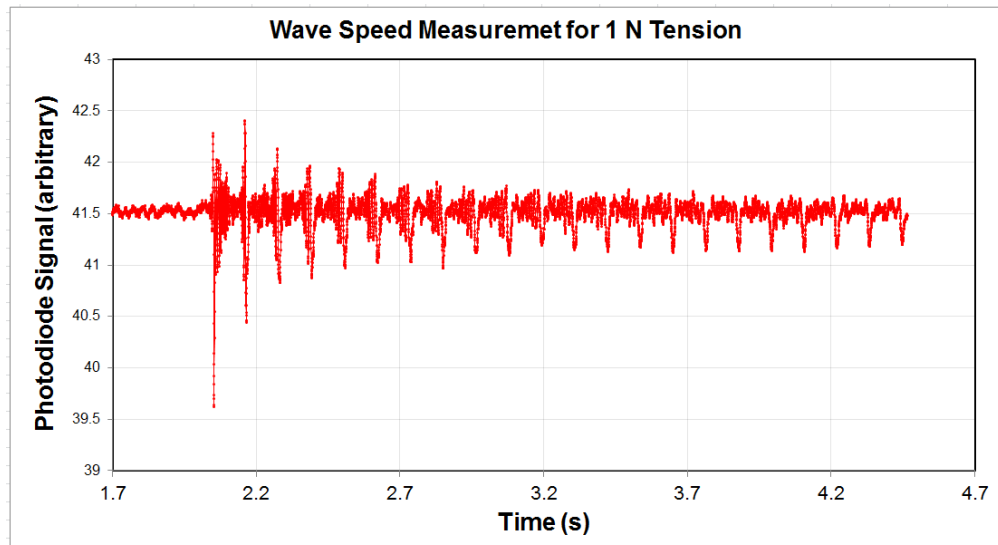


Figure 7.4: Close-up of the signal from a pulse reflecting back and forth from the clamp and pulley. The wave speed can be measured by identifying some feature that repeats and measuring the time duration between repetitions. In this case, the sharp downward spike would probably be a good candidate. The uncertainty in this measurement can be estimated from the width of the spike.

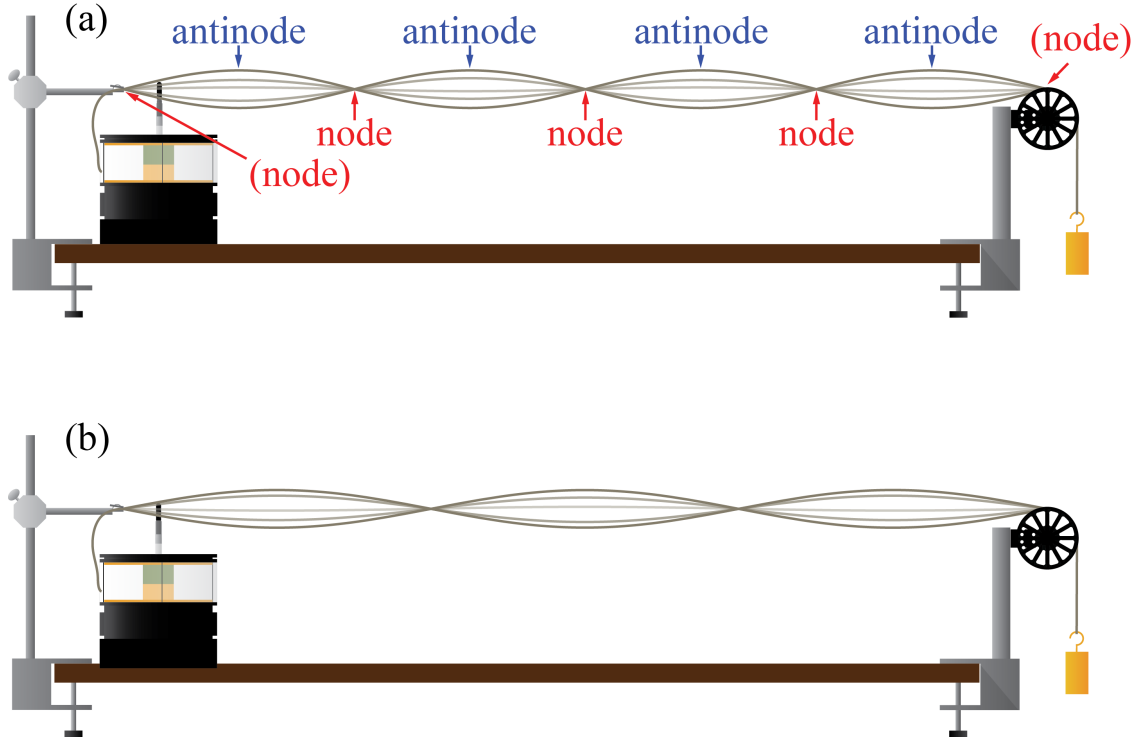


Figure 7.5: Transverse standing waves on a string. The positions where the displacement amplitude is zero are called *nodes*, while the maxima are called *antinodes*. In contrast, a normal *mode* of oscillation in this system is an entire standing wave. The $n = 4$ mode is shown in (a), while an entirely different mode (with a correspondingly different frequency) is shown in (b). The mode in (b) corresponds to $n = 3$.

7.1.2 Part 2: standing waves

For the second part of this experiment, you will be observing standing waves in the vibrating string, as shown in Fig. 7.5. You will probably get the best results if you use your heaviest weight from the first part of the experiment, and be sure to re-position the laser spot and photodiode and optimize the linearity of the signal as mentioned above (driving the wave driver with a sine wave should give you a nice sine wave on the photodiode signal).

Since both ends of the string have fixed boundary conditions, the string will support a series of harmonics of the fundamental standing wave mode. Note: this resonance frequency will probably be less than 20 Hz, so please do not try to turn on the wave driver at 1 kHz, which will primarily produce a painful noise. When driving the fundamental mode on resonance, the string will oscillate with large amplitude (probably clearly visible by eye) and will not have any nodes between end points. We can assign an integer $n = 1$ to this mode. There will be an entire series of harmonics associated with this motion for other integer values of n . Find the resonant frequency for this fundamental mode by monitoring the amplitude of the photodiode signal and finding the frequency for which this amplitude

is maximized. Be sure to make a measurement that is as precise as possible in order to accurately predict the frequency at which higher values of n will also be normal modes of the string. By using the DAQ, it should be possible for you to nail this down to at least 3 digits of precision (10s of mHz) using this “maximum amplitude” method. Record this frequency for your records.

Before moving on to find the frequencies of higher-order modes, recall that you learned last week how to find the undamped resonant frequency ω_0 of an oscillator using the *phase* information of the signal. You created parametric plots of Lissajous figures such as Fig. 6.5, and the resonant frequency was the frequency when the figure was most symmetric. Using what you recall from last week about how to plot the system response (for this week, this is the photodiode signal) vs. the drive signal (in this case, the wave driver output), set up a parametric plot of your system that will allow you to identify resonant frequencies by observing the symmetry of the waveform. You may assume $\omega_R \approx \omega_0$ since the damping time in this system is many oscillation periods. Do this for the fundamental ($n = 1$) mode, and see if you measure the same resonant frequency as you did with the “maximum amplitude” method above. Be sure to record not just the resonant frequency, but also an uncertainty in your measurement of this frequency. How far can you move the frequency before you notice that the Lissajous figure is no longer symmetric?

Using your parametric plot, record the resonant frequencies for a series of harmonics of this fundamental frequency (each harmonic is called a *normal mode* of oscillation). The n th normal mode will have a resonant frequency that is n times the fundamental frequency, so you should use your measured fundamental frequency to predict where to find each harmonic. The n th mode will have n anti-nodes in it (nodes are positions with minimum amplitude, anti-nodes are positions with maximum amplitude). Split up the measurement of the frequencies of the harmonics with your partner up to $n = 9$. For instance, if there are two of you, one can measure the frequencies of modes $n = 1, 3, 5, 7, 9$ and the other can measure $n = 1, 2, 4, 6, 8$. If there are 3 of you sharing an apparatus, each should choose 5 harmonics at random from $n = 2 \dots 9$.

For the higher frequency modes, you may find that it is helpful to turn up the signal generator amplitude. If you have trouble finding those signals, you may have the laser and photodiode too far from the pulley, so moving them closer may help. Try to find the 30th harmonic (you should be able to predict where you think it will occur) and record what you observe.

7.1.3 Part 3: boundary effects

The last part of the experiment is an investigation of intermediate boundary conditions and interference. Using your measured resonant frequencies for $n = 2, 4$, and 5 , drive these modes at some fixed drive amplitude and record the amplitude of the photodiode oscillations for each one (Scope mode is good for this). The “amplitude” you record can simply be the peak-to-peak size of the photodiode signal (because this number will be proportional to the actual wave amplitude for transverse displacement of the string).

For all of the normal modes, the pulley apex and the clamp are always nodes, but for $n = 2$

and higher, there are also nodes between these endpoints. Drive the fundamental ($n = 2$) mode with the same drive amplitude you just used when you measured its amplitude. Using a ring stand and a post, constrain the motion of the string at the node that is in the middle of the string for $n = 2$. You should be able to do this without substantially altering this mode (the signal level should be the same). Record the new signal amplitude you measure for this mode once you have optimized the position of the post to maximize it. Without moving the post, drive the $n = 4$ mode with the same drive amplitude you used before, and compare your new measured signal amplitude to the old one. Do the same (without moving the post!) for $n = 5$ and record what you find.

7.2 Analysis

7.2.1 Part 1 analysis

To measure the wave speed from your data, for each tension, plot the photodiode signal vs. time, as shown in Fig. 7.4. The excitation itself is likely to be a somewhat complicated set of wiggles on the signal, but the important thing is not the shape of the signal so much as it is identifying some feature that repeats itself. Each time the feature repeats, it will be slightly smaller than the previous time, so you will have to make a decision about how far out in time you want to look. Since you know the distance the excitation travels between repetitions, measure the wave speed by dividing this distance by the time delay. Estimate an uncertainty in your measurement based on how well you feel you can localize the excitation feature in time and how well you know the distance traveled.

7.2.2 Part 2 analysis

The frequency of the n th normal mode is predicted to be given by

$$f(n) = n \frac{v}{2L} \quad (7.3)$$

where v is the wave speed (predicted and measured for this tension in Part 1) and L is the distance between the clamp and pulley apex. Using your *measured* value for the wave speed from Part 1, calculate a predicted value for the frequency of the fundamental mode. Using Eq. 7.3, calculate predicted values for the higher-order modes whose frequencies you measured. Compare your results.

7.3 Report guidelines

Write a full, formal lab report that covers Experiments 6 and 7.

1. Cover Sheet

- experiment number and title

- your name
- the date the lab was performed
- your lab section (for instance, “Monday 3pm”)
- your TA’s name
- your lab partners’ names
- the word count of your abstract

2. Guidelines

By this point in Physics 4AL, your experience in writing lab reports should enable you to write a lab report without detailed guidelines. You will be responsible for developing a coherent narrative to connect each of the results you obtained and deciding which figures, plots, tables and analysis will be appropriate to accomplish this. You should look back over your old returned reports and guidelines from earlier in this manual to guide you through this process. If you did the extra credit from this week and/or last, please find a way to include it in your lab report as if it were just another part of your experiment.

3. **Extra Credit** In experiments 6 and 7, you used Lissajous figures to find the resonance frequency of a couple of harmonic oscillators. Using this method for your standing waves, try to find out what the highest mode you can find is. Can you see the $n = 60$ mode? Report your determination of each mode starting from $n = 1$ and going as high in n as you can. State the distance you have between your laser spot on the string and the point where the string touches the pulley. Calculate the frequency of the first mode that will have a node at this location, and describe why this may make your data taking for modes near this one difficult.

7.4 Epilogue

Throughout this course, you have investigated a series of different mechanical phenomena in a laboratory setting. Many of the effect observed in this setting, however, manifest themselves in many different contexts, including electricity and magnetism, atomic physics, nuclear physics, astrophysics, communications, particle physics, et cetera. The material in this course is therefore far more general than mechanics, and it is hoped that working with your hands to investigate these phenomena will help to prepare you to have a more intuitive understanding of these concepts as you move forward.

Appendix A

Laser safety.

Provides information to lab workers/visitors who are NOT authorized laser users about hazards existing at this location.

Location Knudsen 1238, 2115, 2122, 2136

LASERS

- Lasers may only be operated in these labs by **personnel who have received permission to use them** from a suitably qualified class trainer.
- In order to maintain and protect equipment, personnel, and research, no worker, except for trained personnel, can **touch move or interfere with any laser equipment**, materials or processes.
- Personnel should **never use class-supplied laser pointers** as presentation pointers in the classroom.
- Personnel should **never introduce a shiny or mirrored surface** in front of laser beam that might cause uncontrolled specular reflection.
- Classroom laser personnel should **not move or adjust laser equipment** set up by any other class laser operator unless specifically instructed to do so. This includes not detaching the lasers from any stands or moving the stands in any way that could create a hazard for other classroom occupants.
- Laser equipment should be **turned on only when necessary** for presenting the demonstration.
- Laser equipment, whether powered by an external power supply or batteries, should be **turned off following completion of a given classroom demonstration** so as to prevent inadvertent exposure during class dismissal.

EYE HAZARDS

- This lab uses and operates lasers that create light radiation which, if of sufficient power, can cause biological damage to the eyes. Eye damage caused from lasers includes **retinal burns, glaucoma, cataracts and total loss of vision**.
- Personnel should **never stare into a laser or look directly into a beam** and never stand or sit at the same level as the beam path.
- Laser operators must make sure that any laser beam points **away from other members of the class**.
- The person primarily responsible for the class training **can order all personnel to leave the room** if necessary for any reason



**THE PRIMARY PURPOSE
OF THE UCLA LASER
SAFETY PROGRAM IS TO**

**AVOID GETTING A
LASER BEAM IN
YOUR EYE**

**NEVER STARE DIRECTLY
AT A LASER BEAM,
EVEN WITH PROTECTIVE
EYEWEAR**

LASER LIGHT

- *Maintains strength over long distances*
- *Produces significant eye hazards at relatively low levels*
- *Concentrates to a very high intensity when focused by a lens*
- *Occurs in the Visible and Non-visible spectrum*

BIOLOGICAL HAZARDS

- *Can be laser beam and non-beam related*
- *Can occur at all wavelengths*
- *Occur mainly in the eyes and skin*

MOST INJURIES

- *Affect the eyes*
- *Occur during alignment*
- *Result from operator error*

PROTECTION

- *Eyewear must be worn for Class 3B and Class 4 laser use*
- *Eyewear must meet ANSI standards and be marked with Optical Density and Wavelength*
- *Appropriate skin protection is required for Class 4 lasers*

LASER CLASSIFICATION TABLE

Class 1 / 1M	Maximum power output is a few microwatts. Visible spectrum output Considered incapable of producing hazardous eye/skin exposure unless viewed with collecting optics (1M). Does not apply to open Class 1 enclosures containing higher-class lasers
Class 2 / 2M	Maximum power output is < 1 mW. Visible spectrum output Considered incapable of producing hazardous eye/skin exposure within the time period of human eye aversion response (0.25 s) unless viewed with collecting optics (2M)
Class 3R	Maximum power output is 1 mW - < 5 mW. Visible and non-visible spectrum Potentially hazardous under some direct and specular reflection viewing condition if the eye is appropriately focused and stable or if viewed with collecting optics.
Class 3B	Maximum power output is 5 mW - < 500 mW Visible and non-visible spectrum Presents a potential eye hazard for intrabeam (direct) or specular (mirror-like) conditions. Presents a significant skin hazard by long-term diffuse (scatter) exposure if higher powered and operating in 200 – 280 nm UVC ranges
Class 4	Maximum power output is > 500 mW. Visible and non-visible spectrum Presents potential acute hazards to the eye and skin for all intrabeam and diffused conditions Potential hazard for fire (ignition), explosion and emissions from target or process materials.

EYE DAMAGE - WAVELENGTHS

WAVELENGTH	AREA OF DAMAGE	PATHOLOGICAL EFFECT
180 - 315 nm (Ultraviolet UV-B, UVC)	CORNEA ; Deep-ultraviolet light causes accumulating damage, even at very low power	Photokeratitis ; Inflammation of the cornea, similar to sunburn
315 - 400 nm (Ultraviolet UV-A)	CORNEA and LENS	Photochemical cataract ; Clouding of the lens
400 - 780 nm (Visible)	RETINA ; Visible light is focused on the retina	Photochemical damage ; Damage to retina and retinal burns
780 - 1400 nm (Near Infrared)	RETINA ; Near IR light is not absorbed by iris and is focused on the retina	Thermal damage to cataract and retinal burns
1400 - 3000 nm (Infrared)	CORNEA and LENS ; IR light is absorbed by transparent parts of eye before reaching the retina	Aqueous flare ; Protein in aqueous humor, cataract, corneal burn
3000 – 10000 nm (Far Infrared)	CORNEA	Corneal burn



LASER OPERATION GUIDELINES

OPERATORS MUST:

- Review **Standard Operating Procedures**, operating and safety instructions and laboratory-specific laser instructions
- Be trained in **laser safety** and specific laser procedures
- Observe all written procedures, **safety rules** and properly use appropriate **PPE**
- Be authorized by the **Principal Investigator**
- Be directly supervised by a person knowledgeable in laser safety
- Wear appropriate **PPE**, follow safety procedures and SOP's
- Never circumvent **Administrative or Engineering safety controls**
- Know the location and use of the **power kill switch and fire extinguisher**
- Use the buddy system when working with **high voltage equipment**
- Not wear **reflective metal jewelry** when working with laser beams
- Never stare directly into a beam even with eye protection; use indirect viewing
- Give sufficient attention to **non-beam hazards** to prevent possible injury and illness
- Be aware of **plasma and collateral radiation**
- Notify supervisor immediately of potentially hazardous conditions, personal injury, or property damage

IN EACH LAB, PERSONNEL MUST BE ABLE TO OBTAIN:

- Training on equipment, procedures and emergency procedures
- Safety Equipment that is sufficient in numbers for lab staff, appropriate for the equipment in use and in good operating condition
- Standard Operational Procedures for the safe use of all equipment
- Information from the PI or Lab Manager about potential equipment hazards

EMERGENCY INSTRUCTIONS

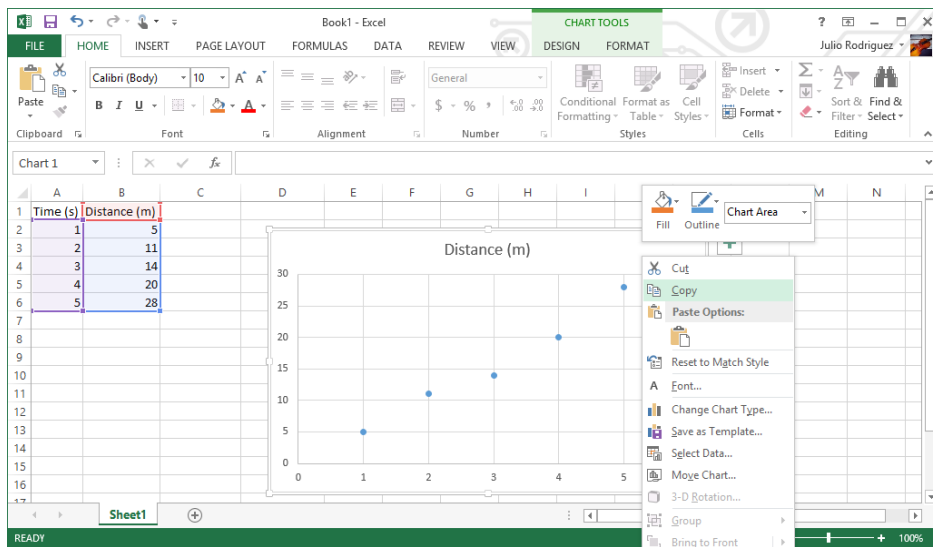
1. Shut the laser off immediately and remove the interlock key. If not possible, alert everyone to exit the laboratory and be the last to leave the laboratory
2. If there is a fire, get everyone out of the laboratory immediately. At the same time shout "FIRE" loudly and frequently. Turn on a fire alarm. Do not try to "fight" the fire from inside the laboratory; do it from the doorway to maintain an escape route
3. In the event of MAJOR injury, Summon Medical Assistance. Call 911 from a campus phone or 310-825-1491 from a cell phone
4. Call Security and/or Fire Department (911) as necessary
5. Call EHS Hotline (59797) to report the incident
Note: ALL incidents must be reported to the Laser Safety Officer
6. Contact the PI and/or Lab Manager and describe the emergency

Appendix B

B.1 Guide for Making and Inserting Plots¹

B.1.1 Obtaining Graph data from Excel

In MS Excel simply click on the white space in your graph, this will select the entire graph. You can then use the **ctrl+c** keyboard shortcut to copy the graph. Alternatively you can right click on the graphs white space and click “copy” from the menu. Simply paste this in Word in the normal way (**ctrl+p**) or right click and selecting “paste.”



B.1.2 Formatting the Graph

Now that the graph is in MS Word, you need to format the graph according to the rules agreed upon by the grading staff. Every graph needs these three things: Axis labels, units, and a title. Additionally, graphs with multiple datasets require some way of determining

¹This section was contributed by Julio S. Rodriguez, Jr. (2014) and revised by Anthony Ransford (2016).

what the data represents (either an explanation or a legend), and some graphs require a trendline with an equation. Many of these things can be set up in Excel beforehand and will be copied over. You may also generate them directly in Word. The lab manual has a pretty good explanation of how to do all of this in Excel and the procedure is largely the same in word. The labels, units, and trendline should appear *on the graph* while title and possibly the trendline equation (with error) should appear *in the caption*. If you use a legend you do not need an explanation of what the data points represent, if you do not have a legend, you should include such an explanation in the caption.

Axis Labels

There is an easy way to add axis labels. Click on the whitespace in your graph and on the ribbon, a few new tabs will open up under the group heading “Chart Tools.” On the “Design” tab there are some preset layouts. In general, you should pick the preset with axis labels (see Figure B.1). You can click on the axis labels to edit their content. I will be working with the assumption that the legend is not necessary since we will have a very descriptive caption. Simply click on the legend and press the “delete” key on the keyboard.

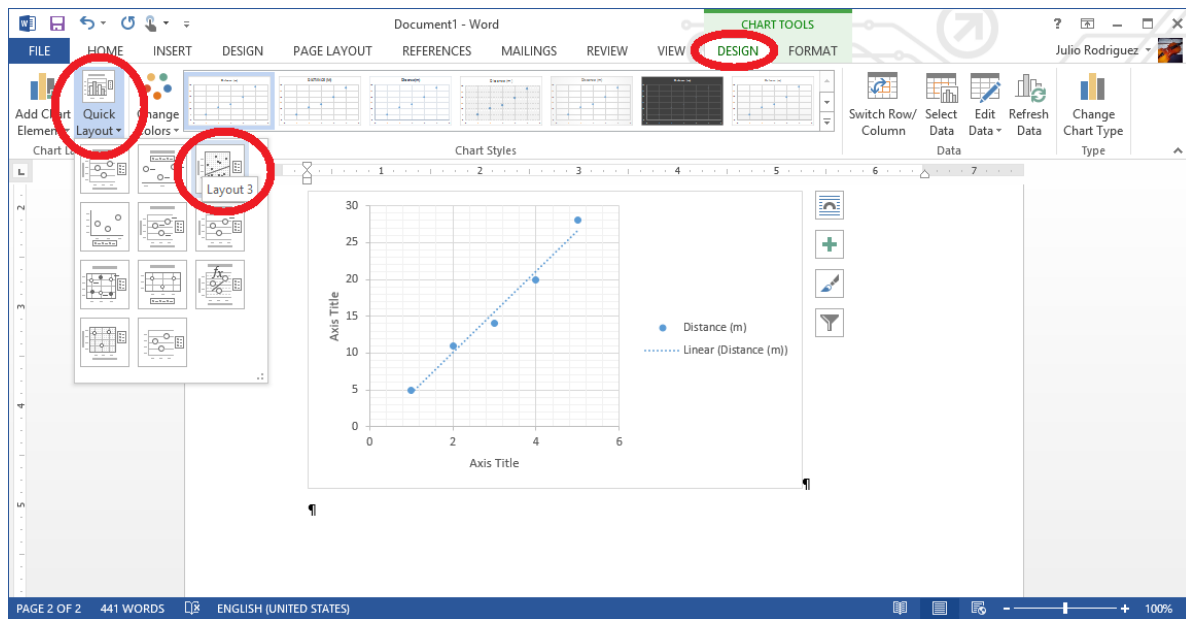
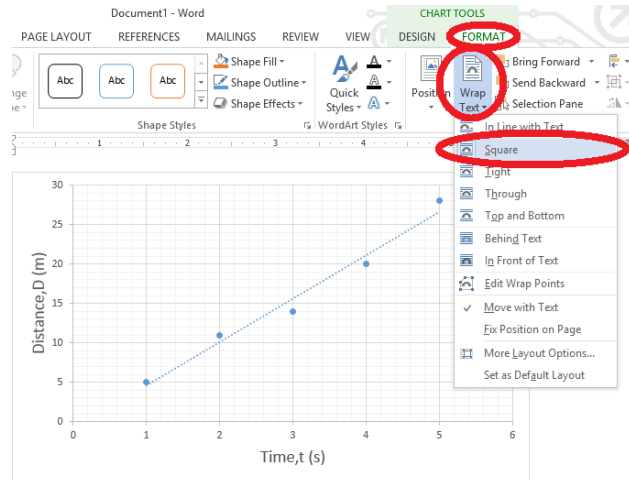


Figure B.1: There are templates in Excel that have axis labels by default, which is a good way to make sure axes don't end up in a report without labels.

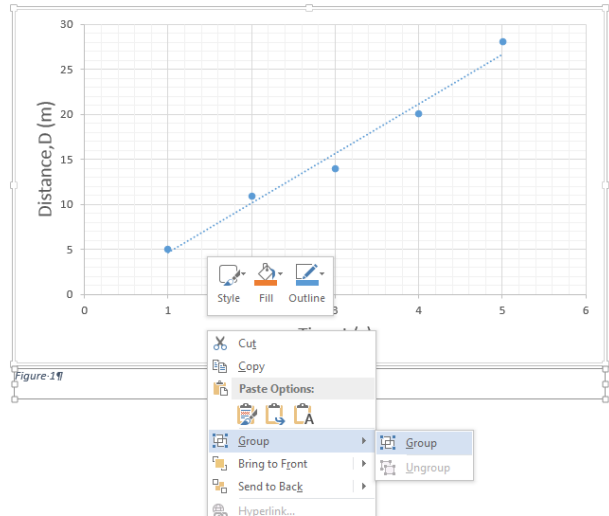
Adding the caption

This is probably the trickiest part of the whole process. The caption function in Word is great in that it auto-numbers things for you, and lets you use different numberings for figure



and tables. The cross-reference tool adds to its functionality, because changing the caption numbering order will not mess up the numbering in the text of your paper. Before we add a caption, we need to change the nature of the graph. Right now Word is treating our graph like an object that takes up its own line, but we want Word to treat the graph as an object embedded in the text (like the image on the right). Click on your graph and this time on the ribbon click on the Format tab under the Chart Tools heading. Here click the Wrap Text button and on the Square option (on older versions of Word, the image for this button looks like a dog instead of an arched curve). Move your graph where you want it to appear in your paper and then add the caption. Right click on the whitespace of your graph and click the insertcaption option. All kinds of options come up, but the default settings are okay for graphs. This will insert the caption as a text box, but we need the caption to be associated with the graph. To do this: If the border and sizing handles on the textbox are not already showing, click on the textbox (anywhere inside). While holding down ctrl, click on the graph. This should select both objects. Release ctrl and right click on either object, then select “Group > Group.”

These two objects will now be treated as a unit; moving one of them will move the other one. Reformat the text in the text box to match rest of your document. You may choose to format the title of the graph in bold font for clarity, but this is not strictly required. To add equations, you can either type things out and use the “symbol” function to include any non-standard symbols, or you can use the equation editor (alt = or insert > equation). A common convention is to italicize variables and leave units un-italicized in equations, remember to leave a space between the units and variables if the two are being multiplied. When referencing your graphs or images in your paper, you should refer to them by their designation. To make this as painless as possible, you may want to use the cross-reference tool in Word. If you change the order of your graphs, insert another graph before one you have already referenced, or anything else along those lines, this tool will keep all of your numbers in order. On the ribbon under the references tab, click “Cross-reference.” Under “Reference Type,” select “Figure,” and under, “Insert Reference To,” select “Only Label and



Number.” You can leave on the “hyperlink” function if you wish. Select which figure you wish to make reference to in the box labeled “For which caption.” This inserts a reference to your chart. For example, Fig. B.2 shows what a proper graph should look like. If you insert any addition graphs or change the order, select your entire document and right click any of the selected text and click “Update Field.”

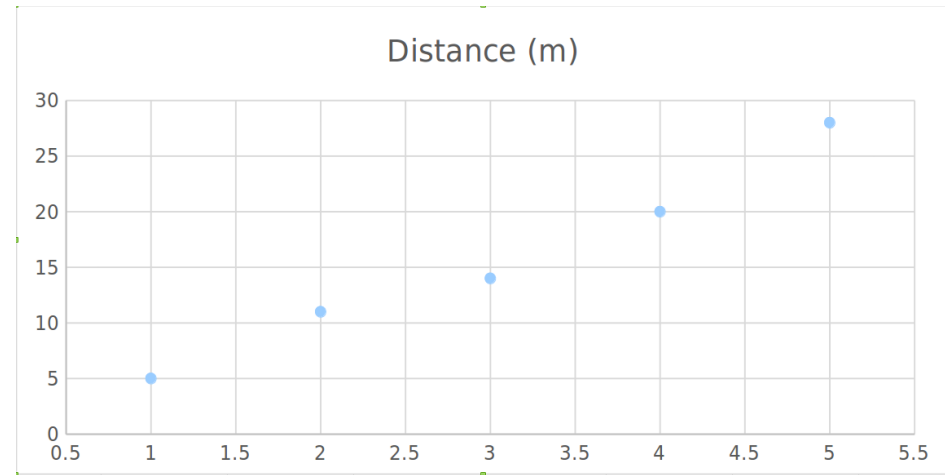


Figure B.2: The blue dots on this graph represent data points taken from the Fakemeter 5000 while on a bicycle ride though Imaginary Park. Distance as a function of time was calculated using the regression tool in Microsoft Excel 365 in order to find the average velocity of the cyclist. The line of best fit is represented by $D = t \times (5.5 \pm 0.5) \frac{\text{m}}{\text{s}} - (1 \pm 2) \text{ m}$.

Appendix C

To help you figure out how to write bibliography entries in the style of Nature formatting, a long example of bibliography formatting from Nature is reproduced here. This example shows entries for published journal articles, journal articles in press, and published books. These are page images taken from the paper reporting sequencing of the human genome [2].

because of the availability of tissues from all developmental time points. A challenge will be to define the gene-specific patterns of alternative splicing, which may affect half of human genes. Existing collections of ESTs and cDNAs may allow identification of the most abundant of these isoforms, but systematic exploration of this problem may require exhaustive analysis of cDNA libraries from multiple tissues or perhaps high-throughput reverse transcription-PCR studies. Deep understanding of gene function will probably require knowledge of the structure, tissue distribution and abundance of these alternative forms.

Large-scale identification of regulatory regions

The one-dimensional script of the human genome, shared by essentially all cells in all tissues, contains sufficient information to provide for differentiation of hundreds of different cell types, and the ability to respond to a vast array of internal and external influences. Much of this plasticity results from the carefully orchestrated symphony of transcriptional regulation. Although much has been learned about the *cis*-acting regulatory motifs of some specific genes, the regulatory signals for most genes remain uncharacterized. Comparative genomics of multiple vertebrates offers the best hope for large-scale identification of such regulatory sites⁴⁴⁰. Previous studies of sequence alignment of regulatory domains of orthologous genes in multiple species has shown a remarkable correlation between sequence conservation, dubbed ‘phylogenetic footprints’⁴⁴¹, and the presence of binding motifs for transcription factors. This approach could be particularly powerful if combined with expression array technologies that identify cohorts of genes that are coordinately regulated, implicating a common set of *cis*-acting regulatory sequences^{442–445}. It will also be of considerable interest to study epigenetic modifications such as cytosine methylation on a genome-wide scale, and to determine their biological consequences^{446,447}. Towards this end, a pilot Human Epigenome Project has been launched^{448,449}.

Sequencing of additional large genomes

More generally, comparative genomics allows biologists to peruse evolution’s laboratory notebook—to identify conserved functional features and recognize new innovations in specific lineages. Determination of the genome sequence of many organisms is very desirable. Already, projects are underway to sequence the genomes of the mouse, rat, zebrafish and the pufferfishes *T. nigroviridis* and *Takifugu rubripes*. Plans are also under consideration for sequencing additional primates and other organisms that will help define key developments along the vertebrate and nonvertebrate lineages.

To realize the full promise of comparative genomics, however, it needs to become simple and inexpensive to sequence the genome of any organism. Sequencing costs have dropped 100-fold over the last 10 years, corresponding to a roughly twofold decrease every 18 months. This rate is similar to ‘Moore’s law’ concerning improvements in semiconductor manufacture. In both sequencing and semiconductors, such improvement does not happen automatically, but requires aggressive technological innovation fuelled by major investment. Improvements are needed to move current dideoxy sequencing to smaller volumes and more rapid sequencing times, based upon advances such as microchannel technology. More revolutionary methods, such as mass spectrometry, single-molecule sequencing and nanopore approaches⁷⁶, have not yet been fully developed, but hold great promise and deserve strong encouragement.

Completing the catalogue of human variation

The human draft genome sequence has already allowed the identification of more than 1.4 million SNPs, comprising a substantial proportion of all common human variation. This program should be extended to obtain a nearly complete catalogue of common variants and to identify the common ancestral haplotypes present in the population. In principle, these genetic tools should make it possible to perform association studies and linkage disequilibrium studies³⁷⁶ to identify the genes that confer even relatively modest risk

for common diseases. Launching such an intense era of human molecular epidemiology will also require major advances in the cost efficiency of genotyping technology, in the collection of carefully phenotyped patient cohorts and in statistical methods for relating large-scale SNP data to disease phenotype.

From sequence to function

The scientific program outlined above focuses on how the genome sequence can be mined for biological information. In addition, the sequence will serve as a foundation for a broad range of functional genomic tools to help biologists to probe function in a more systematic manner. These will need to include improved techniques and databases for the global analysis of: RNA and protein expression, protein localization, protein–protein interactions and chemical inhibition of pathways. New computational techniques will be needed to use such information to model cellular circuitry. A full discussion of these important directions is beyond the scope of this paper.

Concluding thoughts

The Human Genome Project is but the latest increment in a remarkable scientific program whose origins stretch back a hundred years to the rediscovery of Mendel’s laws and whose end is nowhere in sight. In a sense, it provides a capstone for efforts in the past century to discover genetic information and a foundation for efforts in the coming century to understand it.

We find it humbling to gaze upon the human sequence now coming into focus. In principle, the string of genetic bits holds long-sought secrets of human development, physiology and medicine. In practice, our ability to transform such information into understanding remains woefully inadequate. This paper simply records some initial observations and attempts to frame issues for future study. Fulfilling the true promise of the Human Genome Project will be the work of tens of thousands of scientists around the world, in both academia and industry. It is for this reason that our highest priority has been to ensure that genome data are available rapidly, freely and without restriction.

The scientific work will have profound long-term consequences for medicine, leading to the elucidation of the underlying molecular mechanisms of disease and thereby facilitating the design in many cases of rational diagnostics and therapeutics targeted at those mechanisms. But the science is only part of the challenge. We must also involve society at large in the work ahead. We must set realistic expectations that the most important benefits will not be reaped overnight. Moreover, understanding and wisdom will be required to ensure that these benefits are implemented broadly and equitably. To that end, serious attention must be paid to the many ethical, legal and social implications (ELSI) raised by the accelerated pace of genetic discovery. This paper has focused on the scientific achievements of the human genome sequencing efforts. This is not the place to engage in a lengthy discussion of the ELSI issues, which have also been a major research focus of the Human Genome Project, but these issues are of comparable importance and could appropriately fill a paper of equal length.

Finally, it is has not escaped our notice that the more we learn about the human genome, the more there is to explore.

“We shall not cease from exploration. And the end of all our exploring will be to arrive where we started, and know the place for the first time.”—T. S. Eliot⁴⁵⁰

Received 7 December 2000; accepted 9 January 2001.

- Correns, C. Untersuchungen über die Xenien bei Zea mays. *Berichte der Deutsche Botanische Gesellschaft* **17**, 410–418 (1899).
- De Vries, H. Sur la loi de disjonction des hybrides. *Comptes Rendue Hebdomadaires Acad. Sci. Paris* **130**, 845–847 (1900).
- von Tschermack, E. Über Künstliche Kreuzung bei Pisum sativum. *Berichte der Deutsche Botanische Gesellschaft* **18**, 232–239. (1900).
- Sanger, F. et al. Nucleotide sequence of bacteriophage Φ X174 DNA. *Nature* **265**, 687–695 (1977).
- Sanger, F. et al. The nucleotide sequence of bacteriophage ΦX174. *J Mol Biol* **125**, 225–246 (1978).

6. Sanger, F., Coulson, A. R., Hong, G. F., Hill, D. F. & Petersen, G. B. Nucleotide-sequence of bacteriophage Lambda DNA. *J. Mol. Biol.* **162**, 729–773 (1982).
7. Fiers, W. *et al.* Complete nucleotide sequence of SV40 DNA. *Nature* **273**, 113–120 (1978).
8. Anderson, S. *et al.* Sequence and organization of the human mitochondrial genome. *Nature* **290**, 457–465 (1981).
9. Botstein, D., White, R. L., Skolnick, M. & Davis, R. W. Construction of a genetic linkage map in man using restriction fragment length polymorphisms. *Am. J. Hum. Genet.* **32**, 314–331 (1980).
10. Olson, M. V. *et al.* Random-clone strategy for genomic restriction mapping in yeast. *Proc. Natl Acad. Sci. USA* **83**, 7826–7830 (1986).
11. Coulson, A., Sulston, J., Brenner, S. & Karn, J. Toward a physical map of the genome of the nematode *Caenorhabditis elegans*. *Proc. Natl Acad. Sci. USA* **83**, 7821–7825 (1986).
12. Putney, S. D., Herlihy, W. C. & Schimmel, P. A new troponin T and cDNA clones for 13 different muscle proteins, found by shotgun sequencing. *Nature* **302**, 718–721 (1983).
13. Milner, R. J. & Sutcliffe, J. G. Gene expression in rat brain. *Nucleic Acids Res.* **11**, 5497–5520 (1983).
14. Adams, M. D. *et al.* Complementary DNA sequencing: expressed sequence tags and human genome project. *Science* **252**, 1651–1656 (1991).
15. Adams, M. D. *et al.* Initial assessment of human gene diversity and expression patterns based upon 83 million nucleotides of cDNA sequence. *Nature* **377**, 3–174 (1995).
16. Okubo, K. *et al.* Large scale cDNA sequencing for analysis of quantitative and qualitative aspects of gene expression. *Nature Genet.* **2**, 173–179 (1992).
17. Hillier, L. D. *et al.* Generation and analysis of 280,000 human expressed sequence tags. *Genome Res.* **6**, 807–828 (1996).
18. Strausberg, R. L., Feingold, E. A., Klausner, R. D. & Collins, F. S. The mammalian gene collection. *Science* **286**, 455–457 (1999).
19. Berry, R. *et al.* Gene-based sequence-tagged-sites (STSs) as the basis for a human gene map. *Nature Genet.* **10**, 415–423 (1995).
20. Houlgate, R. *et al.* The Genexpress Index: a resource for gene discovery and the genic map of the human genome. *Genome Res.* **5**, 272–304 (1995).
21. Sinsheimer, R. L. The Santa Cruz Workshop—May 1985. *Genomics* **5**, 954–956 (1989).
22. Palca, J. Human genome—Department of Energy on the map. *Nature* **321**, 371 (1986).
23. National Research Council *Mapping and Sequencing the Human Genome* (National Academy Press, Washington DC, 1988).
24. Bishop, J. E. & Waldholz, M. *Genome* (Simon and Schuster, New York, 1990).
25. Keyes, D. J. & Hood, L. (eds) *The Code of Codes: Scientific and Social Issues in the Human Genome Project* (Harvard Univ. Press, Cambridge, Massachusetts, 1992).
26. Cook-Deegan, R. *The Gene Wars: Science, Politics, and the Human Genome* (W. W. Norton & Co., New York, London, 1994).
27. Donis-Keller, H. *et al.* A genetic linkage map of the human genome. *Cell* **51**, 319–337 (1987).
28. Gyapay, G. *et al.* The 1993–94 Genethon human genetic linkage map. *Nature Genet.* **7**, 246–339 (1994).
29. Hudson, T. J. *et al.* An STS-based map of the human genome. *Science* **270**, 1945–1954 (1995).
30. Dietrich, W. F. *et al.* A comprehensive genetic map of the mouse genome. *Nature* **380**, 149–152 (1996).
31. Nusbaum, C. *et al.* A YAC-based physical map of the mouse genome. *Nature Genet.* **22**, 388–393 (1999).
32. Oliver, S. G. *et al.* The complete DNA sequence of yeast chromosome III. *Nature* **357**, 38–46 (1992).
33. Wilson, R. *et al.* 2.2 Mb of contiguous nucleotide sequence from chromosome III of *C. elegans*. *Nature* **368**, 32–38 (1994).
34. Chen, E. Y. *et al.* The human growth hormone locus: nucleotide sequence, biology, and evolution. *Genomics* **4**, 479–497 (1989).
35. McCombie, W. R. *et al.* Expressed genes, Alu repeats and polymorphisms in cosmids sequenced from chromosome 4p16.3. *Nature Genet.* **1**, 348–353 (1992).
36. Martin-Gallardo, A. *et al.* Automated DNA sequencing and analysis of 106 kilobases from human chromosome 19q13.3. *Nature Genet.* **1**, 34–39 (1992).
37. Edwards, A. *et al.* Automated DNA sequencing of the human HPRT locus. *Genomics* **6**, 593–608 (1990).
38. Marshall, E. A strategy for sequencing the genome 5 years early. *Science* **267**, 783–784 (1995).
39. Project to sequence human genome moves on to the starting blocks. *Nature* **375**, 93–94 (1995).
40. Shizuya, H. *et al.* Cloning and stable maintenance of 300-kilobase-pair fragments of human DNA in *Escherichia coli* using an F-factor-based vector. *Proc. Natl Acad. Sci. USA* **89**, 8794–8797 (1992).
41. Burke, D. T., Carle, G. F. & Olson, M. V. Cloning of large segments of exogenous DNA into yeast by means of artificial chromosome vectors. *Science* **236**, 806–812 (1987).
42. Marshall, E. A second private genome project. *Science* **281**, 1121 (1998).
43. Marshall, E. NIH to produce a 'working draft' of the genome by 2001. *Science* **281**, 1774–1775 (1998).
44. Pennisi, E. Academic sequencers challenge Celera in a sprint to the finish. *Science* **283**, 1822–1823 (1999).
45. Bouck, J., Miller, W., Gorrell, J. H., Muzny, D. & Gibbs, R. A. Analysis of the quality and utility of random shotgun sequencing at low redundancies. *Genome Res.* **8**, 1074–1084 (1998).
46. Collins, F. S. *et al.* New goals for the U.S. Human Genome Project: 1998–2003. *Science* **282**, 682–689 (1998).
47. Sanger, F. & Coulson, A. R. A rapid method for determining sequences in DNA by primed synthesis with DNA polymerase. *J. Mol. Biol.* **94**, 441–448 (1975).
48. Maxam, A. M. & Gilbert, W. A new method for sequencing DNA. *Proc. Natl Acad. Sci. USA* **74**, 560–564 (1977).
49. Anderson, S. Shotgun DNA sequencing using cloned DNase I-generated fragments. *Nucleic Acids Res.* **9**, 3015–3027 (1981).
50. Gardner, R. C. *et al.* The complete nucleotide sequence of an infectious clone of cauliflower mosaic virus by M13mp7 shotgun sequencing. *Nucleic Acids Res.* **9**, 2871–2888 (1981).
51. Deininger, P. L. Random subcloning of sonicated DNA: application to shotgun DNA sequence analysis. *Anal. Biochem.* **129**, 216–223 (1983).
52. Chissoe, S. L. *et al.* Sequence and analysis of the human ABL gene, the BCR gene, and regions involved in the Philadelphia chromosomal translocation. *Genomics* **27**, 67–82 (1995).
53. Rowen, L., Koop, B. F. & Hood, L. The complete 685-kilobase DNA sequence of the human beta T cell receptor locus. *Science* **272**, 1755–1762 (1996).
54. Koop, B. F. *et al.* Organization, structure, and function of 95 kb of DNA spanning the murine T-cell receptor C alpha/C delta region. *Genomics* **13**, 1209–1230 (1992).
55. Wooster, R. *et al.* Identification of the breast cancer susceptibility gene BRCA2. *Nature* **378**, 789–792 (1995).
56. Fleischmann, R. D. *et al.* Whole-genome random sequencing and assembly of *Haemophilus influenzae* Rd. *Science* **269**, 496–512 (1995).
57. Lander, E. S. & Waterman, M. S. Genomic mapping by fingerprinting random clones: a mathematical analysis. *Genomics* **2**, 231–239 (1988).
58. Weber, J. L. & Myers, E. W. Human whole-genome shotgun sequencing. *Genome Res.* **7**, 401–409 (1997).
59. Green, P. Against a whole-genome shotgun. *Genome Res.* **7**, 410–417 (1997).
60. Venter, J. C. *et al.* Shotgun sequencing of the human genome. *Science* **280**, 1540–1542 (1998).
61. Venter, J. C. *et al.* The sequence of the human genome. *Science* **291**, 1304–1351 (2001).
62. Smith, L. M. *et al.* Fluorescence detection in automated DNA sequence analysis. *Nature* **321**, 674–679 (1986).
63. Ju, J. Y., Ruan, C. C., Fuller, C. W., Glazer, A. N. & Mathies, R. A. Fluorescence energy-transfer dye-labeled primers for DNA sequencing and analysis. *Proc. Natl Acad. Sci. USA* **92**, 4347–4351 (1995).
64. Lee, L. G. *et al.* New energy transfer dyes for DNA sequencing. *Nucleic Acids Res.* **25**, 2816–2822 (1997).
65. Rosenblum, B. B. *et al.* New dye-labeled terminators for improved DNA sequencing patterns. *Nucleic Acids Res.* **25**, 4500–4504 (1997).
66. Metzker, M. L., Lu, J., & Gibbs, R. A. Electrophoretically uniform fluorescent dyes for automated DNA sequencing. *Science* **271**, 1420–1422 (1996).
67. Prober, J. M. *et al.* A system for rapid DNA sequencing with fluorescent chain-terminating dideoxynucleotides. *Science* **238**, 336–341 (1987).
68. Reeve, M. A. & Fuller, C. W. A novel thermostable polymerase for DNA sequencing. *Nature* **376**, 796–797 (1995).
69. Tabor, S. & Richardson, C. C. Selective inactivation of the exonuclease activity of bacteriophage T7 DNA polymerase by in vitro mutagenesis. *J. Biol. Chem.* **264**, 6447–6458 (1989).
70. Tabor, S. & Richardson, C. C. DNA sequence analysis with a modified bacteriophage T7 DNA polymerase—effect of pyrophosphorylation and metal ions. *J. Biol. Chem.* **265**, 8322–8328 (1990).
71. Murray, V. Improved double-stranded DNA sequencing using the linear polymerase chain reaction. *Nucleic Acids Res.* **17**, 8889 (1989).
72. Guttmann, A., Cohen, A. S., Heiger, D. N. & Karger, B. L. Analytical and micro preparative ultrahigh resolution of oligonucleotides by polyacrylamide-gel high-performance capillary electrophoresis. *Anal. Chem.* **62**, 137–141 (1990).
73. Luckey, J. A. *et al.* High-speed DNA sequencing by capillary electrophoresis. *Nucleic Acids Res.* **18**, 4417–4421 (1990).
74. Swerdlow, H., Wu, S., Harke, H. & Dovichi, N. J. Capillary gel-electrophoresis for DNA sequencing—laser-induced fluorescence detection with the sheath flow cuvette. *J. Chromatogr.* **516**, 61–67 (1990).
75. Meldrum, D. Automation for genomics, part one: preparation for sequencing. *Genome Res.* **10**, 1081–1092 (2000).
76. Meldrum, D. Automation for genomics, part two: sequencers, microarrays, and future trends. *Genome Res.* **10**, 1288–1303 (2000).
77. Ewing, B. & Green, P. Base-calling of automated sequencer traces using phred. II. Error probabilities. *Genome Res.* **8**, 186–194 (1998).
78. Ewing, B., Hillier, L., Wendl, M. C. & Green, P. Base-calling of automated sequencer traces using phred. I. Accuracy assessment. *Genome Res.* **8**, 175–185 (1998).
79. Bentley, D. R. Genomic sequence information should be released immediately and freely in the public domain. *Science* **274**, 533–534 (1996).
80. Guyer, M. Statement on the rapid release of genomic DNA sequence. *Genome Res.* **8**, 413 (1998).
81. Dietrich, W. *et al.* A genetic map of the mouse suitable for typing intraspecific crosses. *Genetics* **131**, 423–447 (1992).
82. Kim, U. J. *et al.* Construction and characterization of a human bacterial artificial chromosome library. *Genomics* **34**, 213–218 (1996).
83. Osoegawa, K. *et al.* Bacterial artificial chromosome libraries for mouse sequencing and functional analysis. *Genome Res.* **10**, 116–128 (2000).
84. Marra, M. A. *et al.* High throughput fingerprint analysis of large-insert clones. *Genome Res.* **7**, 1072–1084 (1997).
85. Marra, M. A. *et al.* A map for sequence analysis of the *Arabidopsis thaliana* genome. *Nature Genet.* **22**, 265–270 (1999).
86. The International Human Genome Mapping Consortium. A physical map of the human genome. *Nature* **409**, 934–941 (2001).
87. Zhao, S. *et al.* Human BAC ends quality assessment and sequence analyses. *Genomics* **63**, 321–332 (2000).
88. Mahairas, G. G. *et al.* Sequence-tagged connectors: A sequence approach to mapping and scanning the human genome. *Proc. Natl Acad. Sci. USA* **96**, 9739–9744 (1999).
89. Tilford, C. A. *et al.* A physical map of the human Y chromosome. *Nature* **409**, 943–945 (2001).
90. Bentley, D. R. *et al.* The physical maps for sequencing human chromosomes 1, 6, 9, 10, 13, 20 and X. *Nature* **409**, 942–943 (2001).
91. Montgomery, K. T. *et al.* A high-resolution map of human chromosome 12. *Nature* **409**, 945–946 (2001).
92. Brüls, T. *et al.* A physical map of human chromosome 14. *Nature* **409**, 947–948 (2001).
93. Hattori, M. *et al.* The DNA sequence of human chromosome 21. *Nature* **405**, 311–319 (2000).
94. Dunham, I. *et al.* The DNA sequence of human chromosome 22. *Nature* **402**, 489–495 (1999).
95. Cox, D. *et al.* Radiation hybrid map of the human genome. *Science* (in the press).
96. Osoegawa, K. *et al.* An improved approach for construction of bacterial artificial chromosome libraries. *Genomics* **52**, 1–8 (1998).
97. The International SNP Map Working Group. A map of human genome sequence variation containing 1.42 million single nucleotide polymorphisms. *Nature* **409**, 928–933 (2001).
98. Collins, F. S., Brooks, L. D. & Chakravarti, A. A DNA polymorphism discovery resource for research on human genetic variation. *Genome Res.* **8**, 1229–1231 (1998).
99. Stewart, E. A. *et al.* An STS-based radiation hybrid map of the human genome. *Genome Res.* **7**, 422–433 (1997).
100. Deloukas, P. *et al.* A physical map of 30,000 human genes. *Science* **282**, 744–746 (1998).
101. Dib, C. *et al.* A comprehensive genetic map of the human genome based on 5,264 microsatellites.

- Nature* **380**, 152–154 (1996).
102. Broman, K. W., Murray, J. C., Sheffield, V. C., White, R. L. & Weber, J. L. Comprehensive human genetic maps: individual and sex-specific variation in recombination. *Am. J. Hum. Genet.* **63**, 861–869 (1998).
 103. The BAC Resource Consortium. Integration of cytogenetic landmarks into the draft sequence of the human genome. *Nature* **409**, 953–958 (2001).
 104. Kent, W. J. & Haussler, D. GigAssembler: an algorithm for the initial assembly of the human working draft. Technical Report UCSC-CRL-00-17 (Univ. California at Santa Cruz, Santa Cruz, California, 2001).
 105. Morton, N. E. Parameters of the human genome. *Proc. Natl Acad. Sci. USA* **88**, 7474–7476 (1991).
 106. Podugolnikova, O. A. & Blumina, M. G. Heterochromatic regions on chromosomes 1, 9, 16, and Y in children with some disturbances occurring during embryo development. *Hum. Genet.* **63**, 183–188 (1983).
 107. Lundgren, R., Berger, R. & Kristoffersson, U. Constitutive heterochromatin C-band polymorphism in prostate cancer. *Cancer Genet. Cytogenet.* **51**, 57–62 (1991).
 108. Lee, C., Wevrick, R., Fisher, R. B., Ferguson-Smith, M. A. & Lin, C. C. Human centromeric DNAs. *Hum. Genet.* **100**, 291–304 (1997).
 109. Riethman, H. C. *et al.* Integration of telomere sequences with the draft human genome sequence. *Nature* **409**, 953–958 (2001).
 110. Pruitt, K. D. & Maglott, D. R. RefSeq and LocusLink: NCBI gene-centered resources. *Nucleic Acids Res.* **29**, 137–140 (2001).
 111. Wolfsberg, T. G., McEntyre, J. & Schuler, G. D. Guide to the draft human genome. *Nature* **409**, 824–826 (2001).
 112. Hurst, L. D. & Eyre-Walker, A. Evolutionary genomics: reading the bands. *Bioessays* **22**, 105–107 (2000).
 113. Saccone, S. *et al.* Correlations between isochores and chromosomal bands in the human genome. *Proc. Natl Acad. Sci. USA* **90**, 11929–11933 (1993).
 114. Zoubak, S., Clay, O. & Bernardi, G. The gene distribution of the human genome. *Gene* **174**, 95–102 (1996).
 115. Gardiner, K. Base composition and gene distribution: critical patterns in mammalian genome organization. *Trends Genet.* **12**, 519–524 (1996).
 116. Duret, L., Mouchiroud, D. & Gautier, C. Statistical analysis of vertebrate sequences reveals that long genes are scarce in GC-rich isochores. *J. Mol. Evol.* **40**, 308–317 (1995).
 117. Saccone, S., De Sario, A., Della Valle, G. & Bernardi, G. The highest gene concentrations in the human genome are in telomeric bands of metaphase chromosomes. *Proc. Natl Acad. Sci. USA* **89**, 4913–4917 (1992).
 118. Bernardi, G. *et al.* The mosaic genome of warm-blooded vertebrates. *Science* **228**, 953–958 (1985).
 119. Bernardi, G. Isochores and the evolutionary genomics of vertebrates. *Gene* **241**, 3–17 (2000).
 120. Fickett, J. W., Torney, D. C. & Wolf, D. R. Base compositional structure of genomes. *Genomics* **13**, 1056–1064 (1992).
 121. Churchill, G. A. Stochastic models for heterogeneous DNA sequences. *Bull. Math. Biol.* **51**, 79–94 (1989).
 122. Bird, A., Taggart, M., Frommer, M., Miller, O. J. & Macleod, D. A fraction of the mouse genome that is derived from islands of nonmethylated, CpG-rich DNA. *Cell* **40**, 91–99 (1985).
 123. Bird, A. P. CpG islands as gene markers in the vertebrate nucleus. *Trends Genet.* **3**, 342–347 (1987).
 124. Chan, M. F., Liang, G. & Jones, P. A. Relationship between transcription and DNA methylation. *Curr. Top. Microbiol. Immunol.* **249**, 75–86 (2000).
 125. Holliday, R. & Pugh, J. E. DNA modification mechanisms and gene activity during development. *Science* **187**, 226–232 (1975).
 126. Larsen, F., Gundersen, G., Lopez, R. & Prydz, H. CpG islands as gene markers in the human genome. *Genomics* **13**, 1095–1107 (1992).
 127. Tazi, J. & Bird, A. Alternative chromatin structure at CpG islands. *Cell* **60**, 909–920 (1990).
 128. Gardiner-Garden, M. & Frommer, M. CpG islands in vertebrate genomes. *J. Mol. Biol.* **196**, 261–282 (1987).
 129. Antequera, F. & Bird, A. Number of CpG islands and genes in human and mouse. *Proc. Natl Acad. Sci. USA* **90**, 11995–11999 (1993).
 130. Ewing, B. & Green, P. Analysis of expressed sequence tags indicates 35,000 human genes. *Nature Genet.* **25**, 232–234 (2000).
 131. Yu, A. Comparison of human genetic and sequence-based physical maps. *Nature* **409**, 951–953 (2001).
 132. Kaback, D. B., Guacci, V., Barber, D. & Mahon, J. W. Chromosome size-dependent control of meiotic recombination. *Science* **256**, 228–232 (1992).
 133. Riles, L. *et al.* Physical maps of the 6 smallest chromosomes of *Saccharomyces cerevisiae* at a resolution of 2.6-kilobase pairs. *Genetics* **134**, 81–150 (1993).
 134. Lynn, A. *et al.* Patterns of meiotic recombination on the long arm of human chromosome 21. *Genome Res.* **10**, 1319–1332 (2000).
 135. Laurie, D. A. & Hulten, M. A. Further studies on bivalent chiasma frequency in human males with normal karyotypes. *Ann. Hum. Genet.* **49**, 189–201 (1985).
 136. Roeder, G. S. Meiotic chromosomes: it takes two to tango. *Genes Dev.* **11**, 2600–2621 (1997).
 137. Wu, T.-C. & Lichten, M. Meiosis-induced double-strand break sites determined by yeast chromatin structure. *Science* **263**, 515–518 (1994).
 138. Gerton, J. L. *et al.* Global mapping of meiotic recombination hotspots and coldspots in the yeast *Saccharomyces cerevisiae*. *Proc. Natl Acad. Sci. USA* **97**, 11383–11390 (2000).
 139. Li, W.-H. *Molecular Evolution* (Sinauer, Sunderland, Massachusetts, 1997).
 140. Gregory, T. R. & Hebert, P. D. The modulation of DNA content: proximate causes and ultimate consequences. *Genome Res.* **9**, 317–324 (1999).
 141. Hartl, D. L. Molecular melodies in high and low C. *Nature Rev. Genet.* **1**, 145–149 (2000).
 142. Smit, A. F. Interspersed repeats and other mementos of transposable elements in mammalian genomes. *Curr. Opin. Genet. Dev.* **9**, 657–663 (1999).
 143. Prak, E. L. & Haig, H. K. Jr Mobile elements and the human genome. *Nature Rev. Genet.* **1**, 134–144 (2000).
 144. Okada, N., Hamada, M., Ogiwara, I. & Ohshima, K. SINEs and LINEs share common 3' sequences: a review. *Gene* **205**, 229–243 (1997).
 145. Esnault, C., Maestre, J. & Heidmann, T. Human LINE retrotransposons generate processed pseudogenes. *Nature Genet.* **24**, 363–367 (2000).
 146. Wei, W. *et al.* Human L1 retrotransposition: cis-preference vs. trans-complementation. *Mol. Cell. Biol.* **21**, 1429–1439 (2001).
 147. Malik, H. S., Henikoff, S. & Eickbush, T. H. Poised for contagion: evolutionary origins of the infectious abilities of invertebrate retroviruses. *Genome Res.* **10**, 1307–1318 (2000).
 148. Smit, A. F. The origin of interspersed repeats in the human genome. *Curr. Opin. Genet. Dev.* **6**, 743–748 (1996).
 149. Clark, J. B. & Tidwell, M. G. A phylogenetic perspective on P transposable element evolution in *Drosophila*. *Proc. Natl Acad. Sci. USA* **94**, 11428–11433 (1997).
 150. Haring, E., Hagemann, S. & Pinsker, W. Ancient and recent horizontal invasions of *Drosophilidae* by P elements. *J. Mol. Evol.* **51**, 577–586 (2000).
 151. Koga, A. *et al.* Evidence for recent invasion of the medaka fish genome by the Tol2 transposable element. *Genetics* **155**, 273–281 (2000).
 152. Robertson, H. M. & Lampe, D. J. Recent horizontal transfer of a mariner transposable element among and between Diptera and Neuroptera. *Mol. Biol. Evol.* **12**, 850–862 (1995).
 153. Simmons, G. M. Horizontal transfer of hobo transposable elements within the *Drosophila melanogaster* species complex: evidence from DNA sequencing. *Mol. Biol. Evol.* **9**, 1050–1060 (1992).
 154. Malik, H. S., Burke, W. D. & Eickbush, T. H. The age and evolution of non-LTR retrotransposable elements. *Mol. Biol. Evol.* **16**, 793–805 (1999).
 155. Kordis, D. & Gubensek, F. Bov-B long interspersed repeated DNA (LINE) sequences are present in *Vipera ammodytes* phospholipase A2 genes and in genomes of Viperidae snakes. *Eur. J. Biochem.* **246**, 772–779 (1997).
 156. Jurka, J. Repbase update: a database and an electronic journal of repetitive elements. *Trends Genet.* **16**, 418–420 (2000).
 157. Sarich, V. M. & Wilson, A. C. Generation time and genome evolution in primates. *Science* **179**, 1144–1147 (1973).
 158. Smit, A. F., Toth, G., Riggs, A. D. & Jurka, J. Ancestral, mammalian-wide subfamilies of LINE-1 repetitive sequences. *J. Mol. Biol.* **246**, 401–417 (1995).
 159. Lim, J. K. & Simmons, M. J. Gross chromosome rearrangements mediated by transposable elements in *Drosophila melanogaster*. *Bioessays* **16**, 269–275 (1994).
 160. Caceres, M., Ranz, J. M., Barbash, A., Long, M. & Ruiz, A. Generation of a widespread *Drosophila* inversion by a transposable element. *Science* **285**, 415–418 (1999).
 161. Gray, Y. H. It takes two transposons to tango: transposable-element-mediated chromosomal rearrangements. *Trends Genet.* **16**, 461–468 (2000).
 162. Zhang, J. & Peterson, T. Genome rearrangements by nonlinear transposons in maize. *Genetics* **153**, 1403–1410 (1999).
 163. Smit, A. F. Identification of a new, abundant superfamily of mammalian LTR-transposons. *Nucleic Acids Res.* **21**, 1863–1872 (1993).
 164. Cordonnier, A., Casella, J. F. & Heidmann, T. Isolation of novel human endogenous retrovirus-like elements with foamy virus-related pol sequence. *J. Virol.* **69**, 5890–5897 (1995).
 165. Medstrand, P. & Mager, D. L. Human-specific integrations of the HERV-K endogenous retrovirus family. *J. Virol.* **72**, 9782–9787 (1998).
 166. Myers, E. W. *et al.* A whole-genome assembly of *Drosophila*. *Science* **287**, 2196–2204 (2000).
 167. Petrov, D. A., Lozovskaya, E. R. & Hartl, D. L. High intrinsic rate of DNA loss in *Drosophila*. *Nature* **384**, 346–349 (1996).
 168. Li, W. H., Ellsworth, D. L., Krushkal, J., Chang, B. H. & Hewett-Emmett, D. Rates of nucleotide substitution in primates and rodents and the generation-time effect hypothesis. *Mol. Phylogenet. Evol.* **5**, 182–187 (1996).
 169. Goodman, M. *et al.* Toward a phylogenetic classification of primates based on DNA evidence complemented by fossil evidence. *Mol. Phylogenet. Evol.* **9**, 585–598 (1998).
 170. Kazazian, H. H. Jr & Moran, J. V. The impact of L1 retrotransposons on the human genome. *Nature Genet.* **19**, 19–24 (1998).
 171. Malik, H. S. & Eickbush, T. H. NeSL-1, an ancient lineage of site-specific non-LTR retrotransposons from *Caenorhabditis elegans*. *Genetics* **154**, 193–203 (2000).
 172. Casavant, N. C. *et al.* The end of the LINE?: lack of recent L1 activity in a group of South American rodents. *Genetics* **154**, 1809–1817 (2000).
 173. Meunier-Rotival, M., Soriano, P., Cuny, G., Strauss, F. & Bernardi, G. Sequence organization and genomic distribution of the major family of interspersed repeats of mouse DNA. *Proc. Natl Acad. Sci. USA* **79**, 355–359 (1982).
 174. Soriano, P., Meunier-Rotival, M. & Bernardi, G. The distribution of interspersed repeats is nonuniform and conserved in the mouse and human genomes. *Proc. Natl Acad. Sci. USA* **80**, 1816–1820 (1983).
 175. Goldman, M. A., Holmquist, G. P., Gray, M. C., Caston, L. A. & Nag, A. Replication timing of genes and middle repetitive sequences. *Science* **224**, 686–692 (1984).
 176. Manuelidis, L. & Ward, D. C. Chromosomal and nuclear distribution of the *HindIII* 1.9-kb human DNA repeat segment. *Chromosoma* **91**, 28–38 (1984).
 177. Feng, Q., Moran, J. V., Kazazian, H. H. Jr & Boeke, J. D. Human L1 retrotransposon encodes a conserved endonuclease required for retrotransposition. *Cell* **87**, 905–916 (1996).
 178. Jurka, J. Sequence patterns indicate an enzymatic involvement in integration of mammalian retrotransposons. *Proc. Natl Acad. Sci. USA* **94**, 1872–1877 (1997).
 179. Arcot, S. S. *et al.* High-resolution cartography of recently integrated human chromosome 19-specific Alu fossils. *J. Mol. Biol.* **281**, 843–856 (1998).
 180. Schmid, C. W. Does SINE evolution preclude Alu function? *Nucleic Acids Res.* **26**, 4541–4550 (1998).
 181. Chu, W. M., Ballard, R., Carpick, B. W., Williams, B. R. & Schmid, C. W. Potential Alu function: regulation of the activity of double-stranded RNA-activated kinase PKR. *Mol. Cell. Biol.* **18**, 58–68 (1998).
 182. Li, T., Spearow, J., Rubin, C. M. & Schmid, C. W. Physiological stresses increase mouse short interspersed element (SINE) RNA expression in vivo. *Gene* **239**, 367–372 (1999).
 183. Liu, W. M., Chu, W. M., Choudary, P. V. & Schmid, C. W. Cell stress and translational inhibitors transiently increase the abundance of mammalian SINE transcripts. *Nucleic Acids Res.* **23**, 1758–1765 (1995).
 184. Filipski, J. Correlation between molecular clock ticking, codon usage fidelity of DNA repair, chromosome banding and chromatin compactness in germline cells. *FEBS Lett.* **217**, 184–188 (1987).
 185. Sueoka, N. Directional mutation pressure and neutral molecular evolution. *Proc. Natl Acad. Sci.*

- USA **85**, 2653–2657 (1988).
186. Wolfe, K. H., Sharp, P. M. & Li, W. H. Mutation rates differ among regions of the mammalian genome. *Nature* **337**, 283–285 (1989).
 187. Bains, W. Local sequence dependence of rate of base replacement in mammals. *Mutat. Res.* **267**, 43–54 (1992).
 188. Mathews, C. K. & Ji, J. DNA precursor asymmetries, replication fidelity, and variable genome evolution. *Bioessays* **14**, 295–301 (1992).
 189. Holmquist, G. P. & Filipski, J. Organization of mutations along the genome: a prime determinant of genome evolution. *Trends Ecol. Evol.* **9**, 65–68 (1994).
 190. Eyre-Walker, A. Evidence of selection on silent site base composition in mammals: potential implications for the evolution of isochore and junk DNA. *Genetics* **152**, 675–683 (1999).
 191. The International SNP Map Working Group. An SNP map of the human genome generated by reduced representation shotgun sequencing. *Nature* **407**, 513–516 (2000).
 192. Bohossian, H. B., Skaletsky, H. & Page, D. C. Unexpectedly similar rates of nucleotide substitution found in male and female hominids. *Nature* **406**, 622–625 (2000).
 193. Skowronski, J., Fanning, T. G. & Singer, M. F. Unit-length LINE-1 transcripts in human teratocarcinoma cells. *Mol. Cell. Biol.* **8**, 1385–1397 (1988).
 194. Boissinot, S., Chevret, P. & Furano, A. V. L1 (LINE-1) retrotransposon evolution and amplification in recent human history. *Mol. Biol. Evol.* **17**, 915–928 (2000).
 195. Moran, J. V. Human L1 retrotransposition: insights and peculiarities learned from a cultured cell retrotransposition assay. *Genetica* **107**, 39–51 (1999).
 196. Kazazian, H. H. Jr *et al.* Haemophilia A resulting from *de novo* insertion of L1 sequences represents a novel mechanism for mutation in man. *Nature* **332**, 164–166 (1988).
 197. Sheen, F.-m. *et al.* Reading between the LINES: Human genomic variation introduced by LINE-1 retrotransposition. *Genome Res.* **10**, 1496–1508 (2000).
 198. Dombroski, B. A., Mathias, S. L., Nanthakumar, E., Scott, A. F. & Kazazian, H. H. Jr Isolation of an active human transposable element. *Science* **254**, 1805–1808 (1991).
 199. Holmes, S. E., Dombroski, B. A., Krebs, C. M., Boehm, C. D. & Kazazian, H. H. Jr A new retrotransposable human L1 element from the LRE2 locus on chromosome 1q produces a chimaeric insertion. *Nature Genet.* **7**, 143–148 (1994).
 200. Sassaman, D. M. *et al.* Many human L1 elements are capable of retrotransposition. *Nature Genet.* **16**, 37–43 (1997).
 201. Dombroski, B. A., Scott, A. F. & Kazazian, H. H. Jr Two additional potential retrotransposons isolated from a human L1 subfamily that contains an active retrotransposable element. *Proc. Natl Acad. Sci. USA* **90**, 6513–6517 (1993).
 202. Kimberland, M. L. *et al.* Full-length human L1 insertions retain the capacity for high frequency retrotransposition in cultured cells. *Hum. Mol. Genet.* **8**, 1557–1560 (1999).
 203. Moran, J. V. *et al.* High frequency retrotransposition in cultured mammalian cells. *Cell* **87**, 917–927 (1996).
 204. Moran, J. V., DeBerardinis, R. J. & Kazazian, H. H. Jr Exon shuffling by L1 retrotransposition. *Science* **283**, 1530–1534 (1999).
 205. Pickeral, O. K., Makalowski, W., Boguski, M. S. & Boeve, J. D. Frequent human genomic DNA transduction driven by LINE-1 retrotransposition. *Genome Res.* **10**, 411–415 (2000).
 206. Miki, Y. *et al.* Disruption of the APC gene by a retrotransposon insertion of L1 sequence in a colon cancer. *Cancer Res.* **52**, 643–645 (1992).
 207. Branciforte, D. & Martin, S. L. Developmental and cell type specificity of LINE-1 expression in mouse testis: implications for transposition. *Mol. Cell. Biol.* **14**, 2584–2592 (1994).
 208. Trelogan, S. A. & Martin, S. L. Tightly regulated, developmentally specific expression of the first open reading frame from LINE-1 during mouse embryogenesis. *Proc. Natl Acad. Sci. USA* **92**, 1520–1524 (1995).
 209. Jurka, J. & Kapitonov, V. V. Sectorial mutagenesis by transposable elements. *Genetica* **107**, 239–248 (1999).
 210. Fraser, M. J., Ciszczon, T., Elick, T. & Bauser, C. Precise excision of TTAA-specific lepidopteran transposons piggyBac (IIP2) and tagalong (TFP3) from the baculovirus genome in cell lines from two species of Lepidoptera. *Insect Mol. Biol.* **5**, 141–151 (1996).
 211. Brosius, J. Genomes were forged by massive bombardments with retroelements and retrosequences. *Genetica* **107**, 209–238 (1999).
 212. Kruglyak, S., Durrett, R. T., Schug, M. D. & Aquadro, C. F. Equilibrium distribution of microsatellite repeat length resulting from a balance between slippage events and point mutations. *Proc. Natl Acad. Sci. USA* **95**, 10774–10778 (1998).
 213. Toth, G., Gaspari, Z. & Jurka, J. Microsatellites in different eukaryotic genomes: survey and analysis. *Genome Res.* **10**, 967–981 (2000).
 214. Ellegrén, H. Heterogeneous mutation processes in human microsatellite DNA sequences. *Nature Genet.* **24**, 400–402 (2000).
 215. Ji, Y., Eichler, E. E., Schwartz, S. & Nicholls, R. D. Structure of chromosomal duplions and their role in mediating human genomic disorders. *Genome Res.* **10**, 597–610 (2000).
 216. Eichler, E. E. Masquerading repeats: paralogous pitfalls of the human genome. *Genome Res.* **8**, 758–762 (1998).
 217. Mazzarella, R. & D. Schlessinger, D. Pathological consequences of sequence duplications in the human genome. *Genome Res.* **8**, 1007–1021 (1998).
 218. Eichler, E. E. *et al.* Interchromosomal duplications of the adrenoleukodystrophy locus: a phenomenon of pericentromeric plasticity. *Hum. Mol. Genet.* **6**, 991–1002 (1997).
 219. Horvath, J. E., Schwartz, S. & Eichler, E. E. The mosaic structure of human pericentromeric DNA: a strategy for characterizing complex regions of the human genome. *Genome Res.* **10**, 839–852 (2000).
 220. Brand-Arpon, V. *et al.* A genomic region encompassing a cluster of olfactory receptor genes and a myosin light chain kinase (MLK) gene is duplicated on human chromosome regions 3q13-q21 and 3p13. *Genomics* **56**, 98–110 (1999).
 221. Arnold, N., Wienberg, J., Ermert, K. & Zachau, H. G. Comparative mapping of DNA probes derived from the V kappa immunoglobulin gene regions on human and great ape chromosomes by fluorescence in situ hybridization. *Genomics* **26**, 147–150 (1995).
 222. Eichler, E. E. *et al.* Duplication of a gene-rich cluster between 16p11.1 and Xq28: a novel pericentromeric-directed mechanism for paralogous genome evolution. *Hum. Mol. Genet.* **5**, 899–912 (1996).
 223. Potier, M. *et al.* Two sequence-ready contigs spanning the two copies of a 200-kb duplication on human 21q: partial sequence and polymorphisms. *Genomics* **51**, 417–426 (1998).
 224. Regnier, V. *et al.* Emergence and scattering of multiple neurofibromatosis (NF1)-related sequences during hominoid evolution suggest a process of pericentromeric interchromosomal transposition. *Hum. Mol. Genet.* **6**, 9–16 (1997).
 225. Ritchie, R. J., Mattei, M. G. & Lalanne, M. A large polymorphic repeat in the pericentromeric region of human chromosome 15q contains three partial gene duplications. *Hum. Mol. Genet.* **7**, 1253–1260 (1998).
 226. Trask, B. J. *et al.* Members of the olfactory receptor gene family are contained in large blocks of DNA duplicated polymorphically near the ends of human chromosomes. *Hum. Mol. Genet.* **7**, 13–26 (1998).
 227. Trask, B. J. *et al.* Large multi-chromosomal duplications encompass many members of the olfactory receptor gene family in the human genome. *Hum. Mol. Genet.* **7**, 2007–2020 (1998).
 228. van Deutekom, J. C. *et al.* Identification of the first gene (FRG1) from the FSHD region on human chromosome 4q35. *Hum. Mol. Genet.* **5**, 581–590 (1996).
 229. Zachau, H. G. The immunoglobulin kappa locus—or—what has been learned from looking closely at one-tenth of a percent of the human genome. *Gene* **135**, 167–173 (1993).
 230. Zimonic, D. B., Kelley, M. J., Rubin, J. S., Aronson, S. A. & Popescu, N. C. Fluorescence in situ hybridization analysis of keratinocyte growth factor gene amplification and dispersion in evolution of great apes and humans. *Proc. Natl Acad. Sci. USA* **94**, 11461–11465 (1997).
 231. van Geel, M. *et al.* The FSHD region on human chromosome 4q35 contains potential coding regions among pseudogenes and a high density of repeat elements. *Genomics* **61**, 55–65 (1999).
 232. Horvath, J. E. *et al.* Molecular structure and evolution of an alpha satellite/non-alpha satellite junction at 16p11. *Hum. Mol. Genet.* **9**, 113–123 (2000).
 233. Guy, J. *et al.* Genomic sequence and transcriptional profile of the boundary between pericentromeric satellites and genes on human chromosome arm 10q. *Hum. Mol. Genet.* **9**, 2029–2042 (2000).
 234. Reiter, L. T., Murakami, T., Koeth, T., Gibbs, R. A. & Lupski, J. R. The human COX10 gene is disrupted during homologous recombination between the 24 kb proximal and distal CMT1A-REPs. *Hum. Mol. Genet.* **6**, 1595–1603 (1997).
 235. Amos-Landgraf, J. M. *et al.* Chromosome breakage in the Prader-Willi and Angelman syndromes involves recombination between large, transcribed repeats at proximal and distal breakpoints. *Am. J. Hum. Genet.* **65**, 370–386 (1999).
 236. Christian, S. L., Fantes, J. A., Mewborn, S. K., Huang, B. & Ledbetter, D. H. Large genomic duplions map to sites of instability in the Prader-Willi/Angelman syndrome chromosome region (15q11-q13). *Hum. Mol. Genet.* **8**, 1025–1037 (1999).
 237. Edelmann, L., Pandita, R. K. & Morrow, B. E. Low-copy repeats mediate the common 3-Mb deletion in patients with velo-cardio-facial syndrome. *Am. J. Hum. Genet.* **64**, 1076–1086 (1999).
 238. Shaikh, T. H. *et al.* Chromosome 22-specific low copy repeats and the 22q11.2 deletion syndrome: genomic organization and deletion endpoint analysis. *Hum. Mol. Genet.* **9**, 489–501 (2000).
 239. Francke, U. Williams-Beuren syndrome: genes and mechanisms. *Hum. Mol. Genet.* **8**, 1947–1954 (1999).
 240. Peoples, R. *et al.* A physical map, including a BAC/PAC clone contig, of the Williams-Beuren syndrome-deletion region at 7q11.23. *Am. J. Hum. Genet.* **66**, 47–68 (2000).
 241. Eichler, E. E., Archidiacono, N. & Rocchi, M. CAGGG repeats and the pericentromeric duplication of the hominoid genome. *Genome Res.* **9**, 1048–1058 (1999).
 242. O'Keefe, C. & Eichler, E. In *Comparative Genomics: Empirical and Analytical Approaches to Gene Order Dynamics, Map Alignment and the Evolution of Gene Families* (eds Sankoff, D. & Nadeau, J.) 29–46 (Kluwer Academic, Dordrecht, 2000).
 243. Lander, E. S. The new genomics: Global views of biology. *Science* **274**, 536–539 (1996).
 244. Eddy, S. R. Noncoding RNA genes. *Curr. Opin. Genet. Dev.* **9**, 695–699 (1999).
 245. Ban, N., Nissen, P., Hansen, J., Moore, P. B. & Steitz, T. A. The complete atomic structure of the large ribosomal subunit at 2.4 angstrom resolution. *Science* **289**, 905–920 (2000).
 246. Nissen, P., Hansen, J., Ban, N., Moore, P. B. & Steitz, T. A. The structural basis of ribosome activity in peptide bond synthesis. *Science* **289**, 920–930 (2000).
 247. Weinstein, L. B. & Steitz, T. A. Guided tours: from precursor snoRNA to functional snoRNP. *Curr. Opin. Cell Biol.* **11**, 378–384 (1999).
 248. Bachellerie, J.-P. & Cavaille, J. In *Modification and Editing of RNA* (ed. Benne, H. G. a. R.) 255–272 (ASM, Washington DC, 1998).
 249. Burge, C. & Sharp, P. A. Classification of introns: U2-type or U12-type. *Cell* **91**, 875–879 (1997).
 250. Brown, C. J. *et al.* The Human Xist gene—analysis of a 17 kb inactive X-specific RNA that contains conserved repeats and is highly localized within the nucleus. *Cell* **71**, 527–542 (1992).
 251. Kickhoefer, V. A., Vasu, S. K. & Rome, L. H. Vaults are the answer, what is the question? *Trends Cell Biol.* **6**, 174–178 (1996).
 252. Hatlen, L. & Attardi, G. Proportion of the HeLa cell genome complementary to the transfer RNA and 5S RNA. *J. Mol. Biol.* **56**, 535–553 (1971).
 253. Sprinzl, M., Horn, C., Brown, M., Ioudovitch, A. & Steinberg, S. Compilation of tRNA sequences and sequences of tRNA genes. *Nucleic Acids Res.* **26**, 148–153 (1998).
 254. Long, E. O. & Dawid, I. B. Repeated genes in eukaryotes. *Annu. Rev. Biochem.* **49**, 727–764 (1980).
 255. Crick, F. H. Codon–anticodon pairing: the wobble hypothesis. *J. Mol. Biol.* **19**, 548–555 (1966).
 256. Guthrie, C. & Abelson, J. In *The Molecular Biology of the Yeast Saccharomyces: Metabolism and Gene Expression* (eds Strathern, J. & Broach J.) 487–528 (Cold Spring Harbor Laboratory Press, Cold Spring Harbor, New York, 1982).
 257. Soll, D. & RajBhandary, U. (eds) *tRNA: Structure, Biosynthesis, and Function* (ASM, Washington DC, 1995).
 258. Ikemura, T. Codon usage and tRNA content in unicellular and multicellular organisms. *Mol. Biol. Evol.* **2**, 13–34 (1985).
 259. Bulmer, M. Coevolution of codon usage and transfer-RNA abundance. *Nature* **325**, 728–730 (1987).
 260. Duret, L. tRNA gene number and codon usage in the *C. elegans* genome are co-adapted for optimal translation of highly expressed genes. *Trends Genet.* **16**, 287–289 (2000).
 261. Sharp, P. M. & Matassi, G. Codon usage and genome evolution. *Curr. Opin. Genet. Dev.* **4**, 851–860 (1994).
 262. Buckland, R. A. A primate transfer-RNA gene cluster and the evolution of human chromosome 1. *Cytogenet. Cell Genet.* **61**, 1–4 (1992).
 263. Gornon, E. S. & Goddard, J. P. Human tRNA-Glu genes: their copy number and organization. *FEBS Lett.* **276**, 138–142 (1990).
 264. Sylvester, J. E. *et al.* The human ribosomal RNA genes: structure and organization of the complete repeating unit. *Hum. Genet.* **73**, 193–198 (1986).

265. Sorensen, P. D. & Frederiksen, S. Characterization of human 5S ribosomal RNA genes. *Nucleic Acids Res.* **19**, 4147–4151 (1991).
266. Timofeeva, M. *et al.* [Organization of a 5S ribosomal RNA gene cluster in the human genome]. *Mol. Biol. (Mosk.)* **27**, 861–868 (1993).
267. Little, R. D. & Braaten, D. C. Genomic organization of human 5S rDNA and sequence of one tandem repeat. *Genomics* **4**, 376–383 (1989).
268. Maden, B. E. H. The numerous modified nucleotides in eukaryotic ribosomal RNA. *Prog. Nucleic Acid Res. Mol. Biol.* **39**, 241–303 (1990).
269. Tykowski, K. T., You, Z. H., Graham, P. J. & Steitz, J. A. Modification of U6 spliceosomal RNA is guided by other small RNAs. *Mol. Cell* **2**, 629–638 (1998).
270. Pavelitz, T., Liao, D. Q. & Weiner, A. M. Concerted evolution of the tandem array encoding primate U2 snRNA (the RNU2 locus) is accompanied by dramatic remodeling of the junctions with flanking chromosomal sequences. *EMBO J.* **18**, 3783–3792 (1999).
271. Lindgren, V., Ares, A., Weiner, A. M. & Francke, U. Human genes for U2 small nuclear RNA map to a major adenovirus 12 modification site on chromosome 17. *Nature* **314**, 115–116 (1985).
272. Van Arsdell, S. W. & Weiner, A. M. Human genes for U2 small nuclear RNA are tandemly repeated. *Mol. Cell. Biol.* **4**, 492–499 (1984).
273. Gao, L. I., Frey, M. R. & Matera, A. G. Human genes encoding U3 snRNA associate with coiled bodies in interphase cells and are clustered on chromosome 17p11.2 in a complex inverted repeat structure. *Nucleic Acids Res.* **25**, 4740–4747 (1997).
274. Hawkins, J. D. A survey on intron and exon lengths. *Nucleic Acids Res.* **16**, 9893–9908 (1988).
275. Burge, C. & Karlin, S. Prediction of complete gene structures in human genomic DNA. *J. Mol. Biol.* **268**, 78–94 (1997).
276. Labit, S. & Kolmerer, B. Titins: giant proteins in charge of muscle ultrastructure and elasticity. *Science* **270**, 293–296 (1995).
277. Stern, D. A., Carlo, T. & Berget, S. M. Architectural limits on split genes. *Proc. Natl Acad. Sci. USA* **93**, 15081–15085 (1996).
278. Sun, Q., Mayeda, A., Hampson, R. K., Krainer, A. R. & Rottman, F. M. General splicing factor SF2/ASF promotes alternative splicing by binding to an exonic splicing enhancer. *Genes Dev.* **7**, 2598–2608 (1993).
279. Tanaka, K., Watakabe, A. & Shimura, Y. Polypurine sequences within a downstream exon function as a splicing enhancer. *Mol. Cell. Biol.* **14**, 1347–1354 (1994).
280. Carlo, T., Stern, D. A. & Berget, S. M. An intron splicing enhancer containing a G-rich repeat facilitates inclusion of a vertebrate micro-exon. *RNA* **2**, 342–353 (1996).
281. Burset, M., Seledtsov, I. A. & Solovyev, V. V. Analysis of canonical and non-canonical splice sites in mammalian genomes. *Nucleic Acids Res.* **28**, 4364–4375 (2000).
282. Burge, C. B., Padgett, R. A. & Sharp, P. A. Evolutionary fates and origins of U12-type introns. *Mol. Cell* **2**, 773–785 (1998).
283. Mironov, A. A., Fickett, J. W. & Gelfand, M. S. Frequent alternative splicing of human genes. *Genome Res.* **9**, 1288–1293 (1999).
284. Hanke, J. *et al.* Alternative splicing of human genes: more the rule than the exception? *Trends Genet.* **15**, 389–390 (1999).
285. Brett, D. *et al.* EST comparison indicates 38% of human mRNAs contain possible alternative splice forms. *FEBS Lett.* **474**, 83–86 (2000).
286. Dunham, I. The gene guessing game. *Yeast* **17**, 218–224 (2000).
287. Lewin, B. *Gene Expression* (Wiley, New York, 1980).
288. Lewin, B. *Genes IV* 466–481 (Oxford Univ. Press, Oxford, 1990).
289. Smaglik, P. Researchers take a gamble on the human genome. *Nature* **405**, 264 (2000).
290. Fields, C., Adams, M. D., White, O. & Venter, J. C. How many genes in the human genome? *Nature Genet.* **7**, 345–346 (1994).
291. Liang, F. *et al.* Gene index analysis of the human genome estimates approximately 120,000 genes. *Nature Genet.* **25**, 239–240 (2000).
292. Roest Crollius, H. *et al.* Estimate of human gene number provided by genome-wide analysis using *Tetraodon nigroviridis* DNA sequence. *Nature Genet.* **25**, 235–238 (2000).
293. The *C. elegans* Sequencing Consortium. Genome sequence of the nematode *C. elegans*: A platform for investigating biology. *Science* **282**, 2012–2018 (1998).
294. Rubin, G. M. *et al.* Comparative genomics of the eukaryotes. *Science* **287**, 2204–2215 (2000).
295. Green, P. *et al.* Ancient conserved regions in new gene sequences and the protein databases. *Science* **259**, 1711–1716 (1993).
296. Fraser, A. G. *et al.* Functional genomic analysis of *C. elegans* chromosome I by systematic RNA interference. *Nature* **408**, 325–330 (2000).
297. Mott, R. EST_GENOME: a program to align spliced DNA sequences to unspliced genomic DNA. *Comput. Appl. Biosci.* **13**, 477–478 (1997).
298. Florea, L., Hartzell, G., Zhang, Z., Rubin, G. M. & Miller, W. A computer program for aligning a cDNA sequence with a genomic DNA sequence. *Genome Res.* **8**, 967–974 (1998).
299. Bailey, L. C. Jr, Searls, D. B. & Overton, G. C. Analysis of EST-driven gene annotation in human genomic sequence. *Genome Res.* **8**, 362–376 (1998).
300. Birney, E., Thompson, J. D. & Gibson, T. J. PairWise and SearchWise: finding the optimal alignment in a simultaneous comparison of a protein profile against all DNA translation frames. *Nucleic Acids Res.* **24**, 2730–2739 (1996).
301. Gelfand, M. S., Mironov, A. A. & Pevzner, P. A. Gene recognition via spliced sequence alignment. *Proc. Natl Acad. Sci. USA* **93**, 9061–9066 (1996).
302. Kulp, D., Haussler, D., Reese, M. G. & Eeckman, F. H. A generalized hidden Markov model for the recognition of human genes in DNA. *ISMB* **4**, 134–142 (1996).
303. Reese, M. G., Kulp, D., Tammam, H. & Haussler, D. Genie—gene finding in *Drosophila melanogaster*. *Genome Res.* **10**, 529–538 (2000).
304. Solovyev, V. & Salamatov, A. The Gene-Finder computer tools for analysis of human and model organisms genome sequences. *ISMB* **5**, 294–302 (1997).
305. Guigo, R., Agarwal, P., Abril, J. F., Burset, M. & Fickett, J. W. An assessment of gene prediction accuracy in large DNA sequences. *Genome Res.* **10**, 1631–1642 (2000).
306. Hubbard, T. & Birney, E. Open annotation offers a democratic solution to genome sequencing. *Nature* **403**, 825 (2000).
307. Bateman, A. *et al.* The Pfam protein families database. *Nucleic Acids Res.* **28**, 263–266 (2000).
308. Birney, E. & Durbin, R. Using GeneWise in the *Drosophila* annotation experiment. *Genome Res.* **10**, 547–548 (2000).
309. The RIKEN Genome Exploration Research Group Phase II Team and the FANTOM Consortium. Functional annotation of a full-length mouse cDNA collection. *Nature* **409**, 685–690 (2001).
310. Basrai, M. A., Hieter, P. & Boeke, J. D. Small open reading frames: beautiful needles in the haystack. *Genome Res.* **7**, 768–771 (1997).
311. Janin, J. & Chothia, C. Domains in proteins: definitions, location, and structural principles. *Methods Enzymol.* **115**, 420–430 (1985).
312. Ponting, C. P., Schultz, J., Copley, R. R., Andrade, M. A. & Bork, P. Evolution of domain families. *Adv. Protein Chem.* **54**, 185–244 (2000).
313. Doolittle, R. F. The multiplicity of domains in proteins. *Annu. Rev. Biochem.* **64**, 287–314 (1995).
314. Bateman, A. & Birney, E. Searching databases to find protein domain organization. *Adv. Protein Chem.* **54**, 137–157 (2000).
315. Futreal, P. A. *et al.* Cancer and genomics. *Nature* **409**, 850–852 (2001).
316. Nestler, E. J. & Landsman, D. Learning about addiction from the human draft genome. *Nature* **409**, 834–835 (2001).
317. Tupler, R., Perini, G. & Green, M. R. Expressing the human genome. *Nature* **409**, 832–835 (2001).
318. Fahrer, A. M., Bazan, J. F., Papathanasiou, P., Nelms, K. A. & Goodnow, C. C. A genomic view of immunology. *Nature* **409**, 836–838 (2001).
319. Li, W.-H., Gu, Z., Wang, H. & Nekrutchenko, A. Evolutionary analyses of the human genome. *Nature* **409**, 847–849 (2001).
320. Bock, J. B., Matern, H. T., Peden, A. A. & Scheller, R. H. A genomic perspective on membrane compartment organization. *Nature* **409**, 839–841 (2001).
321. Pollard, T. D. Genomics, the cytoskeleton and motility. *Nature* **409**, 842–843 (2001).
322. Murray, A. W. & Marks, D. Can sequencing shed light on cell cycling? *Nature* **409**, 844–846 (2001).
323. Clayton, J. D., Kyriacou, C. P. & Reppert, S. M. Keeping time with the human genome. *Nature* **409**, 829–831 (2001).
324. Chervitz, S. A. *et al.* Comparison of the complete protein sets of worm and yeast: orthology and divergence. *Science* **282**, 2022–2028 (1998).
325. Aravind, L. & Subramanian, G. Origin of multicellular eukaryotes—insights from proteome comparisons. *Curr. Opin. Genet. Dev.* **9**, 688–694 (1999).
326. Attwood, T. K. *et al.* PRINTS-S: the database formerly known as PRINTS. *Nucleic Acids Res.* **28**, 225–227 (2000).
327. Hofmann, K., Bucher, P., Falquet, L. & Bairoch, A. The PROSITE database, its status in 1999. *Nucleic Acids Res.* **27**, 215–219 (1999).
328. Altschul, S. F. *et al.* Gapped BLAST and PSI-BLAST: a new generation of protein database search programs. *Nucleic Acids Res.* **25**, 3389–3402 (1997).
329. Wolf, Y. I., Kondrashov, F. A. & Koonin, E. V. No footprints of primordial introns in a eukaryotic genome. *Trends Genet.* **16**, 333–334 (2000).
330. Brunner, H. G., Nelen, M., Breakefield, X. O., Ropers, H. H. & van Oost, B. B. A. Abnormal behavior associated with a point mutation in the structural gene for monoamine oxidase A. *Science* **262**, 578–580 (1993).
331. Cases, O. *et al.* Aggressive behavior and altered amounts of brain serotonin and norepinephrine in mice lacking MAOA. *Science* **268**, 1763–1766 (1995).
332. Brunner, H. G. *et al.* X-linked borderline mental retardation with prominent behavioral disturbance: phenotype, genetic localization, and evidence for disturbed monoamine metabolism. *Am. J. Hum. Genet.* **52**, 1032–1039 (1993).
333. Deckert, J. *et al.* Excess of high activity monoamine oxidase A gene promoter alleles in female patients with panic disorder. *Hum. Mol. Genet.* **8**, 621–624 (1999).
334. Smith, T. F. & Waterman, M. S. Identification of common molecular subsequences. *J. Mol. Biol.* **147**, 195–197 (1981).
335. Tatusov, R. L., Koonin, E. V. & Lipman, D. J. A genomic perspective on protein families. *Science* **278**, 631–637 (1997).
336. Ponting, C. P., Aravind, L., Schultz, J., Bork, P. & Koonin, E. V. Eukaryotic signalling domain homologues in archaea and bacteria: Ancient ancestry and horizontal gene transfer. *J. Mol. Biol.* **289**, 729–745 (1999).
337. Zhang, J., Dyer, K. D. & Rosenberg, H. F. Evolution of the rodent eosinophil-associated Rnase gene family by rapid gene sorting and positive selection. *Proc. Natl Acad. Sci. USA* **97**, 4701–4706 (2000).
338. Shashoua, V. E. Ependymin, a brain extracellular glycoprotein, and CNS plasticity. *Ann. NY Acad. Sci.* **627**, 94–114 (1991).
339. Schultz, J., Copley, R. R., Doerks, T., Ponting, C. P. & Bork, P. SMART: a web-based tool for the study of genetically mobile domains. *Nucleic Acids Res.* **28**, 231–234 (2000).
340. Koonin, E. V., Aravind, L. & Kondrashov, A. S. The impact of comparative genomics on our understanding of evolution. *Cell* **101**, 573–576 (2000).
341. Bateman, A., Eddy, S. R. & Chothia, C. Members of the immunoglobulin superfamily in bacteria. *Protein Sci.* **5**, 1939–1941 (1996).
342. Sutherland, D., Samakovlis, C. & Krasnow, M. A. Branchless encodes a *Drosophila* FGF homolog that controls tracheal cell migration and the pattern of branching. *Cell* **87**, 1091–1101 (1996).
343. Warburton, D. *et al.* The molecular basis of lung morphogenesis. *Mech. Dev.* **92**, 55–81 (2000).
344. Fuchs, T., Glusman, G., Horn-Saban, S., Lancet, D. & Pilpel, Y. The human olfactory subgenome: from sequence to structure to evolution. *Hum. Genet.* **108**, 1–13 (2001).
345. Glusman, G. *et al.* The olfactory receptor gene family: data mining, classification and nomenclature. *Mamm. Genome* **11**, 1016–1023 (2000).
346. Rouquier, S. *et al.* Distribution of olfactory receptor genes in the human genome. *Nature Genet.* **18**, 243–250 (1998).
347. Sharon, D. *et al.* Primate evolution of an olfactory receptor cluster: Diversification by gene conversion and recent emergence of a pseudogene. *Genomics* **61**, 24–36 (1999).
348. Gilad, Y. *et al.* Dichotomy of single-nucleotide polymorphism haplotypes in olfactory receptor genes and pseudogenes. *Nature Genet.* **26**, 221–224 (2000).
349. Gearhart, J. & Kirschner, M. *Cells, Embryos, and Evolution* (Blackwell Science, Malden, Massachusetts, 1997).
350. Barbazuk, W. B. *et al.* The syntenic relationship of the zebrafish and human genomes. *Genome Res.* **10**, 1351–1358 (2000).
351. McLysaght, A., Enright, A. J., Skrabanek, L. & Wolfe, K. H. Estimation of synteny conservation and genome compaction between pufferfish (Fugu) and human. *Yeast* **17**, 22–36 (2000).
352. Trachulec, Z. *et al.* Linkage of TATA-binding protein and proteasome subunit C5 genes in mice and humans reveals synteny conserved between mammals and invertebrates. *Genomics* **44**, 1–7 (1997).

353. Nadeau, J. H. Maps of linkage and synteny homologies between mouse and man. *Trends Genet.* **5**, 82–86 (1989).
354. Nadeau, J. H. & Taylor, B. A. Lengths of chromosomal segments conserved since divergence of man and mouse. *Proc. Natl Acad. Sci. USA* **81**, 814–818 (1984).
355. Copeland, N. G. *et al.* A genetic linkage map of the mouse: current applications and future prospects. *Science* **262**, 57–66 (1993).
356. DeBry, R. W. & Seldin, M. F. Human/mouse homology relationships. *Genomics* **33**, 337–351 (1996).
357. Nadeau, J. H. & Sankoff, D. The lengths of undiscovered conserved segments in comparative maps. *Mamm. Genome* **9**, 491–495 (1996).
358. Thomas, J. W. *et al.* Comparative genome mapping in the sequence-based era: early experience with human chromosome 7. *Genome Res.* **10**, 624–633 (2000).
359. Pletcher, M. T. *et al.* Chromosome evolution: The junction of mammalian chromosomes in the formation of mouse chromosome 10. *Genome Res.* **10**, 1463–1467 (2000).
360. Novacek, M. J. Mammalian phylogeny: shaking the tree. *Nature* **356**, 121–125 (1992).
361. O'Brien, S. J. *et al.* Genome maps 10. Comparative genomics. Mammalian radiations. Wall chart. *Science* **286**, 463–478 (1999).
362. Romer, A. S. *Vertebrate Paleontology* (Univ. Chicago Press, Chicago and New York, 1966).
363. Paterson, A. H. *et al.* Toward a unified genetic map of higher plants, transcending the monocot-dicot divergence. *Nature Genet.* **14**, 380–382 (1996).
364. Jenczewski, E., Prosperi, J. M. & Ronfort, J. Differentiation between natural and cultivated populations of *Medicago sativa* (Leguminosae) from Spain: analysis with random amplified polymorphic DNA (RAPD) markers and comparison to allozymes. *Mol. Ecol.* **8**, 1317–1330 (1999).
365. Ohno, S. *Evolution by Gene Duplication* (George Allen and Unwin, London, 1970).
366. Wolfe, K. H. & Shields, D. C. Molecular evidence for an ancient duplication of the entire yeast genome. *Nature* **387**, 708–713 (1997).
367. Blanc, G., Barakat, A., Guyot, R., Cooke, R. & Delseny, M. Extensive duplication and reshuffling in the arabidopsis genome. *Plant Cell* **12**, 1093–1102 (2000).
368. Paterson, A. H. *et al.* Comparative genomics of plant chromosomes. *Plant Cell* **12**, 1523–1540 (2000).
369. Vision, T., Brown, D. & Tanksley, S. The origins of genome duplications in *Arabidopsis*. *Science* **290**, 2114–2117 (2000).
370. Sidow, A. & Bowman, B. H. Molecular phylogeny. *Curr. Opin. Genet. Dev.* **1**, 451–456 (1991).
371. Sidow, A. & Thomas, W. K. A molecular evolutionary framework for eukaryotic model organisms. *Curr. Biol.* **4**, 596–603 (1994).
372. Sidow, A. Gen(om)e duplications in the evolution of early vertebrates. *Curr. Opin. Genet. Dev.* **6**, 715–722 (1996).
373. Spring, J. Vertebrate evolution by interspecific hybridisation—are we polyploid? *FEBS Lett.* **400**, 2–8 (1997).
374. Skrabaneck, L. & Wolfe, K. H. Eukaryote genome duplication—where's the evidence? *Curr. Opin. Genet. Dev.* **8**, 694–700 (1998).
375. Hughes, A. L. Phylogenies of developmentally important proteins do not support the hypothesis of two rounds of genome duplication early in vertebrate history. *J. Mol. Evol.* **48**, 565–576 (1999).
376. Lander, E. S. & Schork, N. J. Genetic dissection of complex traits. *Science* **265**, 2037–2048 (1994).
377. Horikawa, Y. *et al.* Genetic variability in the gene encoding calpain-10 is associated with type 2 diabetes mellitus. *Nature Genet.* **26**, 163–175 (2000).
378. Hashtack, J. *et al.* The diastrophic dysplasia gene encodes a novel sulfate transporter: positional cloning by fine-structure linkage disequilibrium mapping. *Cell* **78**, 1073–1087 (1994).
379. Tischkoff, S. A. *et al.* Global patterns of linkage disequilibrium at the CD4 locus and modern human origins. *Science* **271**, 1380–1387 (1996).
380. Kidd, J. R. *et al.* Haplotypes and linkage disequilibrium at the phenylalanine hydroxylase locus PAH, in a global representation of populations. *Am. J. Hum. Genet.* **63**, 1882–1899 (2000).
381. Mateu, E. *et al.* Worldwide genetic analysis of the CFTR region. *Am. J. Hum. Genet.* **68**, 103–117 (2001).
382. Abecasis, G. R. *et al.* Extent and distribution of linkage disequilibrium in three genomic regions. *Am. J. Hum. Genet.* **68**, 191–197 (2001).
383. Taillon-Miller, P. *et al.* Juxtaposed regions of extensive and minimal linkage disequilibrium in Xq25 and Xq28. *Nature Genet.* **25**, 324–328 (2000).
384. Martin, E. R. *et al.* SNPing away at complex diseases: analysis of single-nucleotide polymorphisms around APOE in Alzheimer disease. *Am. J. Hum. Genet.* **67**, 383–394 (2000).
385. Collins, A., Lonjou, C. & Morton, N. E. Genetic epidemiology of single-nucleotide polymorphisms. *Proc. Natl Acad. Sci. USA* **96**, 15173–15177 (1999).
386. Dunning, A. M. *et al.* The extent of linkage disequilibrium in four populations with distinct demographic histories. *Am. J. Hum. Genet.* **67**, 1544–1554 (2000).
387. Rieder, M. J., Taylor, S. L., Clark, A. G. & Nickerson, D. A. Sequence variation in the human angiotensin converting enzyme. *Nature Genet.* **22**, 59–62 (1999).
388. Collins, F. S. Positional cloning moves from perditional to traditional. *Nature Genet.* **9**, 347–350 (1995).
389. Nagamine, K. *et al.* Positional cloning of the APECED gene. *Nature Genet.* **17**, 393–398 (1997).
390. Reuber, B. E. *et al.* Mutations in PEX1 are the most common cause of peroxisome biogenesis disorders. *Nature Genet.* **17**, 445–448 (1997).
391. Portsteffen, H. *et al.* Human PEX1 is mutated in complementation group 1 of the peroxisome biogenesis disorders. *Nature Genet.* **17**, 449–452 (1997).
392. Everett, L. A. *et al.* Pendred syndrome is caused by mutations in a putative sulphate transporter gene (PDS). *Nature Genet.* **17**, 411–422 (1997).
393. Coffey, A. J. *et al.* Host response to EBV infection in X-linked lymphoproliferative disease results from mutations in an SH2-domain encoding gene. *Nature Genet.* **20**, 129–135 (1998).
394. Van Laer, L. *et al.* Nonsyndromic hearing impairment is associated with a mutation in DFNA5. *Nature Genet.* **20**, 194–197 (1998).
395. Sakuntabhai, A. *et al.* Mutations in ATP2A2, encoding a Ca²⁺ pump, cause Darier disease. *Nature Genet.* **21**, 271–277 (1999).
396. Gedeon, A. K. *et al.* Identification of the gene (SEDL) causing X-linked spondyloepiphyseal dysplasia tarda. *Nature Genet.* **22**, 400–404 (1999).
397. Hurvitz, J. R. *et al.* Mutations in the CCN gene family member WISP3 cause progressive pseudorheumatoid dysplasia. *Nature Genet.* **23**, 94–98 (1999).
398. Laberge-le Couteux, S. *et al.* Truncating mutations in CCM1, encoding KRIT1, cause hereditary cavernous angiomas. *Nature Genet.* **23**, 189–193 (1999).
399. Sahoo, T. *et al.* Mutations in the gene encoding KRIT1, a Krev-1/rap1a binding protein, cause cerebral cavernous malformations (CCM1). *Hum. Mol. Genet.* **8**, 2325–2333 (1999).
400. McGuire, W. T. *et al.* Mutations in COL11A2 cause non-syndromic hearing loss (DFNA13). *Nature Genet.* **23**, 413–419 (1999).
401. Moreira, E. S. *et al.* Limb-girdle muscular dystrophy type 2G is caused by mutations in the gene encoding the sarcomeric protein telethonin. *Nature Genet.* **24**, 163–166 (2000).
402. Ruiz-Perez, V. L. *et al.* Mutations in a new gene in Ellis-van Creveld syndrome and Weyers acrodermatitis dystostosis. *Nature Genet.* **24**, 283–286 (2000).
403. Kaplan, J. M. *et al.* Mutations in ACTN4, encoding alpha-actinin-4, cause familial focal segmental glomerulosclerosis. *Nature Genet.* **24**, 251–256 (2000).
404. Escarg, A. *et al.* Mutations of SCN1A, encoding a neuronal sodium channel, in two families with GEFS+. *Nature Genet.* **24**, 343–345 (2000).
405. Sacksteder, K. A. *et al.* Identification of the alpha-aminoacidic semialdehyde synthase gene, which is defective in familial hyperlysineuria. *Am. J. Hum. Genet.* **66**, 1736–1743 (2000).
406. Kalaydjieva, L. *et al.* N-myc downstream-regulated gene 1 is mutated in hereditary motor and sensory neuropathy-Lom. *Am. J. Hum. Genet.* **67**, 47–58 (2000).
407. Sundin, O. H. *et al.* Genetic basis of total colourblindness among the Pingelapse islanders. *Nature Genet.* **25**, 289–293 (2000).
408. Kohl, S. *et al.* Mutations in the CNGB3 gene encoding the beta-subunit of the cone photoreceptor cGMP-gated channel are responsible for achromatopsia (ACHM3) linked to chromosome 8q21. *Hum. Mol. Genet.* **9**, 2107–2116 (2000).
409. Avila, K. *et al.* Gene encoding a new RING-B-box-coiled-coil protein is mutated in mulibrey nanism. *Nature Genet.* **25**, 298–301 (2000).
410. Verpy, E. *et al.* A defect in harmonin, a PDZ domain-containing protein expressed in the inner ear sensory hair cells, underlies usher syndrome type 1C. *Nature Genet.* **26**, 51–55 (2000).
411. Bitner-Glindzicz, M. *et al.* A recessive contiguous gene deletion causing infantile hyperinsulinism, enteropathy and deafness identifies the usher type 1C gene. *Nature Genet.* **26**, 56–60 (2000).
412. The May-Hegglin/Fetchner Syndrome Consortium. Mutations in MYH9 result in the May-Hegglin anomaly, and Fechtner and Sebastian syndromes. *Nature Genet.* **26**, 103–105 (2000).
413. Kelley, M. J., Jawien, W., Ortel, T. L. & Korczak, J. F. Mutation of MYH9, encoding non-muscle myosin heavy chain A, in May-Hegglin anomaly. *Nature Genet.* **26**, 106–108 (2000).
414. Kirschner, L. S. *et al.* Mutations of the gene encoding the protein kinase A type I-α regulatory subunit in patients with the Carney complex. *Nature Genet.* **26**, 89–92 (2000).
415. Lalwani, A. K. *et al.* Human nonsyndromic hereditary deafness DFNA17 is due to a mutation in non-muscle myosin MYH9. *Am. J. Hum. Genet.* **67**, 1121–1128 (2000).
416. Matsunaga, T. *et al.* Large expansion of the ATTCT pentanucleotide repeat in spinocerebellar atrophy type 10. *Nature Genet.* **26**, 191–194 (2000).
417. Delettre, C. *et al.* Nuclear gene OPA1, encoding a mitochondrial dynamin-related protein, is mutated in dominant optic atrophy. *Nature Genet.* **26**, 207–210 (2000).
418. Pusch, C. M. *et al.* The complete form of X-linked congenital stationary night blindness is caused by mutations in a gene encoding a leucine-rich repeat protein. *Nature Genet.* **26**, 324–327 (2000).
419. The ADHR Consortium. Autosomal dominant hypophosphataemic rickets is associated with mutations in FGF23. *Nature Genet.* **26**, 345–348 (2000).
420. Bonmont, P. *et al.* The gene encoding gigaxonin, a new member of the cytoskeletal BTB/kelch repeat family, is mutated in giant axonal neuropathy. *Nature Genet.* **26**, 370–374 (2000).
421. Tullio-Pelet, A. *et al.* Mutant WD-repeat protein in triple-A syndrome. *Nature Genet.* **26**, 332–335 (2000).
422. Nicole, S. *et al.* Perlecan, the major proteoglycan of basement membranes, is altered in patients with Schwartz-Jampel syndrome (chondrocytic myotonia). *Nature Genet.* **26**, 480–483 (2000).
423. Rogaev, E. I. *et al.* Familial Alzheimer's disease in kindreds with missense mutations in a gene on chromosome 1 related to the Alzheimer's disease type 3 gene. *Nature* **376**, 775–778 (1995).
424. Sherrington, R. *et al.* Cloning of a gene bearing missense mutations in early-onset familial Alzheimer's disease. *Nature* **375**, 754–760 (1995).
425. Olivieri, N. F. & Weatherall, D. J. The therapeutic reactivation of fetal haemoglobin. *Hum. Mol. Genet.* **7**, 1655–1658 (1998).
426. Drews, J. Research & development. Basic science and pharmaceutical innovation. *Nature Biotechnol.* **17**, 406 (1999).
427. Drews, J. Drug discovery: a historical perspective. *Science* **287**, 1960–1964 (2000).
428. Davies, P. A. *et al.* The 5-HT3B subunit is a major determinant of serotonin-receptor function. *Nature* **397**, 359–363 (1999).
429. Heise, C. E. *et al.* Characterization of the human cysteinyl leukotriene 2 receptor. *J. Biol. Chem.* **275**, 30531–30536 (2000).
430. Fan, W. *et al.* BACE maps to chromosome 11 and a BACE homolog, BACE2, reside in the obligate Down Syndrome region of chromosome 21. *Science* **286**, 1255a (1999).
431. Saunders, A. J., Kim, T.-W. & Tanzi, R. E. BACE maps to chromosome 11 and a BACE homolog, BACE2, reside in the obligate Down Syndrome region of chromosome 21. *Science* **286**, 1255a (1999).
432. Firestein, S. The good taste of genomics. *Nature* **404**, 552–553 (2000).
433. Matsunami, H., Montmayeur, J. P. & Buck, L. B. A family of candidate taste receptors in human and mouse. *Nature* **404**, 601–604 (2000).
434. Adler, E. *et al.* A novel family of mammalian taste receptors. *Cell* **100**, 693–702 (2000).
435. Chandrashekhar, J. *et al.* T2Rs function as bitter taste receptors. *Cell* **100**, 703–711 (2000).
436. Hardison, R. C. Conserved non-coding sequences are reliable guides to regulatory elements. *Trends Genet.* **16**, 369–372 (2000).
437. Onyango, P. *et al.* Sequence and comparative analysis of the mouse 1-megabase region orthologous to the human 11p15 imprinted domain. *Genome Res.* **10**, 1697–1710 (2000).
438. Bouck, J. B., Metzker, M. L. & Gibbs, R. A. Shotgun sample sequence comparisons between mouse and human genomes. *Nature Genet.* **25**, 31–33 (2000).
439. Marshall, E. Public-private project to deliver mouse genome in 6 months. *Science* **290**, 242–243 (2000).
440. Wasserman, W. W., Palumbo, M., Thompson, W., Fickett, J. W. & Lawrence, C. E. Human-mouse genome comparisons to locate regulatory sites. *Nature Genet.* **26**, 225–228 (2000).
441. Tagle, D. A. *et al.* Embryonic epsilon and gamma globin genes of a prosimian primate (*Galago crassicaudatus*). Nucleotide and amino acid sequences, developmental regulation and phylogenetic footprints. *J. Mol. Biol.* **203**, 439–455 (1988).
442. McGuire, A. M., Hughes, J. D. & Church, G. M. Conservation of DNA regulatory motifs and discovery of new motifs in microbial genomes. *Genome Res.* **10**, 744–757 (2000).

Bibliography

- [1] Philip R. Bevington and D. Kieth Robinson. *Data Reduction and Error Analysis for the Physical Sciences*. McGraw-Hill, Inc., 2nd edition, 1992.
- [2] International Human Genome Sequencing Consortium. Initial sequencing and analysis of the human genome. *Nature*, 409:860, 2001.
- [3] T. Kessler, C. Hagemann, C. Grebing, T. Legero, U. Sterr, F. Riehle, M. J. Martin, L. Chen, and J. Ye. A sub-40-mHz-linewidth laser based on a silicon single-crystal optical cavity. *Nature Photonics*, 6:687, 2012.
- [4] Jerry B. Marion and Stephen T. Thornton. *Classical Dynamics of Particles and Systems*. Saunders College Publishing, 4th edition, 1995.
- [5] William J. Murray, 1984.
- [6] Tony Reichhardt. NASA reworks its sums after Mars fiasco. *Nature*, 401:517, 1999.
- [7] T. Rosenband, D. B. Hume, P. O. Schmidt, C. W. Chou, A. Brusch, L. Lorini, W. H. Oskay, R. E. Drullinger, T. M. Fortier, J. E. Stalnaker, S. A. Diddams, W. C. Swann, N. R. Newbury, W. M. Itano, D. J. Wineland, and J. C. Bergquist. Frequency ratio of Al⁺ and Hg⁺ single-ion optical clocks; metrology at the 17th decimal place. *Science*, 319:1808, 2008.
- [8] Barry N. Taylor and Ambler Thompson. NIST special publication 330: The International System of Units (SI). Technical report, National Institute of Standards and Technology, 2008. Available online at <http://physics.nist.gov/Pubs/SP330/sp330.pdf>.
- [9] John R. Taylor. *An Introduction to Error Analysis*. University Science Books, Sausalito, California, 2nd edition, 1997.
- [10] Menglan Zeng and Donald H. Shields. Nonlinear thermal expansion and contraction of asphalt concrete. *Can. J. Civ. Eng.*, 26:26, 1999.